

Muscle-Computer Interface Based on Pattern Recognition of Myoelectric Signals for Control of Dexterous Hand and Finger Movements of Prostheses for Forearm Amputees

John Jairo Villarejo Mayor

Vitoria, Brazil

2017

Muscle-Computer Interface Based on Pattern Recognition of Myoelectric Signals for Control of Dexterous Hand and Finger Movements of Prostheses for Forearm Amputees

John Jairo Villarejo Mayor

Submitted to the Postgraduate Program in Electrical Engineering of the
Federal University of Espirito Santo (UFES)
in partial fulfillment of the
Requirements for the degree of
Doctor of Philosophy in Electrical Engineering

Supervisor: Prof. Dr. Teodiano Freire Bastos Filho

Co-Supervisor: Prof. Dr. Anselmo Frizera Neto

Vitoria, Brazil

2017

Dados Internacionais de Catalogação-na-publicação (CIP)
(Biblioteca Setorial Tecnológica,
Universidade Federal do Espírito Santo, ES, Brasil)

M473m Mayor, John Jairo Villarejo, 1981-
Muscle-computer interface based on pattern recognition of
myoelectric signals for control of dexterous hand and finger
movements of prostheses for forearm amputees / John Jairo
Villarejo Mayor. – 2017.
118 f. : il.

Orientador: Teodiano Freire Bastos Filho.

Coorientador: Anselmo Frizera Neto.

Tese (Doutorado em Engenharia Elétrica) – Universidade
Federal do Espírito Santo, Centro Tecnológico.

1. Membros-superiores – Prótese. 2. Interação homem-
máquina. 3. Mãos – Movimentos. 4. Dedos – Movimentos.
5. Capacidade motora. 6. Eletromiografia. 7. Reconhecimento de
padrões. I. Bastos Filho, Teodiano Freire. II. Frizera Neto,
Anselmo. III. Universidade Federal do Espírito Santo. Centro
Tecnológico. IV. Título.

CDU: 621.3

Muscle-Computer Interface Based on Pattern Recognition of Myoelectric Signals for Control of Dexterous Hand and Finger Movements of Prostheses for Forearm Amputees

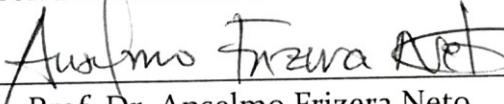
John Jairo Villarejo Mayor

Submitted to the Postgraduate Program in Electrical Engineering of the
Federal University of Espirito Santo (UFES)
in partial fulfillment of the
Requirements for the degree of
Doctor of Philosophy in Electrical Engineering

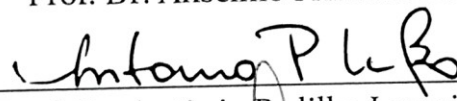
Approved by



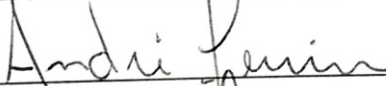
Prof. Dr. Teodiano Freire Bastos Filho



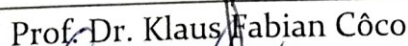
Prof. Dr. Anselmo Frizera Neto



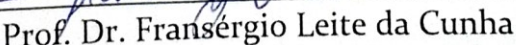
Prof. Dr. Antônio Padilha Lanari Bó



Prof. Dr. André Ferreira



Prof. Dr. Klaus Fabian Côco



Prof. Dr. Fransérgio Leite da Cunha

Vitoria, Brazil

2017

Dedicated to my parents, Maria Eugenia and Jaime

Acknowledgment

Although this dissertation has but one author, many people have contributed in varied but significant ways. I would like to express my sincere appreciation and gratitude to everyone who made this dissertation possible.

Most of people involved in the bioengineering as a researcher believe in one of the most beautiful intention as human being, which is to help other human. Most of time they never meet who are helping. Today, I felt all of people that I met in this area as a big family.

First and foremost, I would like to thank my advisor, Dr. Teodiano Bastos, who since the day I became his student, he has been an enthusiastic believer in me and my capabilities. I have received the most of your support through advices and friendship in many ways. All my gratitude to professor Teodiano.

To Dr. Anselmo, who showed me his tenacity and great effort as a researcher and as a friend, being a guide at this stage; to my professors of the Postgraduate Program in Electrical Engineering of the Federal University of Espirito Santo; for all of them all my gratitude.

My heart and my whole soul thank my family for being always there, present and ant the same time distant, always linked at heart. My parents María Eugenia and Jaime, who taught me how to live, today I thank them for being the best professors. To my brothers, grandparents, uncles, cousins, because they all contributed with a piece to be able to get this achievement today.

Special thanks to all the people who were part of my life during this cycle, to those who I owe a great part of my smiles, my happiness, my memorable days and for which today I have a great affection for the city of Vitória. To my friend Maria Dolores, for becoming a fundamental piece, to whom I owe her friendship, her support and above all her good energies. To my friend Denis, for his friendship, his time and all the collaboration with this thesis. To the group of corporal

consciousness, that left a marked mark and future challenges to do after this thesis. To my best and close Colombian friends, for becoming a great support; to all the foreign friends, for all of them becoming for me as my substitute family; and to all the Brazilian friends, for all of them becoming my home. Without naming everyone, I thank all the friends who arrived, left and stay in the Laboratory of Intelligent Automation, LAI.

Thanks to the same cause of obtaining my doctoral degree, I was able to grow, both as an academic and as a person, knowing my own limits and understanding one of the greatest learning, which today I consider as the convergence of situations throughout my academic life. This learning, which ended up being my greatest strength during the various adversities, is in short, the balance between perseverance, loyalty to principles, physical and spiritual health, and the firm purpose of always being clear about the real purpose of living.

Abstract

Intuitive prosthesis control is one of the most important challenges to reduce the user effort in learning how to use an artificial hand. This work presents the analysis of pattern recognition techniques for low-level myoelectric signals able to discriminate dexterous hand and fingers movements using a reduced number of electrodes in amputees. Ten amputees and ten able-bodied subjects were evaluated and the performance of the techniques was evaluated in both groups of subjects. The techniques here proposed were analyzed to classify individual finger flexion, hand movements and different grasps using four electrodes and taking into account the low level of muscle contraction in these movements. Seventeen features of myoelectric signals were also analyzed considering both traditional magnitude-based features and more recent techniques based on fractal analysis. A comparison was computed for all the techniques using different set of features, for both groups of subjects (able-bodied and amputees) with significant level of 95%. The results with a selected set of features showed average accuracy up to 92.7% of recognition for amputees using support vector machine (SVM), followed very closely by K-nearest neighbors (KNN). The results with the best combination of the analyzed techniques show that the techniques here proposed are suitable for accurately controlling dexterous prosthetic hand/fingers, providing more functionality and better acceptance for amputees.

Keywords: myoelectric signal, upper-limb prosthesis, low-density signals, dexterous hand/finger movements, pattern recognition.

Resumo

O controle intuitivo de uma prótese é um dos desafios mais importantes para reduzir o esforço do usuário em aprender a usar uma mão artificial. Este trabalho apresenta a análise de técnicas de reconhecimento de padrões para sinais mioelétricos de baixo nível para classificar movimentos de destreza dos dedos e da mão em sujeitos com amputação do antebraço. Dez indivíduos com amputação e dez indivíduos sem amputação foram analisados e o desempenho das técnicas propostas no presente estudo foi comparado levando em consideração ambos os grupos. A classificação foi realizada para a flexão de cada um dos dedos, movimentos da mão e diferentes tipos de preensão palmar utilizando quatro eletrodos e considerando a baixa contração muscular durante estes movimentos. Dezesete características dos sinais mioelétricos baseadas na magnitude do sinal e em análise de fractais foram comparadas para os dois grupos de sujeitos (com e sem amputação) com nível de significância de 95%. Os resultados, usando um conjunto de características mostraram uma exatidão máxima das médias de 92,7% de reconhecimento de padrão do movimento para o grupo de indivíduos amputados utilizando máquinas de vetores de suporte (SVM). A segunda melhor exatidão foi obtida utilizando o método de k vizinhos mais próximos (KNN). A melhor combinação das técnicas analisadas mostrou-se adequada para realizar o controle da prótese com precisão e destreza dos dedos e da mão, proporcionando maior funcionalidade e melhor aceitação para os sujeitos com amputação.

Palavras-chave: sinal mioelétrico, prótese de membro superior, sinais de baixa densidade, movimentos de destreza com as mão e os dedos, reconhecimento de padrões. Palavras-chave: sinal mioelétrico, prótese de membro superior, sinais de baixa densidade, movimentos de destreza com as mão e os dedos, reconhecimento de padrões.

Contents

1. Introduction.....	1
1.1. Motivation	2
1.2. State of the art	4
1.3. Problem Statement	8
1.3.1. Problem definition.....	8
1.3.2. Research goal.....	8
1.3.3. Hypothesis	9
1.4. Objectives	9
1.4.1. General objective	9
1.4.2. Specific objectives.....	9
1.5. Thesis contribution.....	10
1.6. Thesis outline	11
2. Theoretical background	13
2.1. Functional hand movements	13
2.2. Brief approach to the physiology of muscle contraction	15
2.2.1. Types of muscle contraction	16
2.3. Electromyography (EMG)	17
2.4. Detection of movement intention for myoelectric control systems.....	19
2.4.1. Myoelectric prosthesis control	20
2.4.2. Myoelectric signal processing.....	21
2.4.3. Feature extraction	23
2.4.4. Dimensionality reduction	28

2.4.5. Classification	30
2.4.6. Post-processing	33
2.4.7. Performance measures	35
3. Materials and methods.....	38
3.1. Experimental procedure	38
3.1.1. Subjects	38
3.1.2. Equipment and electrode placement	39
3.1.3. Experimental protocol	42
3.2. Method for recognition of dexterous hand/fingers movements.....	45
3.2.1. Data extraction and data windowing	47
3.2.2. Feature extraction	49
3.2.3. Feature selection	50
3.2.4. Classification	51
3.2.5. Post-processing.....	52
3.3. Experimental design	53
3.4. Statistical evaluation.....	56
4. Results	58
4.1. Offline study results.....	58
4.1.1. Data extraction	58
4.1.2. Parameter adjustment.....	60
4.1.3. Feature selection analysis.....	65
4.1.4. Proposed MES pattern recognition system	68
4.2. Online study results.....	72
4.2.1. Post-processing.....	80
4.3. Online applications.....	83
4.4. Towards a single-channel recognition system.....	86

4.5.	Assessment of suitable dexterous movements	91
4.5.1.	Individual Finger Movements.....	91
4.5.2.	Grasp Movements	92
5.	Discussion	94
6.	Conclusion.....	101
6.1.	Acknowledgements.....	103
6.2.	Publications	103
7.	References	107

List of Figures

Figure 1. Scheme of a cognitive process in a muscle-computer interface (muCI). Source: Adapted from (BUENO et al., 2008).....	20
Figure 2. Flowchart outlining a proposal for prosthesis control.	21
Figure 3. General scheme for MES pattern recognition for prosthesis control.....	22
Figure 4. Group of amputees who voluntarily participated of the experiments. Details of each one can be seen in Table 2.	39
Figure 5. Touch bionics electrode for MES acquisition.....	40
Figure 6. Forearm muscles by channel adopted in the experimental protocol.....	42
Figure 7. Different kinds of hand and individual finger movements considered in this study (rest state picture is not included).....	44
Figure 8. Experimental protocol to extract the isometric task.	45
Figure 9. General scheme for MES pattern recognition.	46
Figure 10. Diagram of the techniques used for the design of the MES pattern recognition.	47
Figure 11. Diagram of the system for myoelectric pattern recognition of hand/finger movements, using virtual reality environment and robotic hand.	55
Figure 12. Diagram of the low level control (LLC) of the robotic hand for real time validation.	55
Figure 13. Effect of varying the length of the window for individual fingers movements.	59
Figure 14. Effect of varying the sliding of the window on individual fingers movements.	59
Figure 15. Results varying the length of the window and the overlapping for grasp movements.	60
Figure 16. Graphic representation of the accuracy distribution of the different parameters according to the variance among amputees. (a), parameter γ for SVM-RBF; (b), polynomial order for SVM-Polynomial; (c), constant C for all SVM kernels.....	62

Figure 17. Comparison of classification results with amputees in offline mode, for individual fingers (a) movements and grasp movements (b).	63
Figure 18. Comparison of classification results with the control group in offline mode, for individual fingers movements and grasp movements.....	64
Figure 19. Effect of error of classification according to the increment of features.	65
Figure 20. Results of the feature selection experiment for each one of the movements categories. Representation of the selected frequency feature, for the control group and amputees.	66
Figure 21. Graphic representation of the error distribution of the different feature selection methods according to the variance among amputees.....	68
Figure 22. Classification error for control group and amputees using the proposed feature set with SVM.	69
Figure 23. Confusion matrices with average misclassification for amputees.	71
Figure 24. Online results for amputees, for three movements categories.....	73
Figure 25. Confusion matrix for A7 subject, in validation online for CA.....	74
Figure 26. Output stream of predictions for amputee A7, in validation online for individual fingers	75
Figure 27. Confusion matrix for amputee A7, in validation online for grasp movements	76
Figure 28. Output stream of predictions for amputee A7, in validation online for grasp movements.....	76
Figure 29. Confusion matrix for the amputee A3, in validation online for grasp movements.	78
Figure 30. Confusion matrix for the amputee A7, in validation online for all adopted movements.	79
Figure 31. Output stream of predictions for the amputee A7, in validation online for all adopted movements	79
Figure 32. Post-processing response by iteration of level of agreement.....	82
Figure 33. Temporal diagram using post-processing method 1. (Up) predicted decision with discarded patterns; (down) consecutive discarded trials.	83
Figure 34. Histogram of consecutive unclassified samples.....	84

Figure 35. Robotic hand used for the experiments.....	85
Figure 36. Robotic hand built with a 3D printing.....	85
Figure 37. Virtual reality environment for training the control of a myoelectric prosthesis.....	86
Figure 38. Comparison among performance for four-channel to single-channel systems, for all categories of movements.....	89
Figure 39. Graphic representation of the relationship between the number of electrodes and the accuracy of the pattern recognition system.	89

List of Tables

Table 1. Relevant researches for recognition of hand/finger movements using MES.	6
Table 2. Participant demographics. Level of amputation is indicated: wrist disarticulation (WD), Proximal Transradial (PTR), Medial Transradial (MTR) and Distal Transradial (DTR).	40
Table 3. Description and functions of muscle groups covered in this study.	41
Table 4. Movements performed in the experiments.	43
Table 5. Features selected for this study, split in groups. The parameters used for some features are also specified.....	50
Table 6. Parameters selected for features used in this research.	61
Table 7. Parameters selected for the classifiers used in the experiments.	62
Table 8. Average classification accuracy (%) and Kappa's Coefficient of three movement categories, for control group and amputees. Table includes the results for SVM, LDA and KNN classifiers.	70
Table 9. Online results for amputees, for the three movements categories.....	73
Table 10. Online results for control group, for the three movements categories.	73
Table 11. Post-processing analysis results.	81
Table 12. Comparison of accuracy for different number of MES channels.	87
Table 13. Channels selected for the configurations with reduced number of electrodes.....	90
Table 14. Results for PNM index for movements of CA and CB.	91
Table 15. Comparison of previous research with this current work.	98

Abbreviations

AR	Autoregressive model
CA	Category A
CB	Category B
CC	Category C
DFA	Detrended Fluctuation Analysis
EMG	Electromyography
F1	First chirodactyl flexion
F2	Second chirodactyl flexion
F3	Third chirodactyl flexion
F4	Fourth chirodactyl flexion
F5	Fifth chirodactyl flexion
FD	fractals dimensions
GA	Genetics Algorithm
HC	Hand closing
HFD	Higuchi Fractal Dimension
HLC	high-level control
HO	Hand opening
IBGE	Brazilian Institute of Geography and Statistics
KNN	K-nearest neighbor
LD	Large diameter
LDA	Local discriminant analysis
LLC	low-level control
LT	Lateral tripod grasp
MAV	Mean absolute value
MAV1	Modified mean absolute Value 1
MAV2	Modified mean absolute Value 2
MDF	Median frequency

MES	Myoelectric signal
MNF	Mean frequency
MNP	Mean power
MuCI	Muscle-computer interface
MW	Medium wrap
PKF	Peak frequency
PNM	Positive-negative measurement
PPI	Post-processing method 1
PP2	Post-processing method 2
PSR	Power spectrum ratio
RBF	Radial basis function
RMS	Root mean square
sEMG	Surface electromyography
SFS	Sequential forward selection
SM	Small diameter
SSC	Slope sign change
SVM	Support vector machine
TP	Tip pinch
TR	Sphere tripod grasp
TTP	Total power
VAR	Variance of sEMG
WL	Waveform length
ZC	Zero crossing

1. Introduction

Amputation is the partial or total removal of a limb due to trauma or elective surgical process, as a consequence of some accident, disease or congenital malformation (PEERDEMAN et al., 2011). An amputation is considered as a reconstructive process of an extremity with full or limited function, and can be classified into three types: congenital, traumatic or vascular (CARVALHO, 2003). In Brazil, the number of people who evolve to amputation of upper limbs is significant. Over the age of 18, an important cause of amputation becomes the work-related accident. In young adults, due to increased exposure to risks, traumas related to traffic and work accidents, gunshot wounds, and burns are major causes of upper limb amputation.

In Brazil, according to the Brazilian Institute of Geography and Statistics (IBGE), in the Census of 2010, 7% of the population has a motor disability while 1.3% has a physical disability. Moreover, the number of people with disability in Brazil increased from 7.0 million in 2000 to 12.7 million in 2010, which represents 4.2% and 6.7% of the total population, respectively. In relation to people with functional limitations, there was an increment between 2000 and 2010, from 17.2 million (10.1%) to 32.8 million (17.2%). According to the Census 2000, from the group of people with physical disability, 32.8% have lack of a member or part of them, totaling 0.28% of the population. As lack of a member, the Census considered leg, arm, foot, hand and first chirodactyl (IBGE, 2010).

Studies exclusively with amputees are important for the understanding of their particularities, which can help in the design of rehabilitation strategies to achieve a better performance in the execution of more skilled tasks in order to use more modern myoelectric prostheses (ATZORI et al., 2014). Upper limb prostheses offer to users an increased independence in their activities of daily

living to improve the quality of life, making these individuals feel capable of leading a productive life (GOFFI, 2004). There are a variety of prostheses, from purely esthetics to actives prosthetic hands. Myoelectric prostheses use myoelectric signals to generate commands for the control system of the device. Commonly, pattern recognition are used to classify myoelectric signals acquired from a set of hand gestures. However, an ideal prosthesis of this type is still far from current reality, and current hand prostheses often do not satisfactorily restore the ability to hold the first chirodactyl (CARROZZA et al., 2002).

1.1. Motivation

Upper limb prosthetic devices have been constantly evolving, from the old hooks to sophisticated devices with multi-degree of freedom electrically actuated. While old devices are controlled by simple coarse mechanical movements based on the power transmission to the effector, modern devices have finer control based on the user intention (PEERDEMAN et al., 2011).

An ideal upper-limb prosthesis should be recognized as a natural part of the amputee body, supplying motor and sensory functions (ENGLEHART; HUDGINS, 2003). Nevertheless, one of the major problems is the user's acceptance after starting the training process to use prostheses. Some of the common factors of their rejection are the lack of easiness and comfort to use them, their exterior appearance, but most of all, its limited functionality (PEERDEMAN et al., 2011).

An evaluation of the important activities of daily living for users of prosthetic hand was presented by Peerdeman et al. (2011). Opening/closing zipper, making the bed, grasping a glass, holding a ball, and using knife and fork were activities considered as relevant. As a result, grasp tasks were found to be more important than wrist movements, being lateral, cylindrical and tripod grasps the most important one (SENSINGER et al., 2009). Furthermore, the same study

considered that wrist movements, as flexion/extension, and grasp should be taken into account simultaneously. This would avoid non-natural movements with shoulder and elbow. Other study with prosthesis users (ZECCA et al., 2002) reports that 100% of interviewed would like to point the finger, 90% wanted to have individual fingers control and 70% considered useful to have wrist flexion/extension. However, most studies have focused on recognizing power functions and wrist movements, while dexterous movements of prostheses have not been widely addressed, being a lack to improve their functionality. As a result, there is a need for a more functional and reliable control system, and using a minimum number of electrodes.

Advances in the area have been mainly in the development of control strategies often related to pattern recognition of myoelectric signals (MES). The use of MES from residual muscles is one of the current research lines aimed at providing the user with a natural control of the prosthetic device.

Surface electromyography (sEMG) is a common technique used to record electrical activity on the surface of the skin resulting from muscle contraction. Several researchers have used sEMG to control prosthetic devices (OSKOEI; HU, 2007; PONS et al., 2005; SCHULZ et al., 2005). However, systems based on sEMG are currently limited for control basic actions, such as opening and closing the prosthetic hand. There are even more developed prostheses (NAIK; KUMAR, 2012) that open all fingers together simultaneously because it is difficult to characterize myoelectric signals that allow commanding the individual opening of each finger of the hand. The current focus in this area is to find signal processing techniques to allow the identification of different movements, such as opening/closing hand, and finger flexion and extension, in order to control each finger of the hand individually, providing the users a more natural movement of the prosthesis.

For this reason, several researchers in the world have investigated different techniques to control hand and finger movements (ARJUNAN; KUMAR, 2010a; OSKOEI, 2008; PHINYOMARK; PHUKPATTARANONT; LIMSAKUL, 2012a). However, these techniques for classifying MES are unable to accurately identify the actions produced by various active muscles mainly due to the crosstalk problem. This difficulty is even greater when muscle contraction is tiny, which is the case that happens when the muscle is affected by limb amputation. To overcome this problem, some authors have used a great number of electrodes to obtain redundant information from these muscles, in order to identify the actions of each individual finger (TENORE et al., 2009). However, the accuracy is still low.

1.2. State of the art

From the literature, a great variety of methods for feature extraction in time and frequency domains have been explored to recognize MES patterns (ZECCA et al., 2002). Several works have used magnitude-based features to feed classifiers to recognize hand motor tasks involving elbow, forearm, wrist and open/close hand movements (GUO et al., 2015; OSKOEI; HU, 2008; PHINYOMARK; LIMSAKUL; PHUKPATTARANONT, 2009). Other systems have got user's commands for a limited number of hand and individual finger movements (NAIK; KUMAR; ARJUNAN, 2009, 2010; PELEG et al., 2002; TSENOV et al., 2006), and even for combined finger movements (KHUSHABA et al., 2012). However, such attempts did not include dexterous or skillful movements in the hand or fingers. This is mainly because the statistical-based features are not sufficiently reliable due to the weak MES from these movements. Previous works have considered MES from dexterous movements, but only for grasp movements, aiming to improve the functionality of the prosthetic control (CHU; LEE, 2009; HARGROVE et al., 2009; TOMMASI et al., 2013; WANG; CHEN; ZHANG, 2013). In fact, the non-linear relationship between force and electric activity of muscles at low-level of

contractions (NAIK et al., 2010) makes much more difficult the MES analysis. Techniques based on fractals dimensions (FD) have been used to estimate the non-linear properties of MES, which present sensibility at frequency and magnitude to the strength of muscle contraction (Arjunan and Kumar, 2007b). Recently, a combination of Higuchi's fractal dimension (HFD) and detrended fluctuation analysis (DFA) were employed on MES (GUO et al., 2015), in order to have the advantages of features from time and frequency domains.

Another factor that bother the prosthesis users is the high number of electrodes, as the training with many input channels is a long and hard process, resulting in their decision to use only a limited and very simple prosthesis (2-3 degrees of freedom). Moreover, prostheses with electrode array are complex, in addition to the fact that differences in electrode placements lead to variations in the MES and its spectrum (KUMAR; POOSAPADI ARJUNAN; SINGH, 2013a). Some works have sought for systems with low-density (less than six channels) MES (ARJUNAN; KUMAR, 2010b; CASTRO; ARJUNAN; KUMAR, 2015; PHINYOMARK; PHUKPATTARANONT; LIMSAKUL, 2012b), which reduce problems as electrode fixation and computational demand. However, the accuracy reported by these researchers to recognize dexterous movements are still poor and their experiments were only conducted in able-bodied subjects.

Some studies with amputees using few number of electrodes have been conducted in order to fulfil this gap, such as done in (AL-TIMEMY et al., 2013; CIPRIANI et al., 2011; KUMAR; POOSAPADI ARJUNAN; SINGH, 2013b; LI et al., 2011; TENORE et al., 2009). In particular, in (KUMAR; POOSAPADI ARJUNAN; SINGH, 2013b) a method based on wavelet maxima density was proposed as a non-linear parameter to extract relevant information from MES using only one channel, but no grasp movements were considered. Grasp movements were considered in (LI et al. 2011), but using high-density MES (twelve electrodes).

Table 1. Relevant researches for recognition of hand/finger movements using MES.

Authors	Year	Ch	M	Tasks	Features	Feat. Select	Classifier	W/O [ms]	Sub.
Peleg†	2002	2	5	F1-F5	DFT, AR, Bin. Elec. Act.	GA	KNN	1,2	4 C
Englehart	2003	4	4	WF, WE, RD, UD	ZC, SSC, WL, MAV			256/16	12 C
Tsenov †	2006	2	4	F1, F2, F3, HC	MAV,VAR, WL, Norm, ZC, Absolute Max and Min, Max-Min, Med		ANN (MLP, RBF, LVQ)		1 C
Khezri †‡	2007	2	6	HO, HC, FI, TP, WF, WE	MAV, SSC, AR, DWT		Neuro-fuzzy system	200/50	4C
Oskoei and Hu	2008	4	5	Isotonic: HF, HE, Hab, Had, HS	MAV, RMS, WL, VAR, ZCs, SSC, WAMP, MAV1, MAV2, PS, AR2 and AR6, FMN, FMD		SVM, LDA, MLP		11 C
Phinyomark	2009			WF, WE, HC, HO, FP, FS	TD and FD (16)		LDA		3 C
Tenore †	2009	19	12	FFI, FEI, F345	MAV, VAR, WL, WAMP	PCA	MLP	200/25	C 1 A 10 C
Chu and Lee ‡	2009	4	10	WF, WE, radial and ulnar flexion of the wrist, HO,CG, LT,RS	AR4, ZC, WL, SSC, MAV		GMM		7 C
Naik †	2010	2	3	F3, F4, F5	ICA, RMS		ANOVA		C 5 A
Cipriani †	2011	8	7	F1,F2,F345,F2345,T O,TR,LT	MAV		KNN	50/50	C 5 A
Li ‡	2011	12	11	EFE,WF, WE, WP, WS, HO,TP, Power Grip, Tool Grip,RS	MAV, ZC, WL, SSC		LDA		C 8 A 20 C
Phinyomark	2012a	1	2	FP, FS, WF, WE, HO, HC	DFA and TD		LDA		8 C
Khushaba †	2012	2	10	F1-F5, F12, F13, F14, F15, HC	SSC, ZC, WL, HTD, Sample Skewness, AR	LDA	SVM-libsvm and KNN	100	8 C
Phinyomark	2012b	5	8	FP, FS, HO, HC, WE, WF, RD, UD	TD and FD (37)		LDA		20 C
Al-Timemy †	2013	6	12	F1-F5, EI-E5, TA, F12, F234, F1234, RS	TD-AR	PCA OFND A	LDA and SVM		0 C 6 A
Kumar †	2013	1	4	F1, F2, F3, F4, RS	Wavelet Maxima Density (WMD)		T-SVM	300	1 C 1 A 27 C
Tommasi †‡	2013	10	6	TP, LT, TR, PW, PEG, prismatic 4 fingers grasp	MAV		LS-SVM		6 C
Wang ‡	2013	2	8	CG, HG, LT, PT, SG, TR, TP, RS	MAV, VAR, AR4, ZC, MNF, MDF	LDA	LDA	256	4 C
Castro ‡	2015	5	10	TP, TR, HC, HO, RS	PSD-Av		FLD		7 C
Guo	2015	6	8	EFE, FP, FS, WF, WE, Wab, Wad	WP, DFA and Muscle Models		SVM and ANN		

†, works including finger movements; ‡, works including grasp gestures; Ch, number of channels; G, number of gestures; W/O, window length/overlapping; C, control group; A, amputee; F1-F5, flexion of finger 1 to finger 5 and combinations; EI-E5, extension of finger 1 to finger 5; WF= wrist flexion; WE, wrist extension; RD, radial deviation; UD, ulnar deviation; HC, hand close; HO, Hand

open; HF, hand flexion; HE, hand extension; Hab, hand abduction; Had, hand adduction; HS, hand straight; FP, forearm pronation; FS, forearm supination; FF= finger flexion individually; FE, finger extension individually; RS, rest state; TO, thumb opposition; TP, tip pinch; LT, lateral grasp; CG, cylindrical grasp; TR, tripod; EFE, elbow flexion and extension; WP, wrist pronation; WS, wrist supination; TA, thumb abduction; PW, power grasp; PEG, parallel extension grasp; HG, hook grasp; PT= point; SG= spherical grasp; Wab, wrist abduction; Wad, wrist adduction; PSAD-Av, Power Spectral Density Average; DFT, discrete Fourier transform; DWT, discrete wavelet transform; WAMP, amplitude Willison; ICA, independent component analysis; HTD, Hjorth Time Domain; PCA, principal component analysis; OFNDA, orthogonal fuzzy neighborhood discriminant analysis; ANN, artificial neural network; MLP, multilayer perceptron; LVQ, learning vector quantization; RBF, radial basis function; TSVM, twin support vector machine; LS-SVM, least-squares support vector machines; FLD, Fisher's linear discriminant; GMM, Gaussian mixture model; ANOVA, analysis of variance.

Nevertheless, in all these previous works conducted with amputees, a common lack of experiments with hand and individual finger movements can be noticed, and few of these works have even included dexterous movements, and only for high-density. In fact, for our knowledge no studies with low-density for dexterous movements on amputees were found in literature. Table 1 shows very complete details about each one of these works, which are classified according to the year of the research, number of channels, number of movements, kind of tasks, signal features, classifiers, window length for MES analysis and duration of the overlapping window.

However, amputees have to learn muscle contractions to produce specific and repeated patterns to control the prosthesis functions, which is called “motor learning”. Motor learning can be understood as a set of processes associated with the practice and repetition of actions that lead to permanent alterations in the motion performance over time (BOUWSEMA; VAN DER SLUIS; BONGERS, 2014).

Several factors are taken into account both in the motor learning and acquisition of abilities during the training with an upper-limb prosthesis, as verbal instructions, characteristics and variability of practice, active participation and motivation of the user, feedback, among others. Some studies have been focused on developing multifunctional upper limb prosthesis combined to training

environments to provides biofeedback (CUNHA, 2002). However, a methodology to assess the amputees' abilities to control a prosthesis is a lack in the literature (BOUWSEMA; VAN DER SLUIS; BONGERS, 2014).

1.3. Problem Statement

1.3.1. Problem definition

The approval of prostheses by amputees is an important aspect, which could be overcome by improving the functionality of the current prosthetic hands. The level of dexterity of a prosthesis is an important factor contributing to its functionality, as it is related to the ability to perform skilled movements that resemble as much as possible the activities of daily living. The level of dexterity of prosthesis is related to the ability to perform more skilled movements that provide functions for the amputee, which are similar to the activities of daily living. However, few available studies cover the recognition of dexterous hand/fingers movements. Moreover, in most of cases, these dexterous movements are reduced and combined with other tasks with a poor contribution to the functionality. Furthermore, the study of low-density MES from forearm amputees to recognize dexterous movements, without significant modifications of the natural functions during contraction of remnant muscles in the residual limb has not been addressed in the literature.

1.3.2. Research goal

In agreement with the scientific problem, the goal of this thesis is focused on the recognition of the myoelectric pattern of forearm amputees, for control of hand/fingers movements. The method here proposed allows an amputee the ability of exert dexterous hand/fingers movements in a more natural way. To fulfill

this purpose, the processing and pattern recognition of MES is the main action field.

1.3.3. Hypothesis

The main research question of this thesis is derived from the goals:

Is it possible to control dexterous hand/fingers movements of a prosthetic hand by forearm amputees using lower muscle contractions in his residual limb and a reduced number of electrodes?

From the stated scientific problem, the hypothesis formulated in this thesis is: if the pattern recognition combines linear and non-linear features, it is possible to recognize accurately dexterous hand/fingers movements considering low-density MES, from forearm amputees, to control a prosthetic hand in a more natural way.

1.4. Objectives

1.4.1. General objective

Explorer techniques of pattern recognition applied to low-density MES, able to discriminate dexterous hand/fingers movements of forearm amputees, using a reduced number of electrodes in his residual limb.

1.4.2. Specific objectives

- Proposed a muscle-computer interface (MuCI) to recognize patterns of MES of dexterous hand/finger movements

- Analyze the best parameter set of the pattern recognition to obtain a better discrimination of a set of dexterous hand/fingers movements
- Evaluate the proposed pattern recognition method with able-bodied subjects and amputees
- Assess the proposed system on an online pattern recognition system using a virtual environment and a robotic hand, for myoelectric training.

1.5. Thesis contribution

In this research, we propose and evaluate a method to recognize patterns from low-density MES associated with accurate dexterous hand/finger movement intention from forearm amputees, using four electrodes placed in his residual limb, in order to improve the functionality of upper-limb prostheses, more specifically, a hand prosthesis. Individual finger and hand movements are characterized using fractal-based analysis combined with a suitable election of other well-known features on time and frequency domains. The extent of dimension reduction by a feature subset selection is also investigated, through search strategies using sequential and genetic algorithms, considering seventeen features from the MES. In addition, the efficiency of three supervised classifiers is compared as well. From our research, a new system composed of a unique feature set and one classifier is here introduced. Moreover, such system here proposed is validated in online mode. Finally, the study with amputees, including the evaluation of the proposed method in both offline and online execution, the assessment of the movements according their abilities to perform dexterous hand/finger movements, and the analysis toward a single-channel system, are important contributions of this thesis.

In summary, although previous studies have identified different hand and finger movements, a common aspect of most of them is the little inclusion of forearm amputees, which is the focus of our study. In our research, we propose a system to recognize accurate dexterous hand/finger movements from amputees using low-density MES (four electrodes), in order to improve the functionality of upper-limb prostheses.

Hand and individual finger movements are characterized using fractal-based analysis combined with a suitable election of others well-known features on time and frequency domains. The extent of dimension reduction is also investigated, considering seventeen features from the MES, and, in addition, the efficiency of three supervised classifiers is compared as well.

From our research, a new method composed of a unique feature set and one classifier is here introduced, with the aim of obtaining a reliable control, to provide more functionality for forearm amputees in a more natural way to control a multifunctional myoelectric prosthesis.

1.6. Thesis outline

This thesis is organized in seven chapters. The first chapter provides an introduction to the fields of myoelectric prostheses and pattern recognition systems for upper limb amputees. Also, state of art is covered in this chapter. Chapter 2 includes a theoretical background to the understanding of the topics treated in this thesis. This Chapter also presents an overview of the current state of techniques for recognition of dexterous hand gesture recognition. Chapter 3 provides the details of the research methodology, also describing the protocols, materials and participants involved in the experiments. This chapter also explains the techniques used for features extraction, dimension reduction and classification and the steps to be followed in order to develop a successful pattern

recognition system. The results obtained from the experiments and the analysis of the system performance, validated on amputees, are presented in Chapter 4. Chapter 5 discusses the results presented in Chapter 4 and the original contribution of this work, as well as the limitations of this research. Finally, the conclusions of the research are presented and recommendations for future work provided.

2. Theoretical background

2.1. Functional hand movements

The hand and finger movements are highly important for activities of daily living. The immense variability of movements of the hand allows it to be used as a highly specialized instrument that performs very complex manipulations in daily life, requiring multiple levels of force and precision (NEUMANN, 2011). For all this freedom of movement, the hand has twenty-seven bones and uses innumerable intrinsic and extrinsic muscles (NORKIN; LEVANGIE, 2001). The wrist and hand can perform both precision and power movements, due to the number of joints controlled by numerous muscles. The forearm, wrist and hand joints do not act in isolation but as functional groups, as the position of a joint influences the position and action of other joints.

Considering the function of the hand, it is verified that each finger has an individual and specific functional value, and this value of each finger depends on its strength, mobility and relations with the other fingers, especially with the first chirodactyl (TUBIANA; THOMINE; MACKIN, 1996). The five fingers can be divided into three parts, according to importance:

- The first chirodactyl, emphasizing its preponderant role due to its ability to oppose the other fingers;
- The area of the tweezers, which includes the third chirodactyl and, above all, the second chirodactyl, which is indispensable for the formation of tip pinch, (first / second chirodactyls), or tripod grasp (first / second / third chirodactyls);

- The area of the grips, with the annular and minimum fingers, which are indispensable to guarantee the firmness of the grip, with the whole palm or even the grip (KAPANDJI, 2007).

According to the grasp taxonomy of human grasp types established in (FEIX et al., 2015), grasps can be classified into power, intermediate and precision grasp. In the power grip, all movements of the object have to be evoked by the arm. In the precision handling, the hand is able to perform intrinsic movements on the object without the arm movement. Finally, in the intermediate or link grasp, elements of power and precision grasps are present in roughly. Napier, in 1956, defined that power grip is used when full strength is required, as in activities that generate the action of fingers and first chirodactyl against the palm of the hand, for the purpose of transmitting force to an object. In precision gripping, the object is clamped between the flexor surfaces of one or more fingers with the opposing first chirodactyl, being used when necessary accuracy and refinement of touch (MOREIRA, ALVAREZ, 2002).

In particular, the hand wrap grasp, referred as a power grip, uses almost exclusively flexors to bring the fingers around the object and hold the claw. This is performed between the palmar surfaces of the hand and fingers, and is used to hold cylindrical objects like a glass, and the larger the diameter of the object, the lower the grip strength. According to (FEIX et al., 2015), it can be split into three similar grasps: large (LD) and small diameter (SD), and medium wrap (MW). Its differences are related basically to the size and weight of the object to be clamped.

In relation to intermediate grasp, lateral (LT) or side tweezers are considered. The area of contact is between the lateral surface of the fingers and the pulp of the first chirodactyl, or between two fingers. It is used in activities such as holding an object between the fingers as a credit card or triggering a key. It is considered the strongest of the three tweezers.

However, the precision gripper is the most important and most specialized hand function. Two different kind of precision gripping can be considered:

- Tip-pinch: this is done with the fingertips, and the contact area is restricted to the distal end of the digital pulp. This clamp is used to pick up very small objects, such as a needle, being the most delicate and accurate of the tweezers.
- Tripod grasp, three-dimensional tweezers or palmar: are carried out between the pulps of the first chirodactyl, second and third fingers. They are used in about 60% of activities of daily living, such as picking up a pen or to grasp small round subjects, like a tennis ball, and are an intermediate force tweezer (PARDINI JR., 2006; MAGGE, 2010, FERREIRA et al., 2011, KAPANDJI, 2007).

2.2. Brief approach to the physiology of muscle contraction

Skeletal muscles are composed of muscle fibers which are organized into bundles, called fascicles. The myofilaments comprehend myofibrils, grouped together to form as muscle fibers. A muscle contraction occurs from the stimulation to the execution. Initially, an action potential travels via a long nerve motor to its ends in the muscle fibers.

The largest and most frequent source of force generated within the human body is the contraction of muscles. Additional passive forces occur by the tension of fascia, ligaments and non-contractile structures of muscles. Usually, muscles never contract in isolation, instead, several muscles contribute to produce a desired force.

2.2.1. Types of muscle contraction

Muscle contractions are controlled by the central nervous system (CNS). The brain signals travel through the nerves in the form of action potentials, to motor neurons that innervate one or more muscle fibers (CARLSEN; PRIGGE; PETERSON, 2014). Several types of muscle contractions are defined by changes in the length of the muscle during contractions. Muscle contractions can be divided into: Isotonic (meaning same tension), Isometric (meaning same distance or not moving) and Isokinetic (meaning same speed).

2.2.1.1. Isometric Contraction

When a muscle is contracted with a constant force, the contraction is called "isometric". Isometric contractions are often referred to as static or sustained contractions, and are usually used for posture maintenance. Functionally, these contractions stabilize joints, e.g., to reach forward with the hand, the scapula needs to be stabilized against the thorax. The MES recorded during isometric constant force contractions (steady-state) can be considered as a stationary stochastic process, at least for time intervals short enough to exclude fatigue, with Gaussian amplitude distribution and zero mean (BASMAJIAN, 1978; MERLETTI; PARKER, 2004).

This thesis is focused on isometric contraction (steady-state MES) for the representation of the pattern recognition system here proposed. Isometric muscle contractions can be either concentric or eccentric.

2.2.1.2. Concentric Contraction

A shortening of the muscle during contraction is called "concentric contraction" (positive dynamics) or shortening. Examples of such contractions would be the quadriceps muscles when an individual is rising from a chair, or the elbow flexors when an individual is carrying a glass to the mouth. In concentric

contractions the origin and the insertion are approaching, which produces an acceleration of segments of the body, i.e., it accelerates the movement.

2.2.1.3. Eccentric Contraction

When a muscle stretches during contraction, it is called "eccentric contraction" (negative dynamics) or stretching. For example, the quadriceps, when the body is being lowered to sit, or the elbow flexors, when the cup is lowered to the table. In eccentric contractions, the origin and insertion move away, producing the deceleration of the body segments and providing shock absorption (damping) when, e.g., it ends in a jump, or when walking, that is, it stops the movement.

2.3. Electromyography (EMG)

Skeletal muscle consists of several muscle fascicles, formed by cells called muscle fibers (MERLETTI; PARKER, 2004). The muscle consists of parallel axes of muscle fibers. The activation of each muscle fiber is performed by the motor axon that innervates the nerve fiber. According to the position and function of the muscle, the number of muscle fibers innervated by the same axon can range from one to over 1000 (MERLETTI; PARKER, 2004). The group formed by the motor nerve cell of the spine, the axon and the muscle fibers that it innervates, represents the motor unit of the muscular system. When a motor neuron sends an action potential, all the muscle fibers of its motor unit are stimulated. However, in the stimulation process, small delays occur between contractions. The result of the algebraic sum of the n-fiber action potentials is called the motor unit action potential (MUAP) (KONRAD, 2006).

The duration of a MUAP is approximately 2 to 10 ms (KONRAD, 2006). Due to the short duration of a MUAP, the action potentials of the motor units must be

repeated so that a muscle contraction can be generated for longer periods. The sequence of the MUAPs is called the motor unit action potential train (MUAPT). The MES is the sum of the MUAPT of the motor units captured by the detection electrode. Due to the differences between the MUAP, the variations in the firing rate of neurons and the fact that a contraction may include several muscles, the MES has been described as a stochastic process (KONRAD, 2006; MERLETTI; PARKER, 2004).

The MES presents frequency components from 0 to 500 Hz, with the most power located between 10 and 250 Hz. Its range of amplitude varies between 10 μ V and 10 mV, according to the type of muscle analyzed, the level of muscle contraction and the location of the electrodes. Electromyography (EMG) can be understood as the collective electric signal from muscles, which is controlled by the nervous system and produced during muscle contraction (CHOWDHURY et al., 2013b).

According the capture method it can be referred to in two types: surface EMG (sEMG), and intramuscular EMG (FARINA; NEGRO, 2012). SEMG is recorded by non-invasive electrodes unlike the intramuscular EMG, which uses invasive electrodes. A surface electrode is able to pick up EMG activity from all the active muscles in its vicinity, while the intramuscular EMG is highly sensitive, with only minimal crosstalk from adjacent muscles. The non-invasive methods are preferably used to obtain information about the time or intensity of superficial muscle activation (FARINA; NEGRO, 2012).

In addition, surface electrodes are easy to manipulate because of their non-invasive condition. However, they have the disadvantage of registering signals in large areas and in some unnecessary and redundant way. Thus, a trade-off between combine convenience and accuracy is commonly based on the scope and limitations of the problem to the electrode selection. In this thesis, surface electromyography is used.

The MES is a very complex signal, due to it is influenced by many factors related to the electrophysiology and the recording environment, especially when motion occurs. Its complexity represents a challenge in the applications to control powered prosthetic limbs, which is the case of this research. MES can be used to generate control commands for rehabilitation, such as active prostheses among other devices by an interface with the user. Control systems based on the classification of MES are usually known as myoelectric control systems (CHOWDHURY et al., 2013b).

2.4. Detection of movement intention for myoelectric control systems

In recent years, a new tendency of human-computer interfaces is focused on muscle-computer interfaces (muCI), in which users employ the electric activity from their muscles as an input to some robotic device (for example a robotic hand) while they are executing various tasks. The muscle-computer interaction can be seen as a physical interface that implies a coordinated action and an adaptation between both actors, since an unexpected behavior of one of them could generate undesired results.

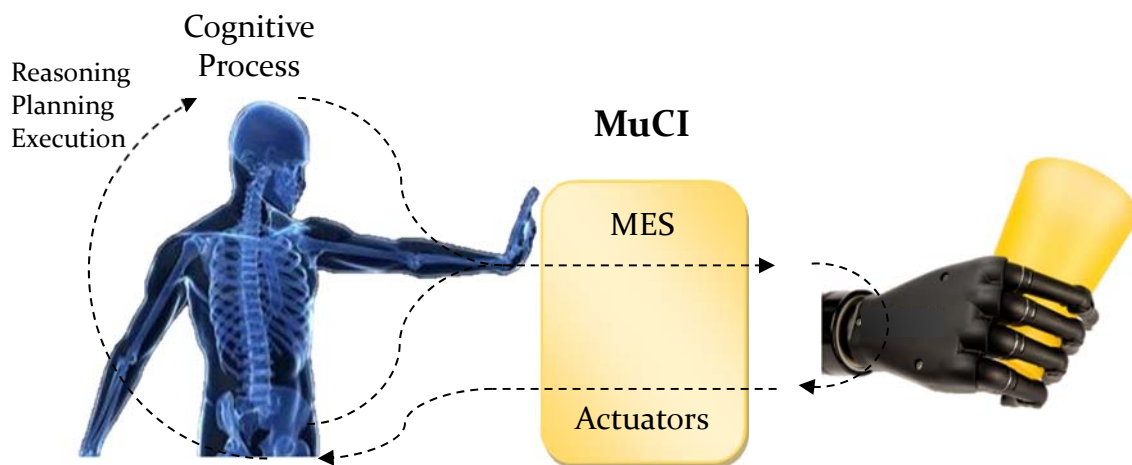
In addition to this physical interface, intelligent sensors, actuators, algorithms and control strategies capable of gathering and decoding complex human movements or physiological phenomena are involved. This interface is designed in order for an artificial system can gather this information to adapt, learn and optimize some body functions, or to generate an answer about a cognitive process that occurs within itself.

A cognitive process is a sequence of tasks that includes reasoning, planning and finally the execution of a previously identified problem or goal, according to the diagram in Figure 1. In the cognitive interaction between the human and the

device, a link is established where the information on cognitive processes is acquired and transmitted in a bidirectional way. These kinds of interactions are evident in applications where the human requires some robotic assistance for the execution of certain tasks.

Although the different strategies used to control movements are determined by low-level control systems, the device needs to know when to apply them and what task the user wants to perform at a given time.

Figure 1. Scheme of a cognitive process in a muscle-computer interface (muCI). Source: Adapted from (BUENO et al., 2008).

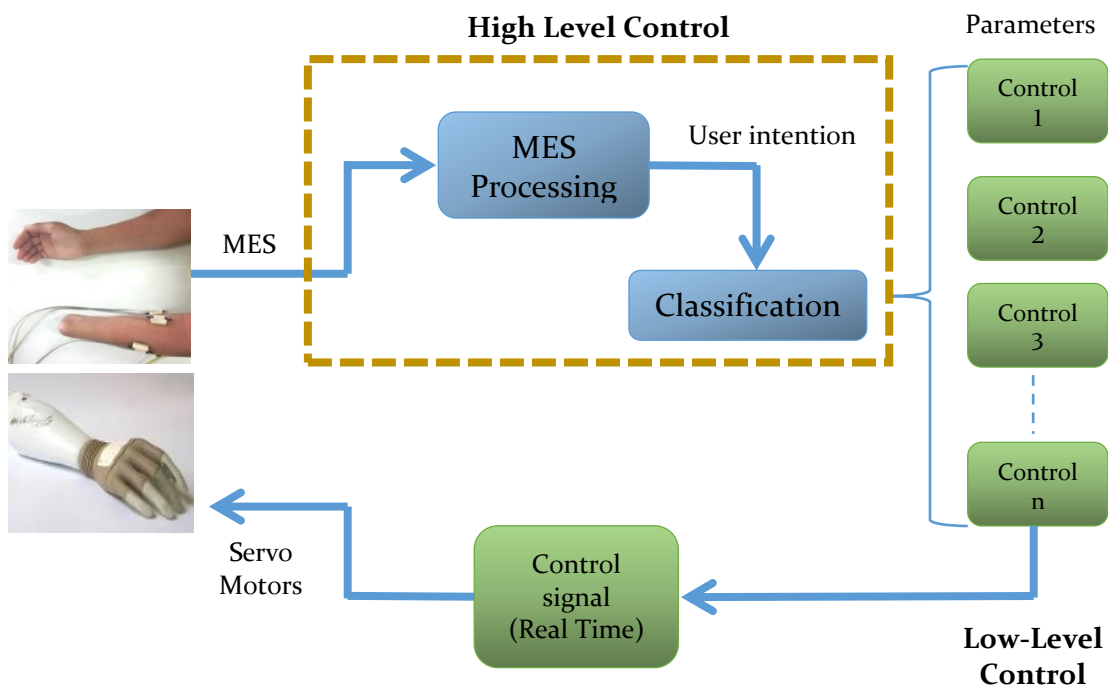


2.4.1. Myoelectric prosthesis control

Myoelectric prosthesis control can be divided into two subsystems: high-level control (HLC) and low-level control (LLC). HLC interprets the subject's intention gathered from patterns extracted from MES, whereas LLC takes the output of the HLC to select a predefined strategy of control angles joint of the prosthesis. HLC includes the MES processing and the pattern classification to detect the user intention. The LLC can be seen as a selector for the control signal of the actuators or servo motors in the prosthesis that executes the movements.

The real challenge for researchers is in the HLC, in which intuitive prosthetic control is one of the most important challenges, in order to reduce the user's learning effort for the prosthesis control. In this aspect, myoelectric control may be considered quite suitable as it allows a more intuitive user interface in a more natural way. However, the still unskillful control, in addition to lack of feedback and training of these prostheses make them unacceptable to several users. The proposal of the HLC for a myoelectric prosthesis control considered in this thesis is shown in Figure 2.

Figure 2. Flowchart outlining a proposal for prosthesis control.



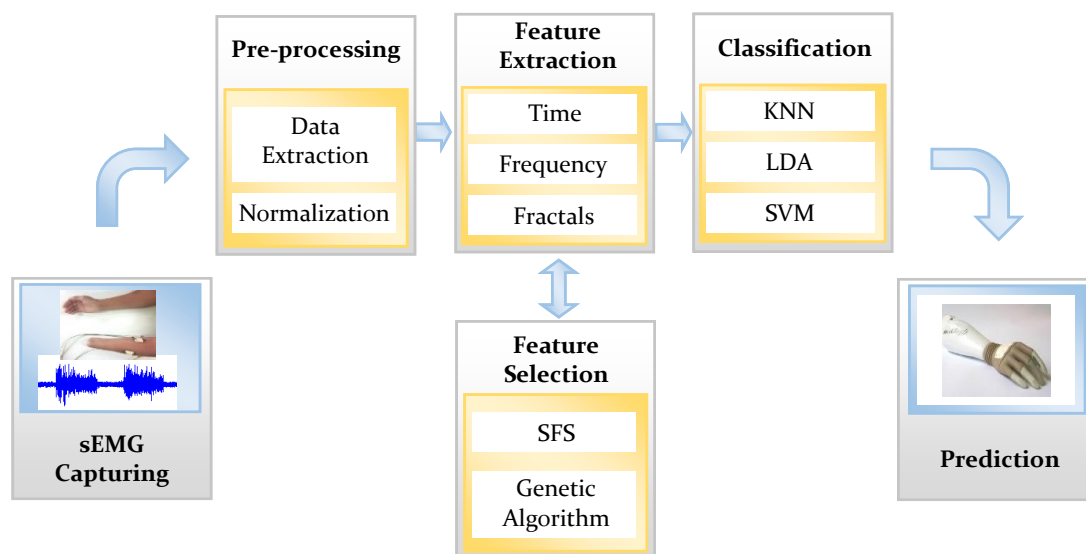
2.4.2. Myoelectric signal processing

The development of applications for detection and identification of signals in real time requires MES analysis techniques, typical of the field of pattern recognition, including signal processing and classification. MES patterns are

represented by a reduced set of features, and their classification is used as a binary action to control a system. In order to solve the defined problem, in this thesis a strategy is here proposed, which is shown in Figure 3. This strategy is composed of the following stages: pre-processing and conditioning of the MES; feature extraction; selection and projection of features; and finally, the classifier. The approach is useful for both offline and online/real-time applications.

In the preprocessing stage, the MES is conditioned by the removal of interferences, in addition to offset and signal data extraction. Subsequently, in the features extraction of the MES, several mathematical methods are used to process the conditioned signal, which are employed to reduce redundant information and extract models in relation to the physiological properties and conditions of the muscles for distinguishing movement patterns. An evaluation of the features is commonly included during training of the machine learning, selecting those with the best performance for discrimination with a better distribution of the feature space. Finally, the classification stage is composed by a machine learning algorithm which associates patterns according to the nature of the executed hand/fingers movements.

Figure 3. General scheme for MES pattern recognition for prosthesis control.



2.4.2.1. Myoelectric signal conditioning

Considering the stochastic and non-stationary nature of the MES, the recommendations proposed by SENIAM (Surface Electromyography for Non-Invasive Assessment of Muscles) (SENIAM, 1996) are taken into account in this study. In addition, digital filters are used to reject interference on the MES. The amplitude of the MES is not constant due to the variation of the impedance between the active muscle fibers and the electrodes (GERDLE et al., 1999). Thus, the rectification and normalization of MES allow its scaling related to the maximum contraction performed by the user, which reduce the variability between subjects and between different samples.

It is widely known that MES can be treated as a stationary process if short time segments between 200 ms and 300 ms are considered. This technique for data extraction leads to generate a stream of MES patterns, in which short data segments are processed using windows, independently. Choosing window width is crucial in implementing online ranking. An overlapping window, or "overlapping", can be applied, which allows an increase of the number of experimental trials, increasing their statistical dependence (MERLETTI; PARKER, 2004).

2.4.3. Feature extraction

The feature extraction stage is one of the most relevant in pattern recognition problems, as is considered as a determinant factor to the success of a pattern recognition system, depending on the quality and optimization of this stage. Presenting the MES directly to a classifier is impractical given the dimension of data. Thus, it is necessary to represent the MES by a vector of reduced dimensions, called the characteristic vector.

Features depend on problem itself, so it is necessary to know the area of interest very well. In the context of the problem addressed in this thesis, the main considerations to be taken into account are: 1) the low levels of muscular contractions for dexterous movements; 2) the low-density signals related to a reduced number of capture channels; 3) the computational cost for real-time applications. Feature extraction can be associated into three different analysis: time domain (TD), (spectrum) frequency domain (FD) and time-frequency domain. The amplitude of MES in TD and some parameters of the power spectrum in FD are commonly used to extract information about the behavior of the MES.

The features in TD do not need to make a signal transformation and are generally faster and easier to calculate. Such features have been very diligent in past decades when the technology developed was not able to perform more complex tasks at reasonable processing times. However, although large-capacity processing systems are currently available, these techniques are still used and provide an efficient distribution of the characteristic space for their discrimination.

The following are the features considered in this research:

Mean Absolute Value (MAV): Provides a maximum likelihood estimate of the amplitude, when a signal is modelled as a Laplacian random process. It is used for low contractions and fatigued muscles analysis (Equation 2.1).

$$MAV = \frac{1}{N} \sum_{n=1}^N |X_n|, \quad 2.1$$

where X_n represents the n^{th} sample of the sEMG signal in a window segment; N denotes the number of sample of the sEMG signal.

Mean Absolute Value modified 1 (MAV1): is a modified version of MAV defined by Equation 2.2:

$$\begin{aligned} \text{MAV1} &= \frac{1}{N} \sum_{n=1}^N |X_n| \\ w_n &= \begin{cases} 1, & \text{if } 0.25N \leq n \leq 0.75N \\ 0.5, & \text{otherwise,} \end{cases} \end{aligned} \quad 2.2$$

where w_n is the continuous weighting window function.

Mean Absolute Value modified 1 (MAV2): is a modified version of MAV defined by Equation 2.3:

$$\begin{aligned} \text{MAV2} &= \frac{1}{N} \sum_{n=1}^N |X_n| \\ w_n &= \begin{cases} 1, & \text{if } 0.25N \leq n \leq 0.75N \\ 4n/N, & \text{if } 0.25N < n \\ 4(1 - n/N), & \text{if } 0.75N > n, \end{cases} \end{aligned} \quad 2.3$$

where w_n is the continuous weighting window function.

Variances (VAR): this parameter is a representation of the EMG signal power, helping to identify onset and contraction (Equation 2.4).

$$\text{VAR} = \frac{1}{N-1} \sum_{n=1}^N X_n^2 \quad 2.4$$

Root Mean Square (RMS): Defined by Equation 2.5:

$$\text{RMS} = \sqrt{\frac{1}{N} \sum_{n=1}^N X_n^2} \quad 2.5$$

Waveform Length (WL): this feature could provide information on the waveform complexity in each segment as indicators for signal amplitude and frequency (Equation 2.6).

$$\text{WL} = \sum_{n=1}^{N-1} |X_{n+1} - X_n| \quad 2.6$$

Zero Crossing (ZC): a simple frequency measure can be obtained by counting the number of times the waveform crosses zero. In order to reduce the noise-induced zero crossing, a threshold must be included. Given two consecutive samples X_n and X_{n+1} , ZC is defined by Equation 2.7:

$$ZC = \sum_{n=1}^{N-1} \left[\text{sgn}(X_n \times X_{n+1}) \bigcap |X_n - X_{n+1}| \geq thld \right] \quad 2.7$$

$$\text{sgn}(x) = \begin{cases} 1, & \text{if } x \geq thld \\ 0, & \text{otherwise} \end{cases},$$

where *thld* denotes a threshold used to avoid low-voltage fluctuations or background noises.

Slop Sign Changes (SSC): frequency measured by counting the number of times the slope of the waveform changes sign (Equation 2.8).

$$SSC = \sum_{n=1}^{N-1} f[(X_n - X_{n-1}) \times (X_n - X_{n+1})] \quad 2.8$$

$$f(x) = \begin{cases} 1, & \text{if } x \geq thld \\ 0, & \text{otherwise} \end{cases}$$

Autoregressive (AR) model: The MES is nonstationary and nonlinear, however, in a short time interval, it can be regarded as a stationary Gaussian process. The MES time series could be modeled as Equation 2.9:

$$x_i = \sum_{p=1}^P a_p x_{i-p} + w_i, \quad 2.9$$

where P is the order of the AR model, a_p are the estimate of the AR coefficients, and w_i is the residual white noise.

In relation to FD, the most common method used to determine the frequency spectrum of MES are the fast and short term Fourier transforms (FFT and SFT, also known as Gabor's transform). These transformation methods assume that MES is stationary, however, MES are non-stationary. To overcome this drawback, several sequential short segments of MES are processed, avoiding this difficulty. Some of the most commons features used in FD are as follow:

Mean Frequency (MNF): Defined by Equation 2.10:

$$MNF = \sum_{j=1}^M f_j P_j / \sum_{j=1}^M P_j, \quad 2.10$$

where P_j is the sEMG power spectrum at the frequency j , M is the length of the sEMG power spectrum.

Median Frequency (MDF): Defined by Equation 2.11:

$$\sum_{j=1}^{MDF} P_j = \sum_{j=MDF}^M P_j = \frac{1}{2} \sum_{j=1}^M P_j \quad 2.11$$

Peak Frequency (PKF): Defined by Equation 2.12:

$$PKF = \max(P_j), \quad j = 1, \dots, M \quad 2.12$$

Mean Power (MNP): Defined by Equation 2.13:

$$MNF = \sum_{j=1}^M P_j / M \quad 2.13$$

Total Power (TTP): Defined by Equation 2.14:

$$TTP = \sum_{j=1}^M P_j \quad 2.14$$

Power Spectrum Ratio (PSR): Defined by Equation 2.15:

$$PSR = \frac{P_0}{P} = \sum_{j=f_0-r}^{f_0+r} P_j / \sum_{j=-\infty}^{\infty} P_j, \quad 2.15$$

where f_0 is a feature value of PKF; r is the integral limit of the ratio ($r = 20$); P_0 is nearby the maximum value of the sEMG power spectrum; P is the whole energy of the sEMG power spectrum in a range of 10 to 500 Hz.

The representation of the time-frequency signal allows to locate the energy of the signal, in time and frequency, making probable a more accurate representation of the physical phenomenon. However, this method generally requires a computationally expensive transformation, such as the SFT, discrete wavelet transform (WT), and wavelet packet decomposition (WPT). This type of transformations applied to non-stationary signals provides a map of spectral characteristics of the signal in time and frequency domain, but with a feature vector of high dimensions, which implies a greater complexity in the learning of the parameters by a classifier. Thus, it is necessary an additional processing to

reduce the data dimension to improve sorting speed and reduce memory requirements without losing classification accuracy.

Moreover, fractal dimension estimates the fractional dimension of the waveform signal in the time domain, which is considered as a geometric figure, quite useful for transient detection. In this aspect, detrended fluctuation analysis (DFA) is one of the most frequently used fractal time-series algorithms, which explores the non-stationary properties of sEMG signals with computational simplicity. DFA is a modified root mean square that provides a self-similarity parameter representing the fractal dimension. This scaling exponent indicates the presence of fractal scaling in a detrended time series of the RMS fluctuation in a succession of random division of the integrated sEMG signal on the time domain (PHINYOMARK; PHUKPATTARANONT; LIMSAKUL, 2012b). DFA offers advantage over methods based on wavelet transformations in the time-scale domain (PHINYOMARK; PHUKPATTARANONT; LIMSAKUL, 2012b). On the other hand, HFD (ESTELLER et al., 2001) is one of the most used fractal dimension feature, as it has shown better performance than other fractal methods (ESTELLER et al., 2001), and has also shown good performance in the classification of EMG signals.

2.4.4. Dimensionality reduction

One of the simplest techniques for reducing data dimensionality is the selection of features, which consists of selecting an appropriate subset of the input data, and discarding the rest. This is possible when there is a strong correlation between the input data sets, so that the same information is repeated several times. For this, it is necessary to define a criterion to determine the best subset and establish a systematic process of analyzing all possible subsets. The ideal criterion for classification should be the minimization of the probability of misclassification, but generally simpler criteria based on class separability are

chosen (ZECCA et al., 2002). One approach is to minimize the probability of classification error, which evaluates the system performance. Other alternative is based on the distribution of features in a clustering scatter. Furthermore, the exhaustive search among all possible subsets is often impractical and other methods can be used.

The commonly used method is the sequential forward selection (SFS), which performs an exhaustive search by an optimization procedure for a high classification accuracy. The method starts with an empty set of features and adds a single feature at each step, with a view of improving the classification accuracy. Since SFS method requires to repeatedly performing the searching procedure for the optimal set of features until obtaining a given number of features, it would take a long computation time to get a relatively optimal subset. Moreover, SFS method must rely on a specific pattern recognition algorithm to obtain the accuracy to execute the selection of the optimal features. Thus, the optimization process would be executed again, in which some parameters of the algorithm would be changed.

Alternatively, a Genetic Algorithms (GA) approach (HUANG; WANG, 2006) for feature selection is used as an alternative to the conventional heuristic methods (THEODORIDIS; KOUTROUMBAS, 2008). GA is a method for solving optimization problems based on some of the process observed in the biological evolution. GA obtains the optimal subset after a series of iterations, being efficient with large search spaces and less chance to get local optimal solution than other algorithms. In addition, a fitness function assesses the mutual information between features and the output like the entropy criteria.

The subsets of features are coded in the form of simple sequences considering the genome of the individuals of a population, as the population changes according to the reproduction of their individuals. For reproduction, operators such as mutation and crosses are applied to the population. The

aptitude of the individuals is represented by the performance of the classification of the corresponding subset of characteristics and determines the possibility of the reproduction. For several generations, the suitability of the population and its individuals are improved. When the criterion is met, a stop is displayed and the feature subset representing the most suitable ones is selected. GAs are optimization strategies that do not assume a continuously differentiable search space. In a population, the subsets of features present are initially covered by random searches (CASTILLO GARCIA, 2015).

2.4.5. Classification

The extracted features must be organized by labels according to the class to which they belong, so they can be associated with the desired movement. A classification system should be able to associate such patterns, overcoming the variations that may arise due to external factors, such as displacement of electrode position, fatigue, sweat, and the intrinsic variability in the nature of the MES. Also, the classifier must be adjusted to meet real-time constraints and efficiency in recognizing new patterns. In this research, we consider supervised learning methods for classification because during training for every input the corresponding target is already known.

2.4.5.1. *K*-nearest neighbors (KNN)

The *K*-nearest neighbors (KNN) is a non-parametric method used for classification. This classifier measures the distance between a trial measured and the *k* closest training samples in the feature space. The trial is classified by the majority vote, being assigned a label with the class of the most common of its nearest neighbor examples. The algorithm commonly uses the Euclidean distance as a metric distance. The number of the *K* neighbors is defined according to the improvement of the classifier performance. A drawback of the majority voting is that the classification depends on the class distribution, and sometimes the

samples of a more frequent class tend to dominate the prediction, resulting in a false positive. Thus, the K value assignment is crucial to define the architecture of the algorithm.

2.4.5.2. Linear discriminant analysis (LDA)

The linear discriminant analysis (LDA) is a parametric method of machine learning, which searches for a linear combination of features to distinguish two or more classes to which the data belong. The objective of the LDA (also known as Fisher Discriminant) is the use of hyperplanes to separate the data representing the different classes (DUDA; HART; STORK, 2001). For a two-class problem, the class of a feature vector depends on its location relative to the hyperplane. LDA assumes normal distribution of data, with a covariance matrix for the equality of both classes. The hyperplane is obtained by finding the projection that maximizes the distance between the mean of the classes and minimizes the interclass variance.

This technique has a very low computational requirement, which makes it suitable for online systems. In addition, this classifier has no parameters to tune, is easy to use and generally delivers good results. The main disadvantage of LDA is its linearity, which can provide poor results with complex and non-linear data. A study conducted by (ZHANG et al., 2013) shows the use of LDA, in an unsupervised adaptation strategy applied to MES pattern recognition, which is based on probability weighting. A variation of this technique uses a quadratic decision surface, which can learn quadratic boundaries with more flexibility. LDA using quadratic discriminant function assumes that the covariance matrix is not identical for each class, then it estimates a matrix by class separately.

2.4.5.3. Support vector machines (SVM)

Support vector machine (SVM) is a learning system for the construction of linear and non-linear classifiers and regression functions. SVM is a non-

parametric technique that explicitly constructs the solution by a linear combination of the training samples. The most salient feature of the SVM is its ability to solve problems where the data is high dimensional, without degrading the solution due to lack of them.

SVM uses a discriminant hyperplane to identify the classes (BURGES et al, 1998; BENNETT et al, 2000), in which the selected hyperplane maximizes the distances between the closest points of the classes. Currently it is possible to train SVM in real-time applications thanks to the improved computing and the development of fast learning algorithms. SVM training builds a model that assigns a new sample to one of two categories, making it a binary linear classifier. For multiclass problem, a common approach consists of decomposing the multiclass problem into several binary sub-problems, building a standard SVM for each class. The most popular strategies are the “*one against all*” and “*one against one*”. The first one builds one SVM per class, training to distinguish a particular class from the other classes. The second one built one SVM for each pair of classes and the result is decided by majority voting. Some studies have reported that “one against one” approach has similar results as the other approach, and it has been stated to be more practical because the training process is quicker.

The effectiveness of SVM depends on the selection of the kernel, the kernel's parameters, and soft margin parameter C (HSU; CHANG; LIN, 2016). A common choice is a Gaussian kernel (also known as radial basis function, RBF), which has a single parameter γ . The best combination of C and γ is often selected by a grid search with growing sequences of C and gamma. The C value in the SVM classifier is a throttling parameter that allows the removal of atypical data and tolerates errors in the training set to avoid misclassifying of training samples. The C value configures the margin separating the hyperplane, such that large values configure small margin to classify all training trials correctly. However, small values configure a larger margin, even getting possible misclassified trial.

2.4.5.4. Repeated k -fold cross-validation

In addition, repeated k -fold cross-validation method with all trials of the experiments is used to assess how accurately the predictive model performs in the offline validation. This method folds all dataset into k subsets, where one subset is used to validate the model while the others are used as a training set. All subsets are crossed so that each one of them has a chance to be used as a validation set. The accuracy is the metric used to measure the overall performance of the classifiers. This process is repeated n times and the average accuracy is calculated.

2.4.6. Post-processing

Post-processing techniques can be used as an attempt to improve classification accuracy. The output vector of the classifier is composed of scores with the probabilities of association of the current pattern with each one of the classes. Before obtaining a class decision, it is convenient to compare these scores to yield a reliable final decision. The class with the higher probability among all others is a common criterium to establish the output classifier. However, it is found that a comparison of this output vector with a level of confidence could improve the classification performance, in order to reject likely false positives by giving a wrong decision.

One method used for post-processing is the comparison between the score vector with a level of agreement, which is based on the metric Kappa (k), that indicates a substantial agreement between the class expected and the predicted decision for k values above 0.6, taking into account the *a priori* probability of a classification system defined in 2.16,

$$P_e = \frac{1}{\text{Number of classes}}, \quad 2.16$$

where P_e denotes the chance agreement of a class to be assigned.

The Kappa coefficient is a parameter proposed by Cohen (JAPKOWICZ and SHAH, 2011), which represents the concordance between the targets and the prediction values. The Kappa's coefficient (k) can be defined by Equation 2.17:

$$k = \frac{P_o - P_e}{1 - P_e}, \quad 2.17$$

where P_o denotes the probably of overall agreement over the class decision and the true class; and P_e denotes the chance of agreement of a class to be assigned. Values of $K < 0$ indicate no agreement; between 0 and 0.20 are considered as slight; between 0.21 and 0.40 as fair; between 0.41 and 0.60 as moderate; between 0.61 and 0.80 as substantial, and finally, between 0.81 and 1 as almost perfect agreement.

Stating a level of agreement $k_1 = 0.6$, then, the minimum probability to obtain a reliable class decision, $P_{o_{min}}$, can be defined by Equation 2.18 using the value of P_o in Equation 2.17, as follow:

$$P_{o_{min}} = k_1 - k_1 * P_e - P_e. \quad 2.18$$

For example, for the eight-class problem of individual finger movements, the minimum probability of a sample to be reliable is 0.65. Finally, the output vector of the classifier is compared with the value obtained by $P_{o_{min}}$, and a class decision is assigned, if and only if, some class gets a higher probability value.

Additionally, a second method for pros-processing uses a defined threshold to compare each one of the class probabilities in the score vector among the others. A class decision can be given, if and only if, a maximum class probability is sufficiently greater than the other ones in the score vector. Considering a multiclass system for 5 movements, the a priori probability for each class is 20%, supposing all class has the same chance of happening, with no difference between each one of classes. For this purpose, it is necessary to define a threshold for difference between two similar classes.

Finally, a simple approach for post-processing seeks to smooth the outcome accuracy using a Majority Vote (MV) (KHUSHABA et al., 2012). This method is intended to combine adjacent outputs in a stream of class decisions to reduce false positives. The MV uses the current decision combined with a defined number of last decisions to obtain the mode as the current output. A ponderation in a modified scheme is used to add weight to the samples in the decision stream, so that the last sample contributes more to the average than the more distant ones. The maximum pondered value among all classes would correspond to the final decision. By trial and error different weight combinations were tested, and it was found the following values to be most appropriated to improve the performance:

Decision n , weight = 4;

Decision $n-1$, weight = 3;

Decision $n-2$, weight = 2;

where n is the actual state of the decision stream, which is intended to avoid the perseverance of past values, rejecting the tendency to prevail past decisions.

The error rate using majority vote scheme is roughly lower than the error with unprocessed stream decisions, and it does not depends on the feature set and window increment (ENGLEHART; HUDGINS; PARKER, 2001). It has also to be taken into account that this scheme can induce errors in the classification performances, especially in the transition regions between hand/fingers movements. For real-time applications, the improvement due to using a majority vote scheme may serve to smooth the stream of class decisions and reduce spurious errors.

2.4.7. Performance measures

The performance measures for a MuCI draw information mainly from the confusion matrix. In order to have a detailed analysis by classes of the classifier performance, a confusion matrix is also calculated to obtain the average accuracy

for all classes. The confusion matrix is generated from results of classification, where information about accuracy and misclassification for each class can be analyzed. This confusion matrix considers the correct classification in the diagonal cells as the positive predictions and the misclassification in the other cells as the negatives.

For multiclass system, the confusion matrix is a square matrix and can be defined by Equation 2.19:

$$C = \left\{ C_{ij} = \sum_{x \in T} [(l = i) \cdot (p = j)] \right\}, \quad 2.19$$

where each element C_{ij} of the confusion matrix denotes the number of examples belonging to a class i label, and the classifier recognizes as a class j . For a test sample, l denotes the corresponding label and p the predicted class.

Specificity (Sp), also known as True Negative Rate (TNR), is the proportion of negative instances (movements) that are detected, defined by the Equation 2.20

$$Sp = \frac{TN}{FP + TN}, \quad 2.20$$

where TN denotes the true negatives, and FP the false positives.

Further, Positive-Negative Measurement index (PNM) takes into account the sensitivity and specificity of the system (CASTRO; ARJUNAN; KUMAR, 2015). This index combines the correct classification of each class, referred as positive, with the misclassification in the prediction, caused by counting false positives instead negatives, as is shown in Equation 2.21.

$$PNM_i = \frac{(C_{ii} - \sum_{j \neq i}^g C_{ij}) + (C_{ii} - \sum_{i \neq j}^g C_{ij})}{\sum_{i,j=1}^g C_{ij} + \sum_{j,i=1}^g C_{ij}}, \quad 2.21$$

where C_{ij} corresponds to the element in row i and column j in the confusion matrix; and g is the total number of classes. The PNM index is used to measure the performance of an individual movement related to how well the movement

was correctly recognized and to how well the same movement was discriminated by other ones. The index ranges from 1, if all predictions are correct, to -1 if all predictions are wrong.

3. Materials and methods

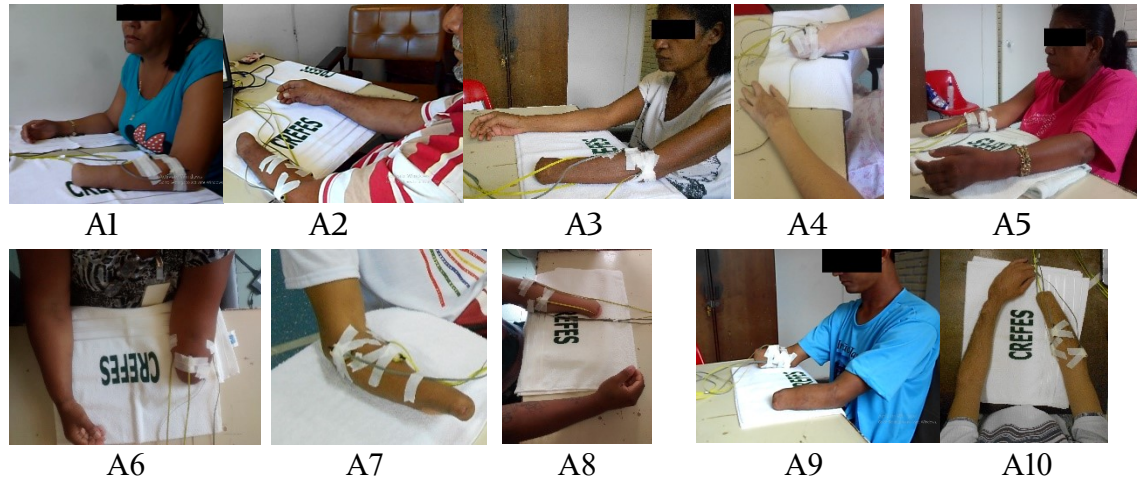
In this chapter, a detailed description about the implementation of the blocks for pre-processing, feature extraction, feature selection and classification, shown in the Figure 3, and the different techniques used is addressed. Moreover, the experimental procedure conducted in this thesis is described.

3.1. Experimental procedure

3.1.1. Subjects

This study was conducted on a control and amputees groups. MES was recorded from the dominant forearm of ten able-bodied subjects (five males and five females), from the control group, aged 22-35 years, with no history of neurological or neuromuscular disorders. Moreover, ten forearm amputee subjects (five females and five males), aged 19-64, participated in this study. All the amputees are outpatients from the *Centro de Reabilitação Física do Espírito Santo* (CREFES/Brazil), which are shown in Figure 4. All amputees have traumatic amputation. The amputees (A) were previously evaluated by a physiotherapist, with an assessment (Appendix B) including aspects as participant identification and physical examination (anamnesis, inspection, palpation, range of motion and sensitivity). All subjects did not have any experience of attending this kind of study before. The inclusion criteria adopted in this research were as follows: (1) transradial or wrist disarticulation amputation; (2) no evidence, in their medical history, of peripheral neuropathy, diseases of the central nervous system or any neurological or muscular disease; (3) no evident abnormal motion restriction; and (4) no earlier experience with myoelectric prosthesis.

Figure 4. Group of amputees who voluntarily participated of the experiments. Details of each one can be seen in Table 2.



All transradial levels (distal, medial or proximal) of amputation were accepted because it is possible to capture MES from the muscle groups selected for this research. All participants were informed about the objectives and methodology of the study, through oral presentation. After knowing the detailed procedures, the participants signed the free consent form, according to the ethical principles of the *Universidade Federal do Espirito Santo (UFES/Brazil)*. The study was approved by the Human Ethics Committee of UFES, conducted in strict adherence to the Declaration of Helsinki (protocol number 302/II, Appendix A). A physical and functional assessment was accomplished for each participant. Baseline sociodemographic and amputee characteristics from all subjects are presented in Table 2.

3.1.2. Equipment and electrode placement

MES data were acquired using reusable bipolar active electrodes (PL091060A - 60Hz) manufactured by Touch Bionics, with inbuilt 60Hz notch filter, pre-amplification and conditioning circuits, with adjustable gain (Figure 5). The MES was sampled (1 kHz) via an NI USB-6009 data acquisition system. The software *Matlab 2014a (The Mathworks, Inc)* running on a laptop battery powered,

with *Windows 10* 64-bits operational system, and an *Intel Core i-7* processor (2.2 GHz) and RAM of 8 GB, was used to process the data. Electrodes were positioned in contact with the unbroken skin in suitable locations to capture the activation of specific muscle groups as detailed below. All three metal pads of the electrodes were correctly attached to the subject's skin by adding conductive gel in order to make good electric contact.

Table 2. Participant demographics. Level of amputation is indicated: wrist disarticulation (WD), Proximal Transradial (PTR), Medial Transradial (MTR) and Distal Transradial (DTR).

Amputee	Gender	Age	Missing Hand	Time since amputation	Prosthesis used	Level of amputation
A1	Female	45	Right	4 years	Esthetic	WD
A2	Male	64	Left	42 years	Esthetic	WD
A3	Female	48	Right	1 year	Non	WD
A4	Female	23	Right	4 years	Non	PTR
A5	Female	48	Right	2 years	Non	WD
A6	Female	50	Left	25 years	Non	PTR ‡
A7	Male	34	Both †	2 years	Non	WD
A8	Male	21	Left	2 years	Non	MTR
A9	Male	27	Both †	1 year	Non	PTR
A10	Male	24	Right	1 year	Non	DTR

† Bilateral amputation, not same level on both sides

‡ Cause of amputation due to poor circulation

Figure 5. Touch bionics electrode for MES acquisition



Some technical specifications of these electrodes are:

- Power Supply: powered by USB port supply via NI USB-6009 DAQ
- Temperature Range: -15°C to 60°C
- Frequency Bandwidth: 90 - 450 Hz
- Sensitivity Range: 2000 – 100,000 fold

Four electrodes were placed on the selected muscle groups of the subject, according to their relation with the functions of the hand/finger movements, as described in Table 3.

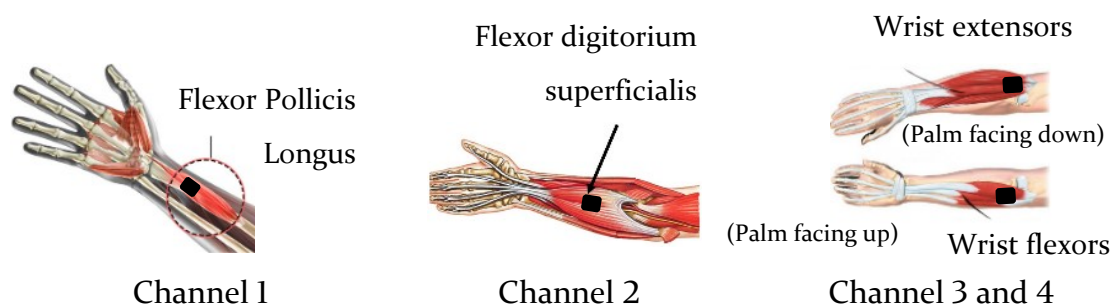
Table 3. Description and functions of muscle groups covered in this study.

Ch	Muscle	Origin	Insertion	Primary functions	Electrode placement
1	Flexor pollicis longus	1/3 of the anterior face of the radius and interosseous membrane	Palmar base of the first chirodactyl Distal Phalanx	Flexes the first chirodactyl interphalangeal and metacarpophalangeal Joints	1/3 of the anterior face of the radius and interosseous membrane
2	Flexor digitorum superficialis	Medial epicondyle of the humerus	Base of the middle phalanx of the 2nd to 5th finger	Flexion of proximal interphalangeal and metacarpophalangeal joints, from 2nd to 5th finger	Ventral face of the forearm, approximately 5 cm distal from the elbow fold
3	1. Flexor carpi radialis	Medial epicondyle of the humerus	Base of 2nd and 3rd metacarpals	Flexion and radial deviation of the wrist	Ventral face of the forearm, approximately 5 cm distal from the elbow fold
	2. Flexor carpi ulnaris	Humeral head and ulnar head	Base of the small metacarpal	Flexion and ulnar deviation of the wrist	
4	1. Extensor carpi radialis longus	Humerus (lateral supracondylar)	Dorsal base of the Index Metacarpal	Extends, radially deviates the Wrist	Center of muscular mass, 5 cm distal of the elbow
	2. Extensor carpi radialis brevis	Humerus (lateral epicondyle)	Dorsal base of the Middle Metacarpal	Extends and radially deviates the Wrist	
	3. Extensor carpi ulnaris	Distal humerus	dorsal base of the Small Metacarpal	Extension and ulnar deviation of the Wrist	

The electrode placement procedure was the same for able-bodied subjects and amputees. All the electrodes were placed according to SENIAM recommendations (HERMENS et al., 2000). Prior to place the electrodes on the forearm, the skin was previously cleaned with 70% alcohol, and conductive gel was used before attaching the electrodes, in order to reduce skin impedance. The same experimental conditions were maintained to guarantee the repeatability of experiments across different days. A temperature of 24 °C was conditioned to avoid the presence of sweat. A minimal inter-electrode distance on the forearm of 2 cm was ensured for all subjects. To find the best location for positioning the electrodes, a graphical representation of the patient's MES was provided. Three near points around each specific muscle area were tested to identify the more suitable point with the strongest signal.

The selected muscles for this research, shown in Figure 6, are associated to the first chirodactyl flexion (channel 1), fingers flexions (channel 2), wrist flexion (channel 3) and wrist extension (channel 4).

Figure 6. Forearm muscles by channel adopted in the experimental protocol. Source: adapted from ANATOMY OF THE HAND (2017)



3.1.3. Experimental protocol

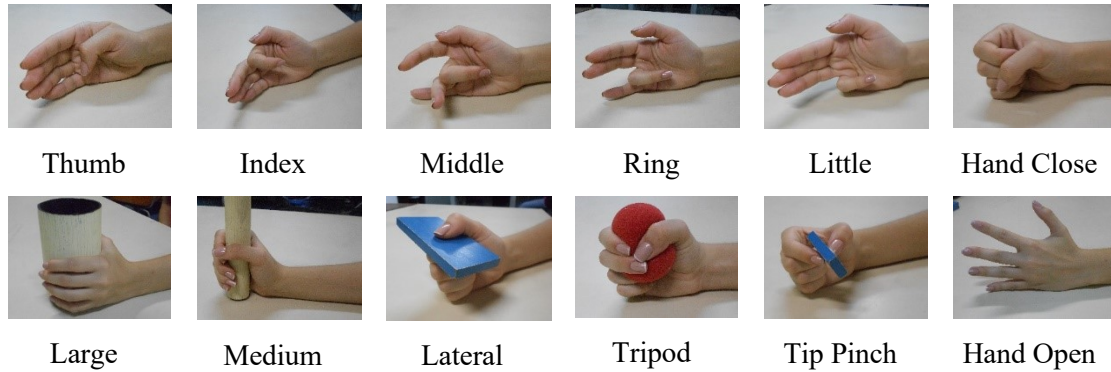
All the subjects (amputees and able-bodied) performed each hand/finger movement, shown in Figure 7, separately. Thirteen movements (described in Table 4) were considered in this study, arranged into three

movement categories: category A (CA) for individual fingers, which includes first chirodactyl flexion (F1), second chirodactyl flexion (F2), third chirodactyl flexion (F3), fourth chirodactyl flexion (F4), fifth chirodactyl flexion (F5), hand closing (HC) and hand opening (HO); category B (CB), for hand grasp, which was arranged within the following taxonomy: into power, intermediate and precision grasps. As power grasps, two kind of full hand wrap grasps were considered: large diameter (LD: diameter = 9 cm, height = 11 cm) and medium wrap (MW: diameter = 5 cm, height = 14 cm). The lateral grasp (LT) was included as intermediated grasp. For the precision grasps, sphere tripod grasp (TR) and tip pinch (TP) were considered. Finally, the category C (CC), which includes all the thirteen movements. The rest state (RT) was included in all categories. The movements, described in Figure 7 were selected because of their importance to the improvement of prosthesis functionality (BOUWSEMA, 2008).

Table 4. Movements performed in the experiments.

Category	No.	Abbreviation	Hand/fingers movements	
-	0	RT	Resting	
CA	1	F1	First chirodactyl flexion	
	2	F2	Second chirodactyl flexion	
	3	F3	Third chirodactyl flexion	
	4	F4	Fourth chirodactyl flexion	
	5	F5	Fifth chirodactyl flexion	
	6	HC	Hand closing	
	7	HO	Hand opening	
CB	8	LD	Large diameter	Dim = 9 cm
	9	MW	Medium wrap	Dim = 5 cm
	10	LT	Lateral tripod grasp	
	11	TR	Sphere tripod grasp	
	12	TP	Tip pinch	
CC	-	-	All movements	

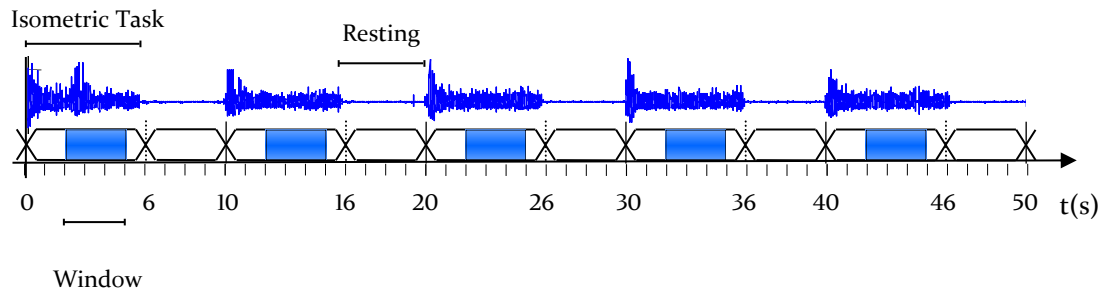
Figure 7. Different kinds of hand and individual finger movements considered in this study (rest state picture is not included).



For the experiments, a preliminary assessment (day 0) and three experimental sessions in different days (days 1-3) were conducted. Prior to the recording, the subjects were encouraged to familiarize themselves with the experimental protocol. They were seated in a chair with both arms resting on a table. During the familiarization stage, it was given a time to they imagine the movement performance with the missing limb, at the bilateral action training modality. The amputee subjects were asked to produce muscle contractions while they imagined specific movements with their phantom stump. At the same time, they performed a mirrored bilateral movement with the intact limb to facilitate the contraction of the affected side.

Afterwards, during the experiments, the subjects were instructed by both visual and oral cues to elicit a contraction from the rest state and hold that task for 6 s, followed by a background activity (rest state) of 4 s, switching between isometric contraction and relaxation. Each hand gesture was repeated five times consecutively, as shown in Figure 8, with a resting period of 3 minutes between each movement, in order to avoid fatigue. Each performed repetition and background period are referred to in this thesis as “trial”. Within each trial, the contraction period was split roughly into a phase of onset and a subsequent steady-state (isometric) phase. Moreover, to enhance generalization ability due to the fluctuation of MES, the experiments were repeated on three different days, referred to herein as sessions.

Figure 8. Experimental protocol to extract the isometric task.

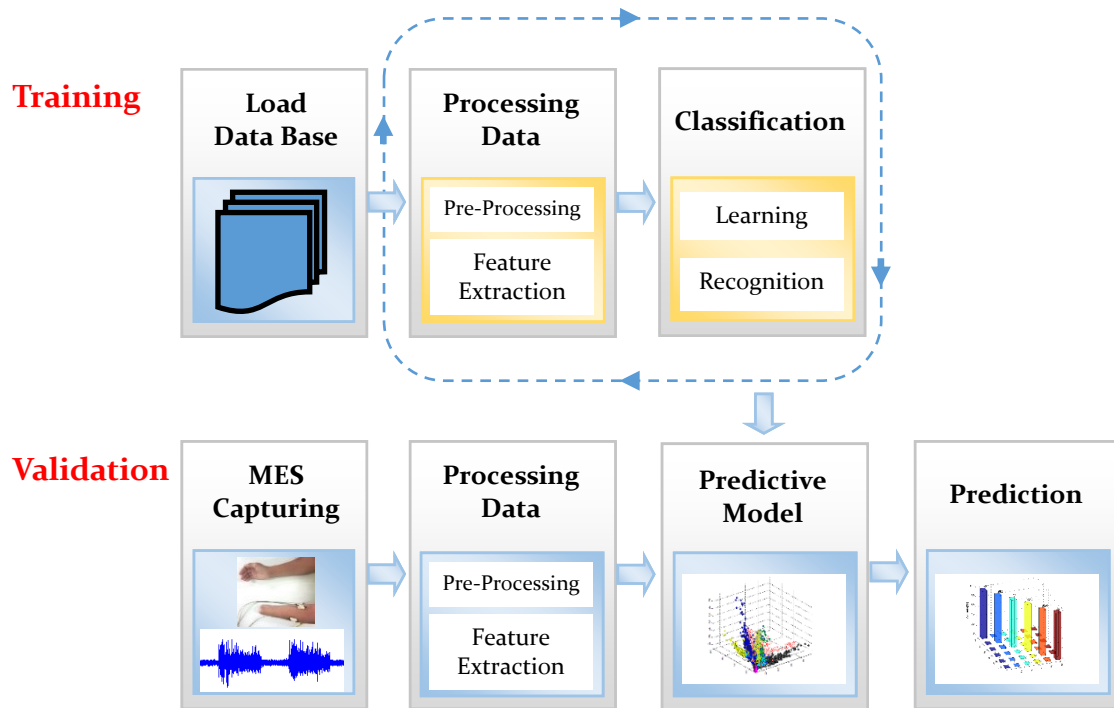


3.2. Method for recognition of dexterous hand/fingers movements

The muscle-computer interface (muCI) proposed in this thesis is composed of MES pattern recognition, such as that described in the diagram shown in Figure 9.

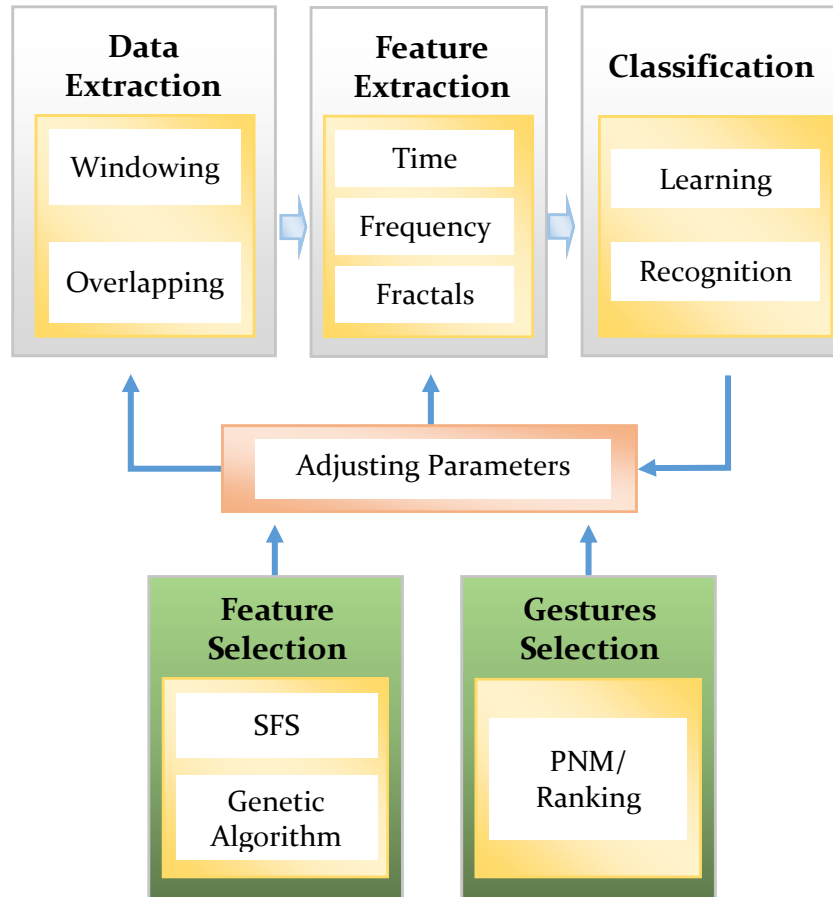
The system can be divided, according to the recognition stages, into two subsystems: training and validation. The first one is intended to define a predictive model, which is trained by a supervised learning machine through loading of a data base of processed MES patterns with known movement. This processing is performed in offline mode. Furthermore, the predictive model is used in the validation subsystem to predict new MES patterns and recognize the movement originated from this signal. This recognition originated from the user's intention is taken as a control command for the prosthesis. This processing is performed in online mode. Both subsystem include a processing data stage, in which pre-processing and feature extraction are performed. In the online mode, MES capturing and data processing are accomplished using two threads concurrently. The data processing is performed for a short segment of signal captured previously while a new segment is captured simultaneously. The *Data Acquisition System Toolbox* of *Matlab* was used to accomplish this stage of research.

Figure 9. General scheme for MES pattern recognition.



Processing data and supervised learning block shown in Figure 9 are widely detailed in the Figure 10. The data processing block can be divided into data extraction, feature extraction and classification stages. Moreover, two adjacent blocks (feature selection and gesture selection) can be noted, which are used in order to find the best parameters during system design with the aim to improve the performance. The first one is intended to obtain a subset of features by the selection of the best parameter to characterize the myoelectric patterns. The second one is used to assess the suitable movements for each voluntary according to its abilities to performed the contractions and generate different patterns. Both are blocks executed just at the designing phase of the recognition system.

Figure 10. Diagram of the techniques used for the design of the MES pattern recognition.



3.2.1. Data extraction and data windowing

All the raw MES are preprocessed for conditioning and to remove unwanted DC level. It is not necessary to use digital filters due to the analog Notch filters embedded in the active electrodes circuits. Due to the zero average of the signal, the rectification is intended to obtain only positive values preserving all the information from magnitude of muscle contractions. The unwanted DC level is removed subtracting the average of the MES, and, subsequently, a rectification (full wave) is performed. The MES is not normalized due to the analysis is performed for each channel individually and not comparison of signal magnitudes is needed between muscles and among voluntaries.

Afterwards, a data extraction stage is carried out, which is determinant for a real-time implementation of the myoelectric control. As stated by Englehart and Hudgins (2003), using transient MES for control has some obstacles, as the requirement of initiating a movement from the rest-state in order to produce a single command, which makes continuous control of devices cumbersome and slow (SHENOY et al., 2008). This makes awkward and slow the continuous control. Thus, in this research steady-state signals are considered for the learning patterns during offline experiments. However, continuous MES (both transient and steady-state) are considered for online classification.

The onset and offset of the muscle contraction is identified by the cues given to the subject during experiments. This process is made manually because of the low amplitude of the background activity, which is similar to the isometric activity itself and noise magnitude. The steady-state MES (isometric task) is extracted from each trial, and the transient stages (i.e. during movement changes) are removed. The data from the two first seconds and last second of the 6-second trial are removed from all observation to extract only the steady-state of the isometric contraction of each trial. In this sense, three seconds from each trial are used to be processed. This time is enough to ensure that the subject starts the movement, the transient is performed and the steady-state is achieved.

Before feature extraction stage, the MES are windowed, and from each window a control command is conveyed. It is important to note that the window length (denoted here as M) for recording and the window increment or overlapping (denoted here as N) have influence in the characterization of patterns and the classifier's performance. The maximum delay possible for data processing is limited by the N value, while the required memory to store the data to be processed is defined by M value. It is worth to mention that an evaluation of the effects of the window length and window increment on the classification accuracy for all subjects is also performed in this research. The window length is varied for

M = 100, 200, 300, 400 and 500 ms, while the overlapping was varied for N = 20, 40, 60, 80 and 100 ms.

It is actually expected that a larger window improves the accuracy, but increases the response time. However, a very short overlapping reduces the effects of the delay, increasing the computational cost. The minimum and maximum values for both parameters are defined to agree with the real-time constraint required by human being for detection of user intention using MES, whose response time should be less than 300 ms, in order to not introduce a perceivable delay by the user (ENGLEHART; HUDGINS, 2003).

3.2.2. Feature extraction

Seventeen features detailed before in the second chapter are considered in this study, which are based on time domain (TD), frequency domain (FD) and non-linear analysis related to Fractals, as shown in Table 5. Each feature was normalized individually based on the average and standard deviation values. For each data window, the features extracted from all channels are concatenated, which yield a twenty-dimensional feature vector per channel. It is important to remark that each one of the autoregressive (AR) coefficients are here considered as one-dimension feature for each channel.

After the feature extraction stage, a normalization is necessary to reduce the variability of magnitude levels among features. For this, the method based on mean and standard deviation of the data was used, following Equation 3.1.

$$|X| = \frac{X - \bar{x}}{\sigma} \quad 3.1$$

where X is the value of the feature to be normalized, \bar{x} and σ are the mean and standard deviation of the feature vector and $|X|$ is the value normalized, respectively.

Table 5. Features selected for this study, split in groups. The parameters used for some features are also specified.

Domain	Feature	Abbr.	Dim/Ch
Time Domain	Mean absolute value	MAV	1
	Modified mean absolute Value 1	MAV1	1
	Modified mean absolute Value 2	MAV2	1
	Variance	VAR	1
	Root mean square	RMS	1
	Waveform length	WL	1
	Zero crossing	ZC	1
	Slope sign change	SSC	1
Frequency Domain	Autoregressive model	AR	4
	Mean frequency	MNF	1
	Median frequency	MDF	1
	Peak frequency	PKF	1
	Mean power	MNP	1
	Total power	TTP	1
	Power spectrum ratio	PSR	1
Fractal Features	Detrended Fluctuation Analysis	DFA	1
	Higuchi Fractal Dimension	HFD	1

Dim/Ch, dimensions per channel; *thld*, threshold.

3.2.3. Feature selection

It is known that multiple feature sets are more feasible to accomplish a high accuracy for the classifier (ENGLEHART; HUDGINS, 2003). However, despite the analysis of all aforementioned features may provide redundant information, the use of more features will increase also the computation cost. Hence, it is

imperative to use techniques for feature reduction for optimal subsets in a point of view of class separability. Two methods are considered in this study: Sequential Forward Selection (SFS) and Genetic Algorithms (GA). These two methods are chosen to compare the selection of features using traditional solutions and models to solve optimization problems based on machine learning. The SFS method performs the search using the classification accuracy as a criteria for the selection. On the other hand, GA approach is based on the feature space distribution, which minimizes the within-cluster scatter and maximizes the between-cluster separation, such as proposed by (HUANG; WANG, 2006).

Both methods are carried out following two approaches: in the first one, features from the four channels are considered as a whole dataset using all-channel analysis (GA and SFS). In the second approach, features from each channel are selected using an individual-channel analysis (denoted as GA-CH and SFS-CH). All methods were performed by each subject for both control group and amputees, yielding an own feature subset in each case. Data classification was also performed, in order to determine the performance of each method.

3.2.4. Classification

For the experiments, a comparison among different classification techniques was performed to identify the most appropriated classifier for the pattern recognition system here proposed. Linear Discriminant Analysis (LDA), K-Nearest Neighbors (KNN) and multi-class Support Vector Machine (SVM) (one-against-one approach) were the selected classifiers. These classifiers were selected due to their low computational complexity (Chowdhury et al., 2013). Also, they are recommended as robust classifier and have been employed in several studies (CHOWDHURY et al., 2013a; CIPRIANI et al., 2011; GUO et al., 2015; KHUSHABA et al., 2012; OSKOEI, 2008; PHINYOMARK; PHUKPATTARANONT; LIMSAKUL, 2012a; WANG; CHEN; ZHANG, 2013).

For each one of these topologies, tests of different architectures and parameters were performed. K is usually chosen as an odd value for an even number of classes. Also, small K -values lead to a high noise influence on the results and a low generalization capability. For KNN classifier implementation, the K -value was iterated taking odd numbers from 5 to 9. Even values were not considered to avoid score results with two class with the same probability. The LDA does not require parameter adjustment, and a quadratic function was chosen for its implementation.

For SVM, three different kernels were considered: linear, Gaussian (also known as RBF) and polynomial. For the Gaussian kernel, the parameter γ and the regularization parameter, C , were empirically optimized by minimizing the error rate on the validation dataset. The γ parameter for RBF kernel was set for the following values: 0.01, 0.1, 0.5, 1, 2 and 5. In the polynomial kernel, the order have to be set, using polynomials of second, third and fourth order. For all kernels, the C was iterated for: 0.01, 0.1, 1, 2, 5 and 10. These values were defined according to the revision in literature (CHEN et al., 2013; HSU; CHANG; LIN, 2016; LIU, 2015; OSKOEI; HU, 2007). In addition, a repeated k -fold cross-validation is used in the offline validation for $k = 5$ subsets and repeated $n = 3$ times.

3.2.5. Post-processing

Post-processing techniques were used to prevent overwhelming the prosthetic controller with varying classification decisions, in an attempt to improve the classifier performance by eliminating spurious misclassification, as previously done by (ENGLEHART & HUDGINS, 2003). Three methods were tested for post-processing: by comparison using Kappa (k) as a level of agreement; by comparison using a defined threshold among score vector; and finally, by using a pondered majority vote (MV) technique. For the first one, a value of $k \geq 0.6$ was used to ensure a substantial agreement between the decision and the class

expected. For the second method, a threshold of 0.2 was established, which corresponds to a 20% of difference among the selected class and the other classes. For the MV method, the maximum pondered value among all classes would correspond to the final decision. Different weight combinations are tested using the following values to be most appropriated to improve the performance:

Decision n , weight = 4;

Decision $n-1$, weight = 3;

Decision $n-2$, weight = 2;

being n the actual state of the decision stream, which is intended to avoid the perseverance of past values, rejecting the tendency to prevail past decisions.

3.3. Experimental design

The experiments conducted in this thesis can be organized into two specific studies, according to the objective for each one, such as offline and online studies. The offline study is aimed to obtain a predictive model of a MES pattern recognition, validated both on control group and amputees. The online study is considered as a subsequent phase in the validation of the previous results, considering specific conditions for real-time implementations, performing the recognition simultaneously with the movement execution.

In the offline study, the data collected from the first two sessions are used to analyze the structure of an optimal system and finally obtaining a trained classification system. After the feature extraction stage on both control group and amputees, an analysis for feature selection is carried out for each movement category, in order to determinate an optimal feature subset. This optimal feature subset is intended to obtain the best characterization of the MES patterns by extraction of the most relevant information, rejecting redundant information and reducing computational costs. The accuracy of the results is used to establish a

ranking of frequency for each feature, to yield a new feature subset for each method. Finally, an overall method is adopted to recognize patterns related to all aforementioned movement groups.

In the online study, a third session is performed for the validation of the classification system trained with the results of two first sessions with the structure proposed by the offline study. The same protocol used to perform hand/finger movements is followed in the online study, and its performance is also evaluated. To achieve the online application, two concurrent threads are executed to capture and process data, using the proposed data extraction scheme. No visual feedback to the users during the system validation was considered, to assess the repeatability of the patterns in a spontaneous way.

Additionally, two alternative schemes were proposed for training the motor learning and acquisition of abilities to use a myoelectric prosthesis and performing distinguishable muscle patterns associated with individual finger flexion and grasp movements. In the first scheme, a virtual hand designed in a virtual reality environment (VRE) was used. The human movements were adapted to the hand in the VRE, which is controlled by the motion command provided by the pattern recognition system. The second scheme, referred to as a prototype of a robotic hand, can be controlled through a low level control (LLC) system. Figure 11 details the system design for this study.

The predicted commands yielded by the high level control (HLC) system are used as input for the LLC. The LLC system, shown in Figure 12, is composed of a microprocessor, which controls five servomotors that reproduce the flexion and extension of each finger of the robotic hand. In this study, both schemes offer a biofeedback (visual response) to the user about the predicted movement.

Figure 11. Diagram of the system for myoelectric pattern recognition of hand/finger movements, using virtual reality environment and robotic hand.

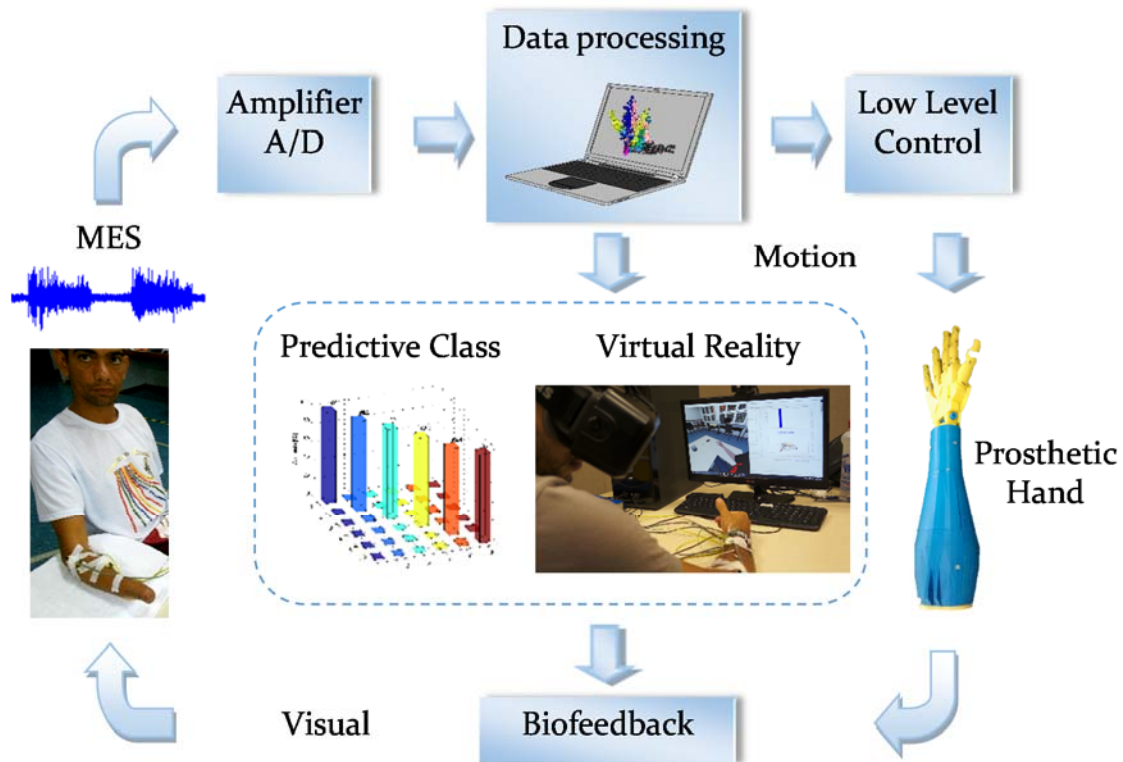
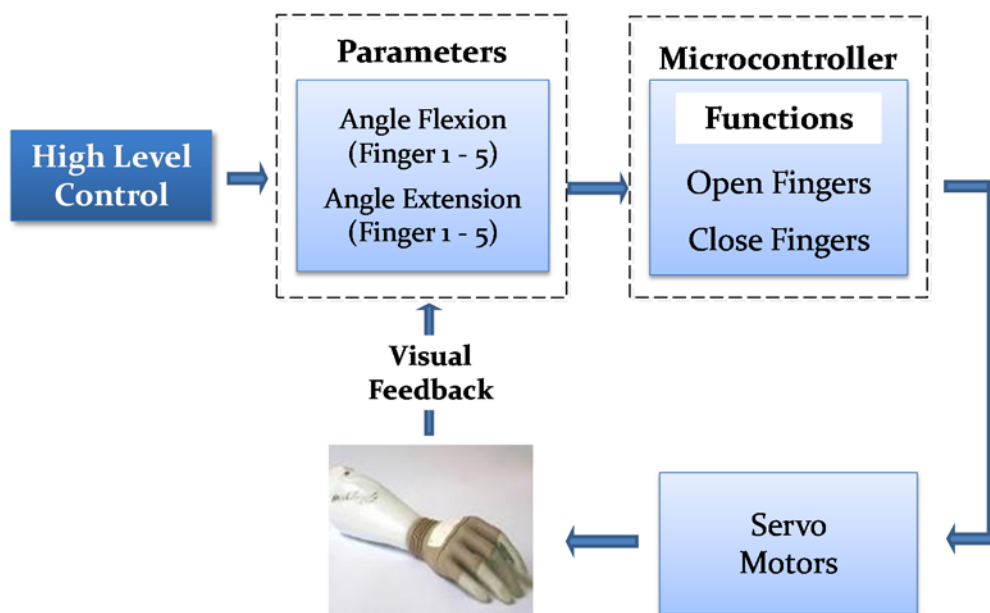


Figure 12. Diagram of the low level control (LLC) of the robotic hand for real time validation.



Finally, the results obtained in the online study were used to carry out two analyses, after the experiments. The first one is intended to develop a system towards a MES single-channel recognition system, in which the information provided from each one of the muscle contractions is assessed. The second one is an analysis for the selection of a suitability set of movements, according to the abilities of the amputees. The accuracy is used to compare the extent of discrimination of the movements. This analysis was carried out independently for movements of categories CA and CB. The positive-negative performance (PNM) measurement index (CASTRO; ARJUNAN; KUMAR, 2015) is then used to measure the performance (recognition/discrimination) of the movement in relation to the other ones. This index is compared for all subjects, while average and variance are considered to compare the easiness to exert specific contractions for determined movement and to maintain constant patterns and separated among the movements proposed in this study.

3.4. Statistical evaluation

Accuracy (Acc), mean percentage error (MPE), specificity (Sp), Kappa's coefficient (k) and positive-negative measurement (PNM) are used to evaluate the performance of each classifier. For the analysis of the results obtained in this research, and taking into account the low number of observations and their unknown distribution, non-parametric approaches were used, which are strongly suggested in the literature (CIPRIANI et al., 2011) due to not require the assumption of normality. Statistical differences among experimental results were also evaluated, firstly using the Wilcoxon rank-sum test to compare two groups with unpaired data, and the Friedman test for simultaneous comparison of more than two groups. Post hoc pairwise comparisons using Wilcoxon rank-sum test with a Bonferroni correction factor were also conducted, in which a level of $p < 0.05$ was selected as the threshold for statistical significance. The outcome of

these tests were interpreted in this research to establish if there was a statistically significant difference in accuracy for each category of movements between different subjects.

4. Results

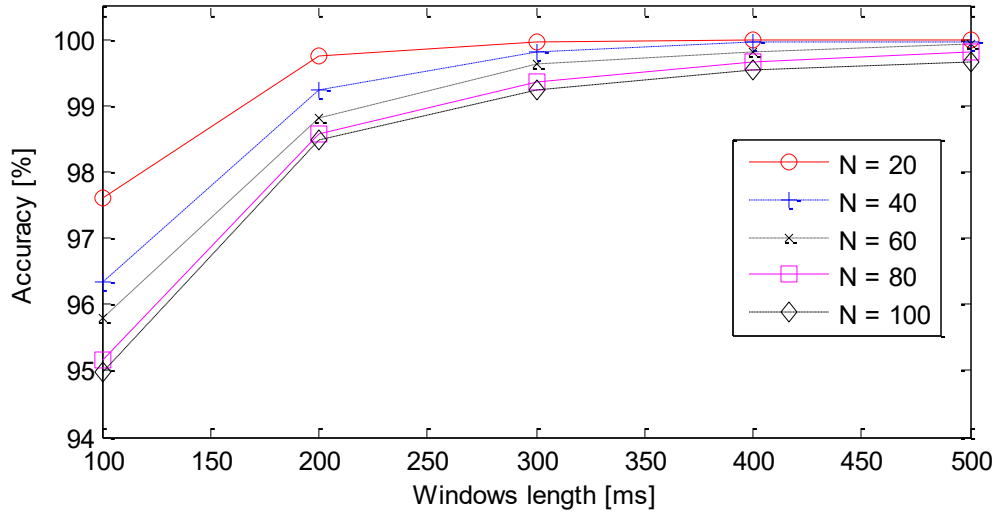
4.1. Offline study results

4.1.1. Data extraction

In the first part of the experiments, the effects of the window length and its overlapping were evaluated. The windowed data evaluation was performed to compare the classification accuracy using all the features included in this research. The window length (M) was varied for $M = 100, 200, 300, 400$ and 500 ms, while the window increment or overlapping (N) was varied for $N = 20, 40, 60, 80$ and 100 ms.

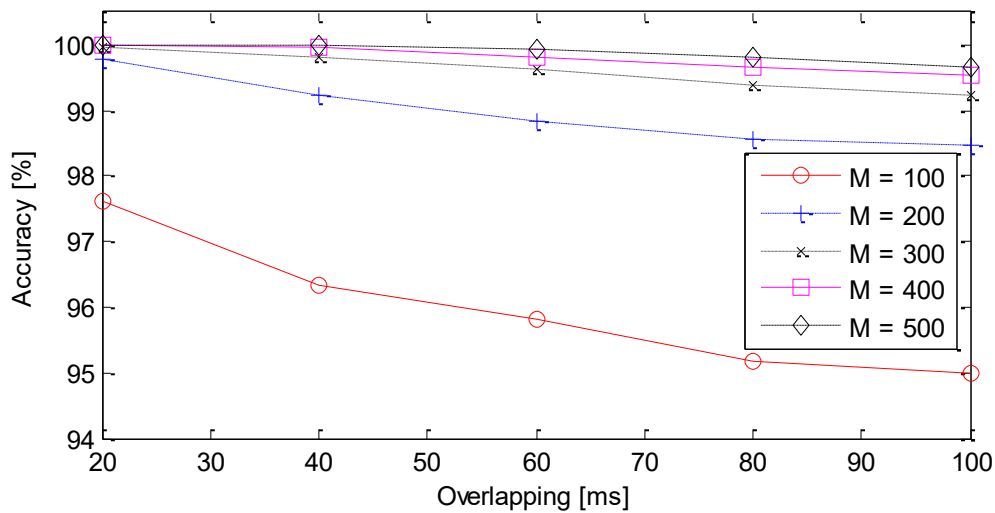
Results of the experiments with amputees, varying the window length (described in Figure 13), showed a direct correlation between the classification accuracy and size of the window length: the more length of the window the more accuracy, such as expected. Figure 13 shows the average accuracy for all amputees, for different lengths, iterating overlapping from $N = 20$ up to 100 ms, with increments of $N = 20$ ms. It can be noted that the accuracy was above 98% for $M = 200$ ms onwards, being $M = 500$ ms the value with best performance achieved. The classification accuracy at values of $M = 300, 400$ and 500 ms was found to be closely the same. Moreover, the accuracy was found to be improved with the reduction of N .

Figure 13. Effect of varying the length of the window for individual fingers movements.



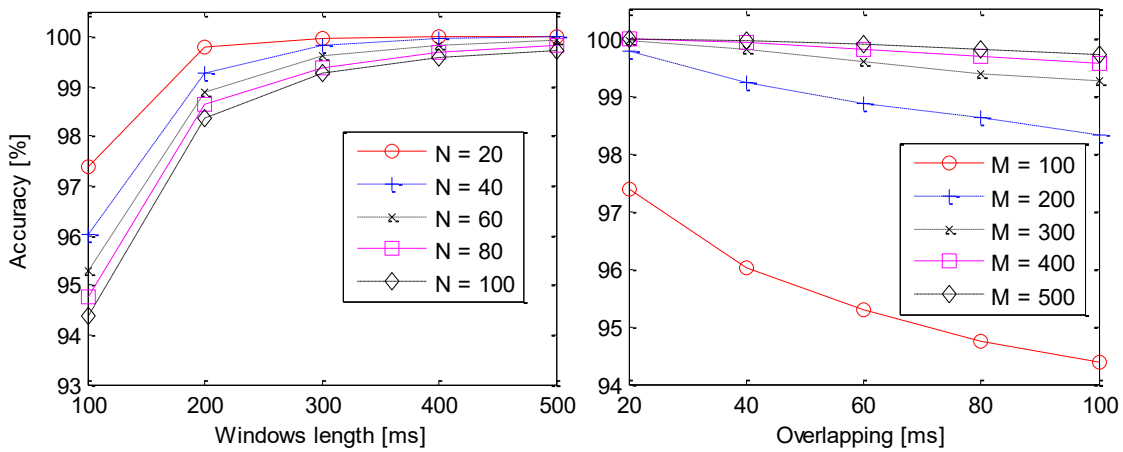
The window increment determines the real-time constraint of the system, i.e., the features must be computed and processed to generate a command before the next data segment arrives. After data analysis the classification accuracy was found to be increased with a progressive reduction of the overlapping time. However, the performance was not significant affected by this increment for window lengths from 200 samples onwards, as shown in Figure 14.

Figure 14. Effect of varying the sliding of the window on individual fingers movements.



From these results, a trade-off between these two parameters was taken into account in this research, being chosen in this study a window length $M = 300$ ms and an overlapping $N = 100$ ms. These parameters were selected to conduct the next experiments, to accomplish the real-time application purpose. The same behavior in classification accuracy was observed (last results: $M = 300$ ms and $N = 100$ ms) for the group of grasp movements, such as shown in Figure 15.

Figure 15. Results varying the length of the window and the overlapping for grasp movements.



4.1.2. Parameter adjustment

The setting of some parameters for the features considered in this research (Table 5), were optimized iteratively using trial and error method, seeking to improve the classification accuracy. Particularly, for ZC and SSC, the thresholds values obtained were 0.0005 and 0.001, respectively. Other parameters were chosen according to the literature, such as: for AR model(order = 4) (OSKOEI; HU, 2007), DFA ($L = 10$) (PHINYOMARK; PHUKPATTARANONT; LIMSAKUL, 2012b), PSR ($N = 20$) (PHINYOMARK et al., 2012) and HFD ($K_{max} = 10$) (ESTELLER et al., 2001). All parameters are summarized in the Table 6.

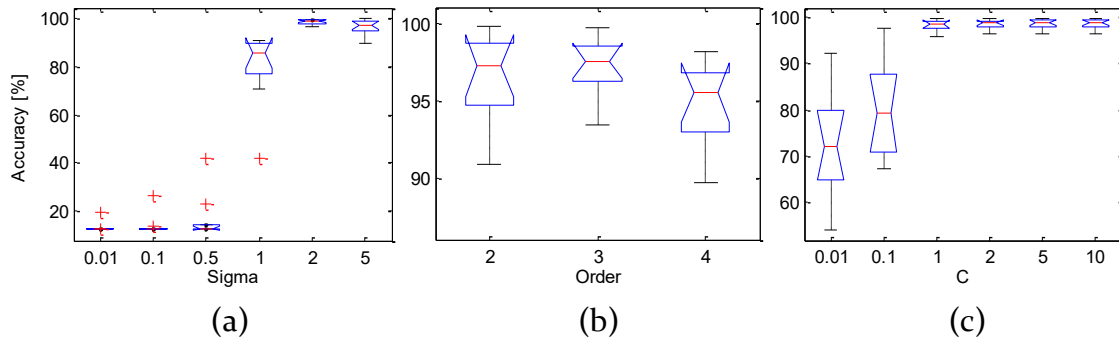
Table 6. Parameters selected for features used in this research.

Feature	Abbreviation	Parameters
Zero Crossing	ZC	$thld = 0.0005$
Slope Sign Change	SSC	$thld = 0.001$
Autoregressive Model	AR	$P = 4$
Power Spectrum Ratio	PSR	$r = 20$
Detrended Fluctuation Analysis	DFA	$L = 10$
Higuchi Fractal Dimension	HFD	$Kmax = 10$

Additionally, the parameters of the classifiers were selected by comparing the classification rate for the different values for each topology, such as defined in the methodology. Three different classifiers were tested in the experiments of this research, being considered KNN, LDA and three variants of SVM. For KNN, it was found an improvement at the performance (accuracy = 96.6%) for most of amputees using $K = 7$ neighbors. This is true for the three group of categories (hand/finger, grasp and all movements). However, using $K = 9$ a similar performance was obtained with differences in accuracy below of 5%.

For SVM, three kernels were used in its architecture, such as above mentioned in the methodology. Using a linear kernel (SVM-Lin), no additional adjustments were needed other than the C constant. From the results with Gaussian kernel (SVM-RBF), in most of cases, with $\gamma = 2$ led the results to an improvement (accuracy = 98.5%), as shown in Figure 16. Using the polynomial kernel (SVM-Polynomial), a third-order polynomial was found to get the best performance (accuracy = 97.1%) in most of cases, followed closely by the second order with no significant difference (accuracy = 96.5%). Finally, for all kernels, variations of the constant C were also analyzed. From the overall results, the classification accuracy at higher values of C was found to be improved (accuracy = 98.5%). However, no significant difference was found for $C > 1$ (accuracy = 98.2%). This tendency was found to be similar for all groups of movements.

Figure 16. Graphic representation of the accuracy distribution of the different parameters according to the variance among amputees. (a), parameter γ for SVM-RBF; (b), polynomial order for SVM-Polynomial; (c), constant C for all SVM kernels.



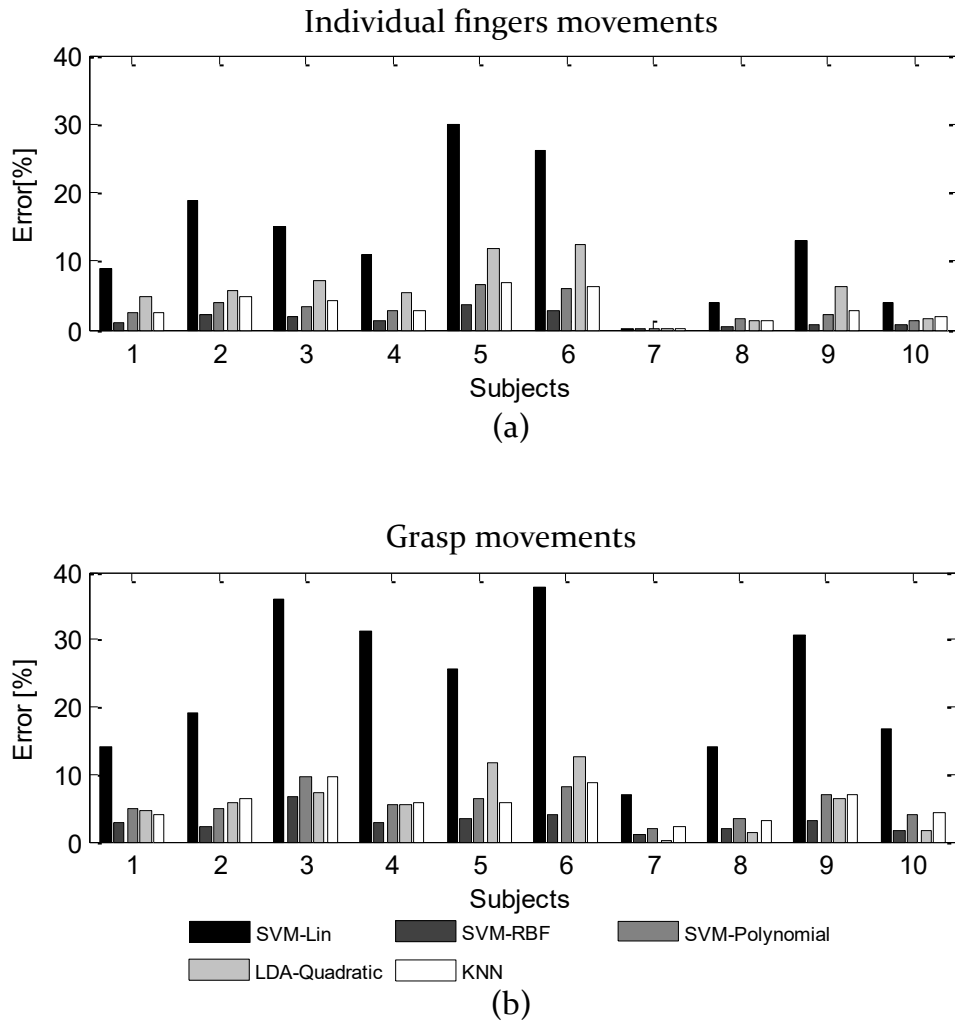
This study was also carried out with the control group getting similar results. A summary of the parameters selected for all classifiers can be summarized in Table 7.

Table 7. Parameters selected for the classifiers used in the experiments.

Classifier	Function	Parameters	Value
SVM	Linear	-	-
	RBF	γ	2
	Polynomial	Order	3 rd
	All kernels	C	1
KNN	-	K	7
LDA	Quadratic	-	-

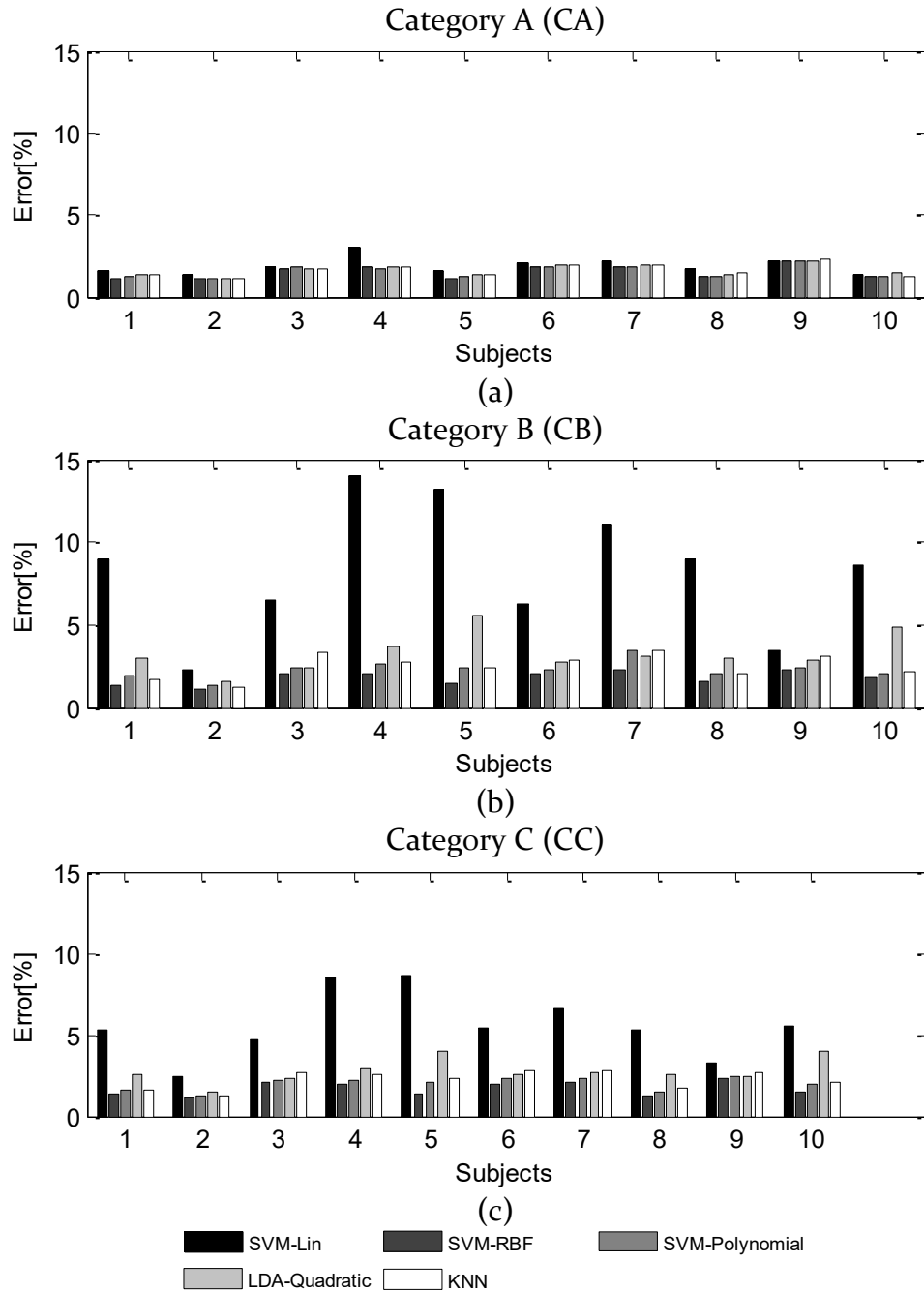
Overall results for the classifiers architectures implemented (three for SVM, KNN and LDA) by each one of the amputees are shown in Figure 17. Despite differences found between subjects, it can be noted a similar behavior in the performance of different classifiers tested. SVM-RBF was found to have the best performance in all subjects, while SVM-Lin showed the higher error, as shown in Figure 17, for individual fingers movements (a) and grasp movements (b). No differences were found among groups of movements in relation to the performance between classifiers.

Figure 17. Comparison of classification results with amputees in offline mode, for individual fingers (a) movements and grasp movements (b).



From the results with the control group, a similar performance was found among classifiers, as shown in Figure 18. However, when compared error results from Figure 17 and Figure 18, it can be noted a difference on the error between amputees and control groups, respectively.

Figure 18. Comparison of classification results with the control group in offline mode, for individual fingers movements and grasp movements.



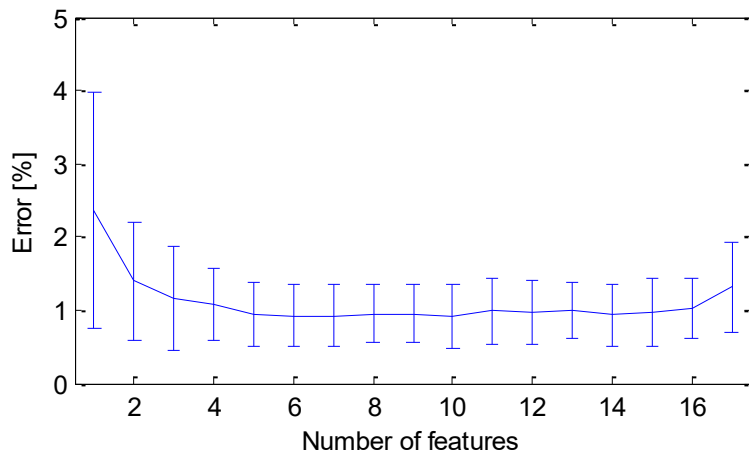
In summary, according to the selected parameters from previous analysis, an architecture for each one of the classifiers was chosen to be used in the following experiments. Thus, KNN was configured with $K = 7$, and for LDA, the quadratic function was used. In the case of SVM, the RBF kernel was chosen due

to its better performance in comparison with the other two kernels analyzed. Hereinafter, the selected configuration SVM-RBF will be referred as SVM.

4.1.3. Feature selection analysis

First of all, in the experiment using SFS method, the relation between average classification and number of selected features was studied. Classification accuracy was found to increase in most of cases when including more features, as shown in Figure 19. However, it can also be noted that there was no substantial improvement in the error using more than six features, which agrees with the findings of (PHINYOMARK; PHUKPATTARANONT; LIMSAKUL, 2012a). Thus, from the feature selection analysis a suitable subset composed of six features was adopted to form the MES patterns.

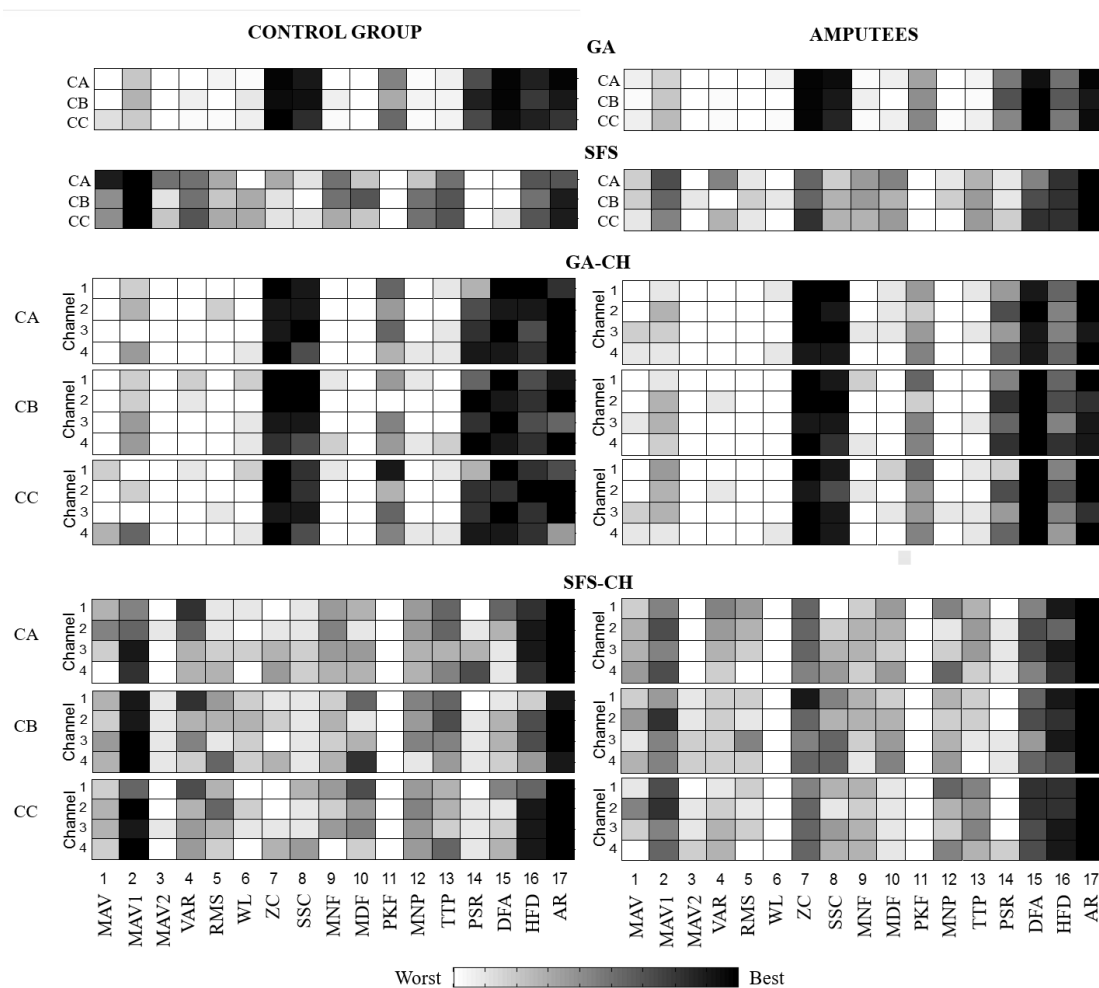
Figure 19. Effect of error of classification according to the increment of features.



In the experiments, the feature selection methods proposed in the methodology were evaluated for each movement category. In relation to GA and GA-CH methods, the ZC and DFA features were the most frequently selected, followed by SSC, AR, HFD and PSR, as shown in Figure 20. Specifically, ZC and DFA were selected in all movement categories for all amputees. Moreover, time domain features were little considered as relevant, with MAVI as the most relevant

feature from this set. Similarly, PKF, computed in the frequency domain, was considered in lesser extent. The analysis with AG-CH, using the individual-channel approach, showed similarity in the selected features between channels. Moreover, from AG and AG-CH, the features were found to be similar between movement categories and subjects.

Figure 20. Results of the feature selection experiment for each one of the movements categories. Representation of the selected frequency feature, for the control group and amputees.



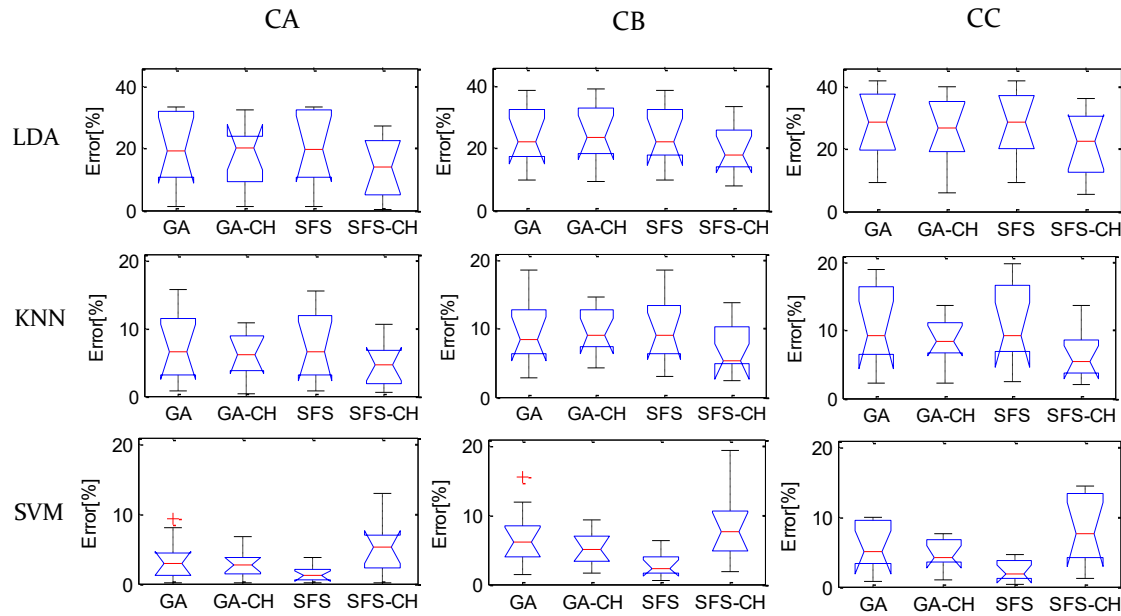
In relation to SFS and SFS-CH methods, from the results AR model was the most frequently feature selected, followed by HFD and MAV1. Different features from time and frequency domains were included in the subsets for both control and amputees. However, outcomes using SFS and SFS-CH approaches showed strong differences among the features selected, categories and subjects.

All resulting feature subsets were used as input for the chosen classifiers (LDA, KNN and SVM), in order to compare the performance of the proposed methods to select the most suitable approach. In general, the comparison of error variance distribution of the methods had similar mean and standard deviation for all movement categories, as shown in Figure 21, in which the results are related to all categories. Due to the similar performance of both control group and amputees, only results of amputees have been widely discussed here. KNN and LDA showed similar error variance distributions among the methods, unlike SVM, which showed a different behavior.

From the results, SFS had the best classification performance with SVM ($MPE < 2.8\%$), followed closely by GA-CH and GA methods, with similar performances ($MPE < 6.1\%$) and no significant differences ($p > 0.954$). In contrast, SFS showed the lowest performance using KNN and LDA, having a significant difference when compared with SFS-CH ($p < 0.009$). The SFS-CH method achieved the best performance for KNN and LDA classifiers, followed closely by GA-CH. In addition, the performance of SFS-CH was found to be significantly better when compared to GA and SFS ($p < 0.028$). In contrast, SFS-CH method showed the lowest performance among other methods when using SVM. However, from Figure 21, GA and GA-CH approaches did not present significant differences ($p > 0.618$) using KNN. In addition, improved results were found using the features from GA-CH with KNN ($MPE < 9.6\%$) and LDA ($MPE < 25.1\%$).

In summary, the error variance in the box plots of Figure 21 shows high dispersion in different movement categories for SFS (i.e. classification of CB and CC using KNN and LDA) and for SFS-CH (i.e. CA, CB and CC using SVM). The results indicate that features of SFS, GA and GA-CH with SVM classifier provide lower classification error rates for both control group and amputees. From these findings, a ranking of the selection frequency from all cases was employed to obtain a feature subset for each method.

Figure 21. Graphic representation of the error distribution of the different feature selection methods according to the variance among amputees.



From GA and GA-CH, the ranking resulted in the same feature sets, which were DFA, HFD, AR model, ZC, SSC and PSR. Likewise, from SFS, the features obtained were DFA, HFD, AR model, ZC, MAVI and MNF. For SFS-CH, the features were different for each category, in which the ranking was not significant and therefore, it was not suitable to be considered. Afterwards, an evaluation with the subsets obtained from the ranking for each method was performed, having no significant differences between SFS and GA ($p < 0.918$). As a result, taking into account all of the above, the features selected by GA were chosen as the proposed feature set to be used for the analyses conducted in this study.

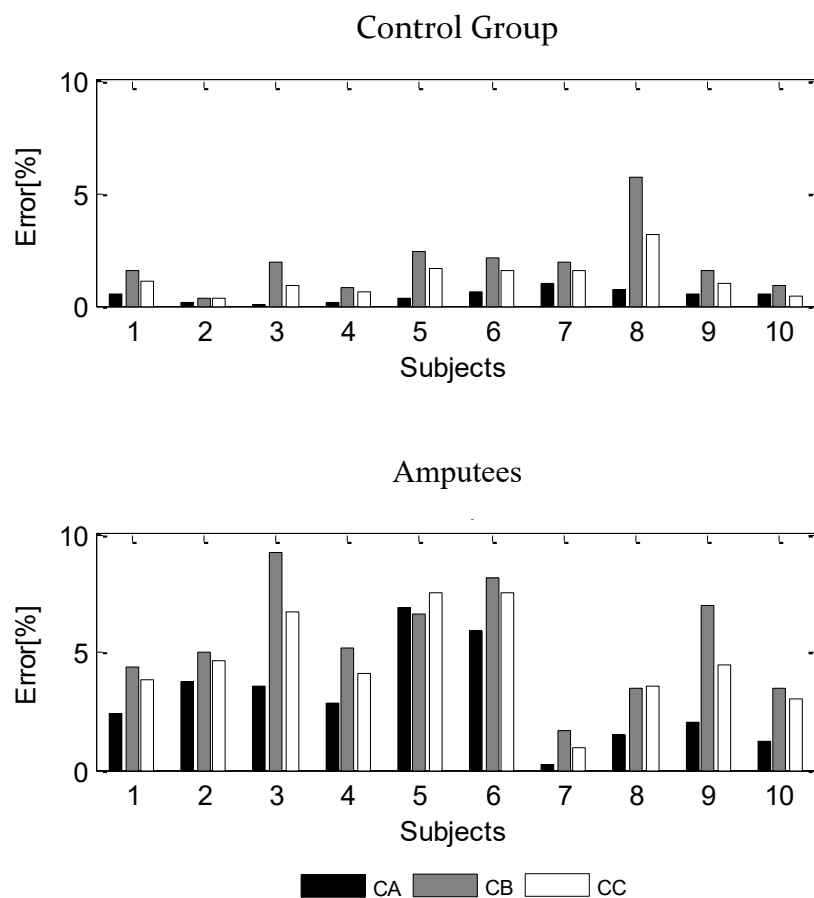
4.1.4. Proposed MES pattern recognition system

A comparison from results for KNN, LDA and SVM classifiers using the proposed feature set was carried out. From all movement categories, SVM showed the best performance, followed by KNN and LDA, respectively. Moreover, SVM had a significant difference with LDA ($p < 0.024$) for all cases, but did not have a

significance difference with KNN ($\rho > 0.062$), except for the control group for movements of CB ($\rho < 0.032$). Figure 22 shows the classification error for both control group and amputees using SVM. From the results with amputees, the average accuracy for CA, CB and CC categories using SVM were $97.0 \pm 2.0\%$, $94.6 \pm 2.2\%$ and $95.4 \pm 2.0\%$, respectively, with the grasp movements (CB) obtaining the lowest performance.

For all categories, values of Kappa's coefficient and specificity were higher than 0.9 and 98.4%, respectively. The accuracy among subjects ranged from 99.8% (A7 for CA) to 90.8% (A3 for CB). In all experiments, the highest performances per subject were for the amputees A7, A10 and A8, sorted by performance, respectively.

Figure 22. Classification error for control group and amputees using the proposed feature set with SVM.



For category C, which includes thirteen movements, the best accuracies were achieved by amputee A7 ($99.5 \pm 1.0\%$) followed closely by A10 ($97.0 \pm 2.4\%$). However, the worst result was for amputee A3, for CB ($90.8 \pm 3.6\%$), while for CA and CC categories, amputee A5 and A6 showed the worst performance (although, above 92.4%). Results using KNN showed average accuracies above 90.4% (CB), while for LDA the performance was above 74.9% . From the results for the control group, accuracies ranged from 99.9% to 96.8% , with average accuracy of $98.8 \pm 1.2\%$, specificity ($Sp > 99\%$) and Kappa ($k > 0.97$). Table 8 summarizes the results for the control group and amputees for accuracy and Kappa.

The confusion matrices for each movement category provide the average mistaken classification for all amputees, as shown in

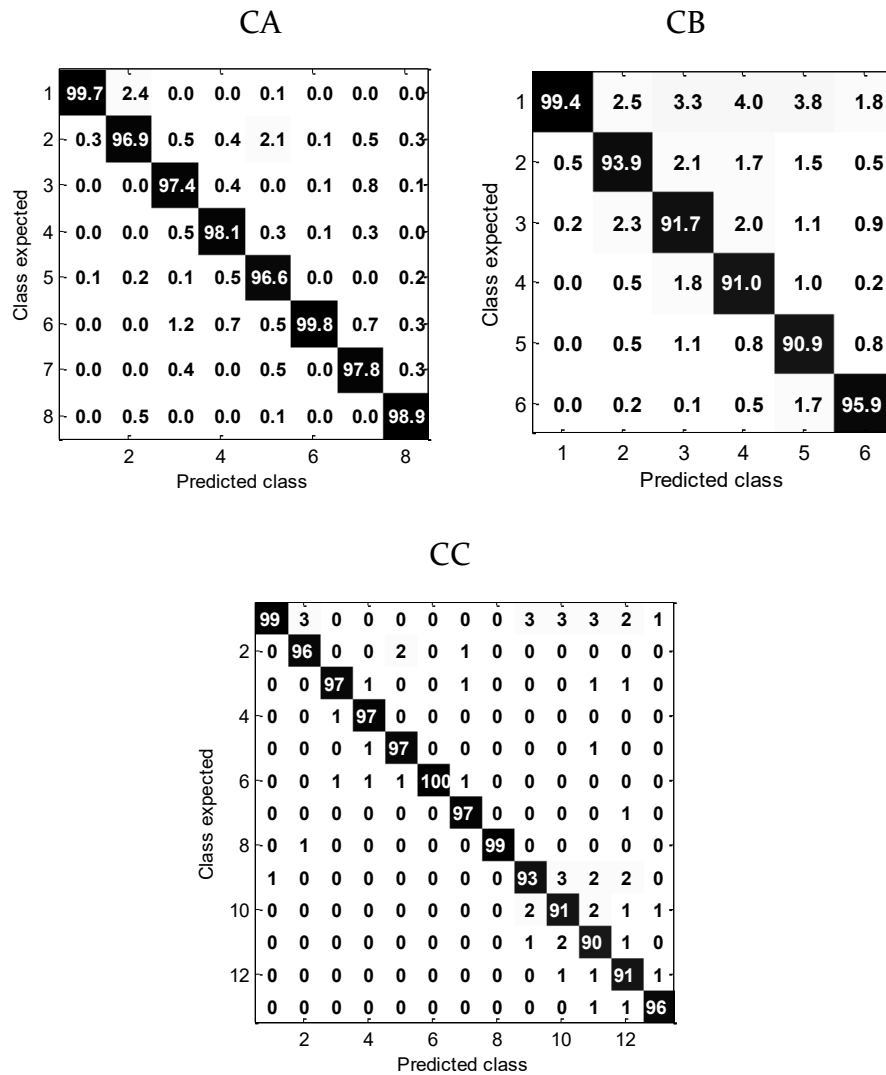
Figure 23. The confusion matrix for CA shows that the recognition of finger movements was mainly confused with flexions of the near fingers. However, the fifth chirodactyl (F5) was found to be easily confused with most of the movements. Furthermore, hand closing (HC) was confused with all fingers (F1-F5).

Table 8. Average classification accuracy (%) and Kappa's Coefficient of three movement categories, for control group and amputees. Table includes the results for SVM, LDA and KNN classifiers.

Cat	Sub	SVM		LDA		KNN	
		Acc	K	Acc	K	Acc	K
CA	C	99.17 ± 0.6	0.99 ± 0.0	95.06 ± 2.5	0.92 ± 0.0	99.55 ± 0.2	0.96 ± 0.0
	A	98.94 ± 0.8	0.97 ± 0.0	80.21 ± 10.8	0.78 ± 0.2	96.98 ± 1.9	0.92 ± 0.1
CB	C	97.64 ± 0.8	0.98 ± 0.0	89.35 ± 3.4	0.84 ± 0.0	98.07 ± 1.4	0.93 ± 0.1
	A	96.94 ± 1.0	0.94 ± 0.0	76.06 ± 9.7	0.75 ± 0.1	94.58 ± 2.2	0.84 ± 0.1
CC	C	98.77 ± 0.7	0.99 ± 0.0	88.19 ± 3.2	0.88 ± 0.0	97.89 ± 0.7	0.97 ± 0.1
	A	97.19 ± 0.9	0.95 ± 0.0	71.91 ± 10.7	0.75 ± 0.1	95.36 ± 2.0	0.89 ± 0.1

Control group (C); Amputees (A).

Figure 23. Confusion matrices with average misclassification for amputees.



For CB, the confusion matrix shows that most movements were confused among them. Specifically, confusion matrices for the subjects show that tripod (TP) is easily mistaken with all other classes. However, the highest mistaken was found between the full hand wrap grasps (for 2.9% of times LD was confused as MD). Finally, the results for CC resemble with previous observations, in which TP was found to be the most difficult movement to be recognized. It was also found from the results that movements belonging to CA were rarely confused with CB (below 0.1% of mistaken).

4.2. Online study results

An important issue discussed in this thesis is whether the recognition scheme can meet the real-time constraints of the problem. To accomplish it, the system must perform pre-processing, feature extraction and classification in the window increment time $N = 100$ ms, previously established. The processing delay was empirically tested using an Intel Core i-7 processor (2.2GHz) for this system computing and the computation performed in Matlab. No real-time operational system was used for the testing. For the experiments, this processing system was tested on online mode, without a perceivable delay in the visual response in the laptop screen. This preliminary test showed that the system used was enough for the experimental design here proposed. Although it is possible, the implementation of the proposed method on an embedded hardware is beyond the scope of this thesis.

The results shown in Figure 24, describes the error from each amputee for the three movement categories. Table 9 summarizes the accuracy of classification for each amputee and the mean accuracy for all of them. According to the results, the highest performance (accuracy = 92.7%) was achieved for the finger individual movements, followed by the grasp movements.

From the results in Table 9, an analysis of the overall performance of the experiments shows a mean of recognition for all participants of 62.5% (SD = 15.1) for CA, 54.1% (SD = 12.7) for CB and 47.4% (SD = 10.8) for CC. It is worth to note that each category groups a different number of hand/finger movements, which is directly related to the demand of the classifier to discriminate the classes. Moreover, it was found a significant variance among subject's performances for all categories.

Figure 24. Online results for amputees, for three movements categories.

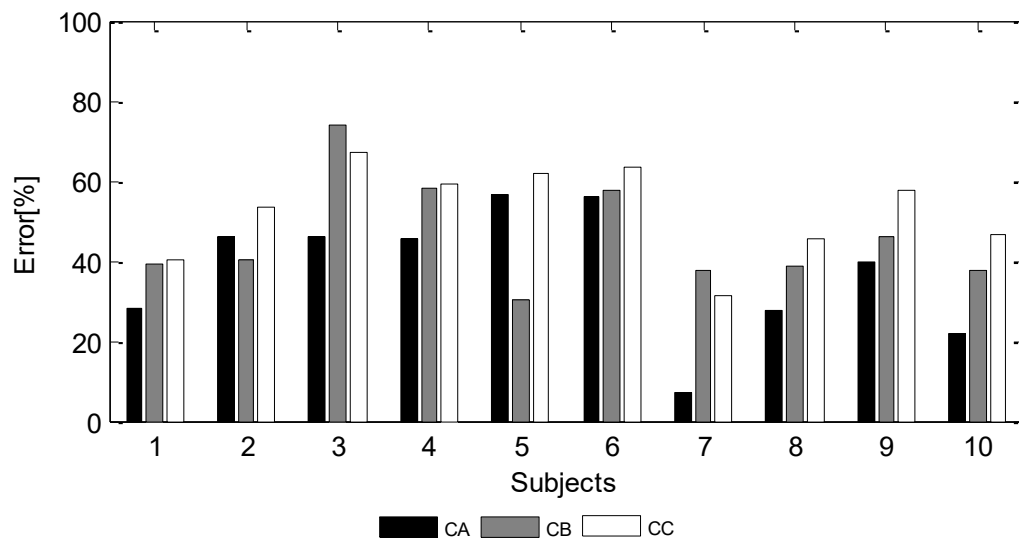


Table 9. Online results for amputees, for the three movements categories.

	Subjects										Mean
Cat	1	2	3	4	5	6	7	8	9	10	
CA	71.7	53.7	54.1	54.6	43.2	44.2	92.7	72.3	60.4	78.4	62.5
CB	61.0	59.5	25.8	42.0	69.9	42.3	62.6	61.3	53.9	62.4	54.1
CC	59.5	46.8	32.8	40.7	38.3	36.4	68.7	54.6	42.3	53.3	47.4

For CA, e.g., the performances were between 44% and 93%, being a significant difference. Similar results were found for the control group, which can be found in Table 10.

Table 10. Online results for control group, for the three movements categories.

	Subjects										Mean
Cat	1	2	3	4	5	6	7	8	9	10	
CA	82.2	88.8	68.5	56.9	82.4	71.8	63.4	82.2	67.9	76.8	74.1
CB	67.5	79.9	55.7	51.5	70.8	63.9	53.5	67.5	79.7	76.5	66.6
CC	65.2	63.7	42.8	42.9	63.1	58.2	36.1	65.2	50.7	59.8	54.8

Conducting a deeper analysis for each one of the categories, with the individual finger movements belonging to the CA, some subjects showed ease to discriminate individual finger movements, while others showed difficulty to accomplish it. The best performance was achieved by amputee A7, with 92.7% of accuracy, followed by A10 with 78.4%. A1 and A8 also showed a good recognition rate, with accuracies above 71%. However, the lowest performance corresponded to A5 and A6, with accuracies below 44%. A2, A3 and A4 had also difficulty to recognize the movements, obtaining accuracy of 54%, approximately.

In particular, amputee A7 showed to have good abilities to contract the selective muscles to discriminate individual fingers. In Figure 25, the confusion matrix shows that high values of recognition were related in the diagonal, which means that the classifier's output matches the correct target, corresponding to the performed movement. It can be seen that when the classifier received patterns of second chirodactyl flexion, it was confused by recognizing them as fourth chirodactyl flexion (8.62%) or fifth chirodactyl flexion (5.5%).

Figure 25. Confusion matrix for A7 subject, in validation online for CA

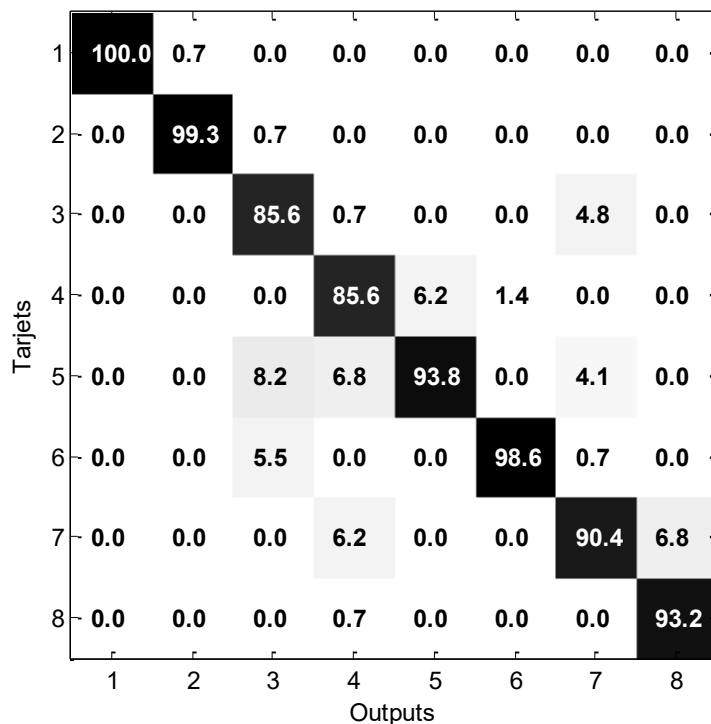
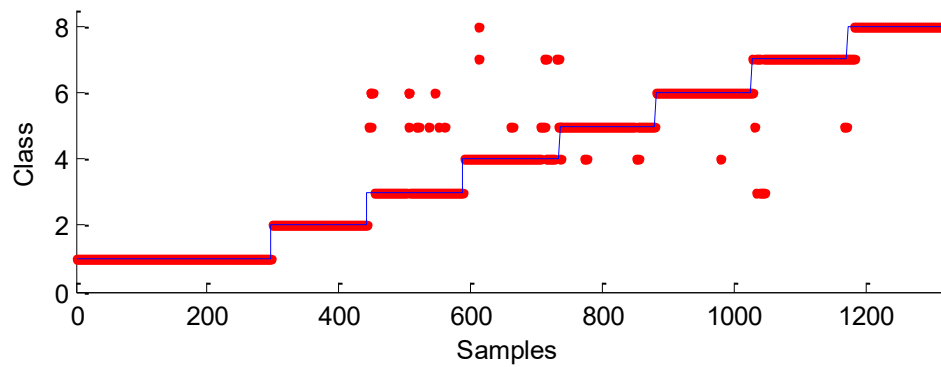


Figure 26. Output stream of predictions for amputee A7, in validation online for individual fingers



Similarly, the third chirodactyl flexion was confused with fourth chirodactyl flexion (6.8%) or hand closing (6.2%). Figure 26 shows the stream of the class decisions in the online experiments. The continuous blue line represent the target while the red point describes the samples referred to the recognized patterns. It can be seen that most of confused patterns are referred to movements of close muscle in the arm, such as adjacent fingers.

Furthermore, for the grasps movements grouped in CB, most of subjects showed similar performance, with accuracies between 60% and 70%. The best performance was achieved by amputee A5, with 69.9% of accuracy, followed by A7 with 62.6%. Taking into account the amputee A7 again, which was analyzed for the movements from CA, Figure 27 shows the confusion matrix, while Figure 28 shows the responses on the time of validation. A7 showed to have abilities to contract specific muscles for grasp movements, as well as to perform individual finger flexion movements.

However, the grasp movements imply a greater difficulty in the muscle selectivity to accomplish more complex movements, which involves more finger movements at the same time. In Figure 27, the highest accuracy of true positive for the movements, different to the rest state, was achieved for full hand medium

wrap (86.3%), with a similar accuracy for sphere tripod grasp. Both medium wrap and sphere tripod grasp were referred as power and precision grasp, respectively.

Figure 27. Confusion matrix for amputee A7, in validation online for grasp movements

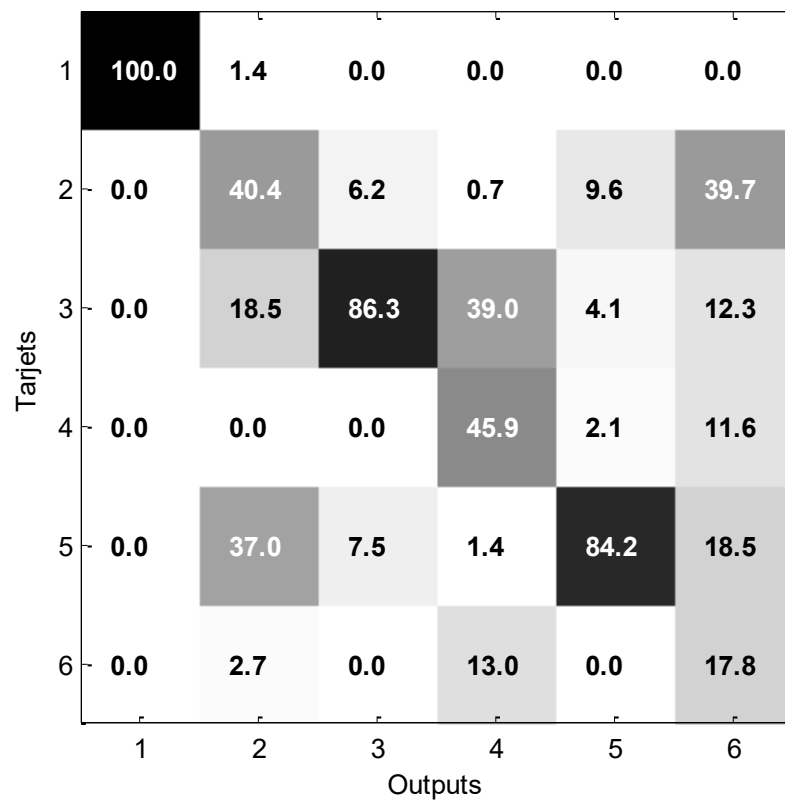
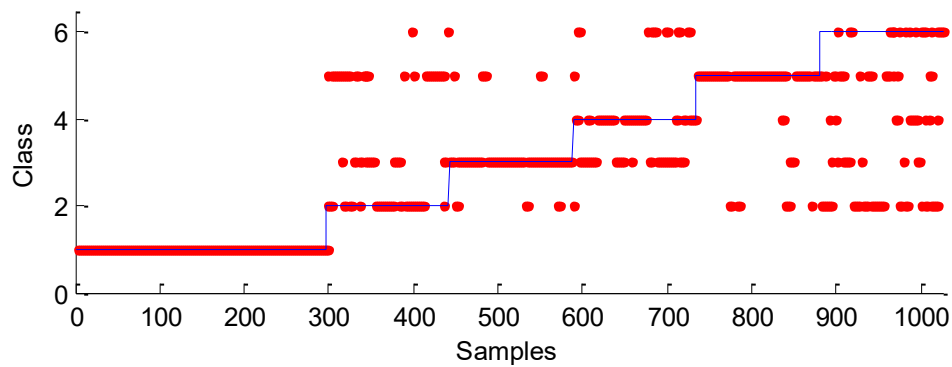


Figure 28. Output stream of predictions for amputee A7, in validation online for grasp movements.



The most difficult movement to be recognized was the tip pinch, which was confused with all other grasp movements, mainly with full hand large grasp

(39.7%), being above of the movement itself (17.8%). Lateral grasp was confused with high percentage of false positive for full hand medium wrap (39.0%). Similar behavior was found in other amputees, whose accuracies were above 54%, such as for A1, A2, A5, A7, A8, A9 and A10.

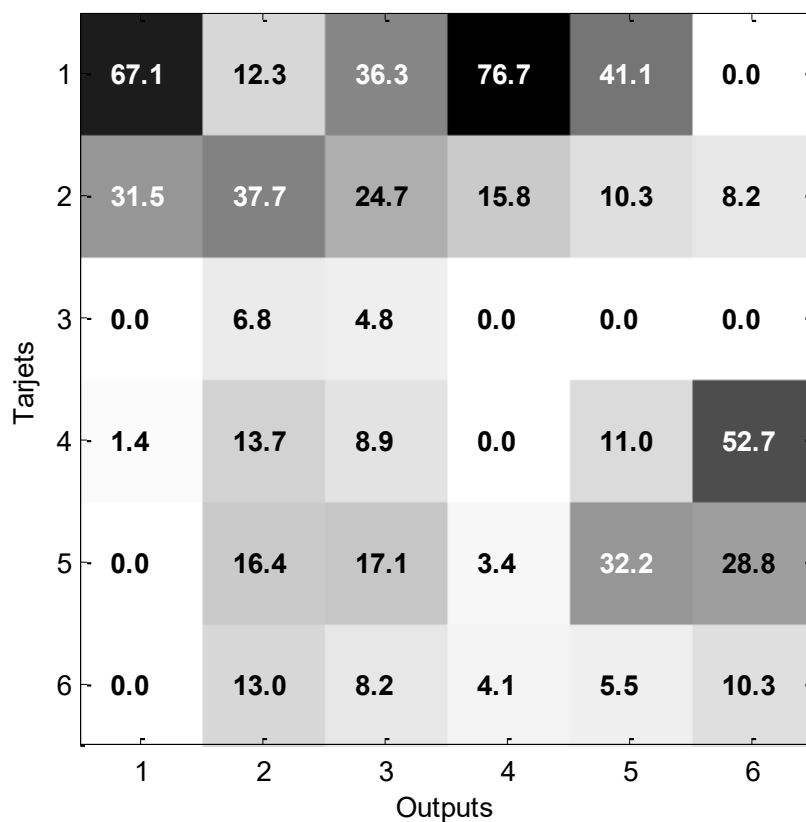
Furthermore, some amputees had a low performance, around 42%, such as A4, A6 and A9. In particular, the amputee A3 had the lowest performance, with 25.8% of accuracy, being that a high recognition rate for the rest state class was achieved with 67.1%. It is worth to mention that the accuracy by itself it is no able to assess the results on the validation of the classification, whereby it is necessary to interpret the other indices of evaluation. However, the sensibility (25.8%) and the specificity (85.1%) also indicated a very low performance. In relation to the Kappa's coefficient, a slight agreement between targets and outputs was found ($K = 0.10$), which means that the achieved results are not reliable to be used as control command.

An overall assessment about this subject (A3) can be obtained by inspection of the confusion matrix in Figure 29. The rest state, referred to no voluntary contraction to execute any movement, was wrongly recognized when the subject was asked to perform most of movements. A significant number of false positive was found, up to 76.7%, when performed lateral grasp. Also, it was found that full hand large grasp was recognized as false positive when other movements were performed. The spherical tripod grasp had the higher recognition among the grasps, with 32.2%.

In summary, it can be noted that in the online experiment, this subject could no perform voluntarily the selected muscle contraction to discriminate movements, neither maintain repeated patterns in relation to the experiments conducted in the training of the recognition system. Moreover, it could be understood as there was not an enough voluntary contraction, in most of trials in the experiment, to be recognized as a movement.

Finally, in CC, for the recognition of all proposed movements, results showed accuracies between 32.8% and 68.7%. The best performance was achieved by amputee A7 again (68.7%), followed by A1 (59.5%). In particular, for the confusion matrix of A7 in Figure 30, it was possible to identify a tendency in the misclassification, in relation to the similarities in the movement executed.

Figure 29. Confusion matrix for the amputee A3, in validation online for grasp movements.



The grasp movements, e.g., which involves the actuation of more than one finger to accomplish the movement, were confused mainly among themselves. Similarly, the individual finger movements seem to be confused mainly with other movements in this category. However, a few false positives were noted when some movements, like spherical tripod and lateral grasps, were recognized as first chirodactyl or third chirodactyl flexions.

Figure 31 shows the stream of outputs in the sequence of the execution of each movement in the experiment.

Figure 30. Confusion matrix for the amputee A7, in validation online for all adopted movements.

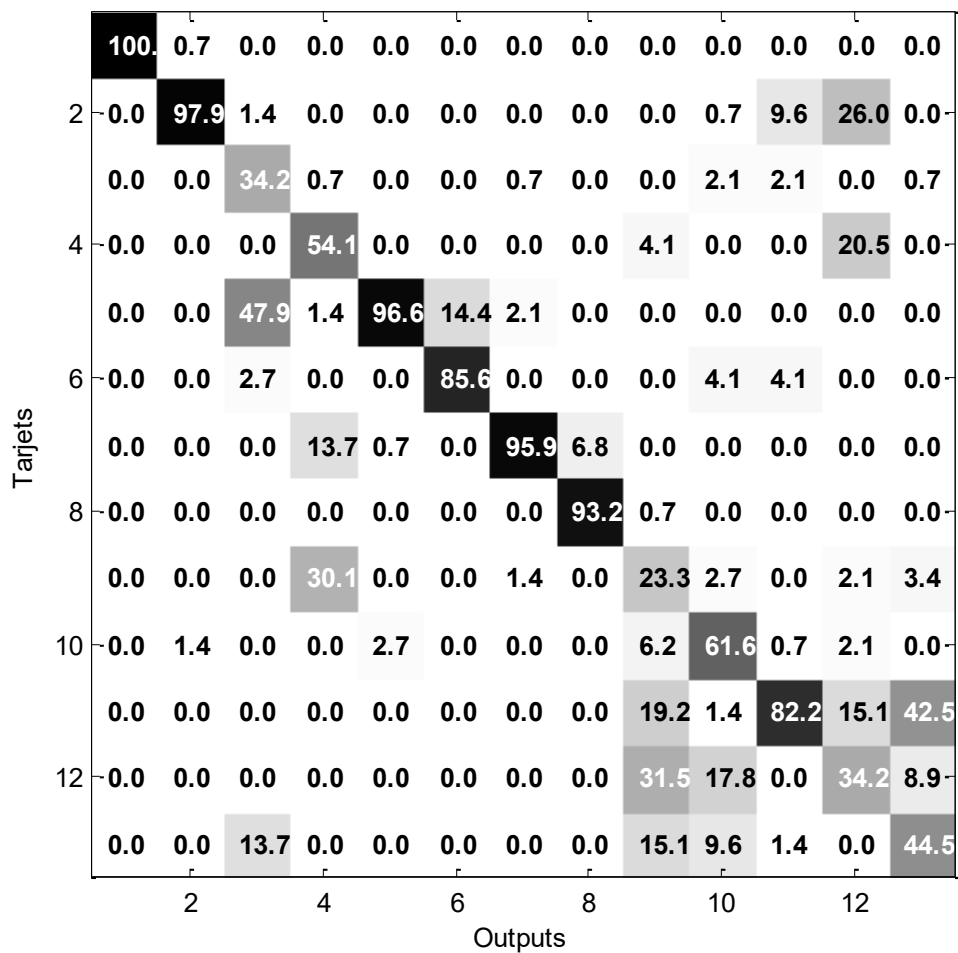
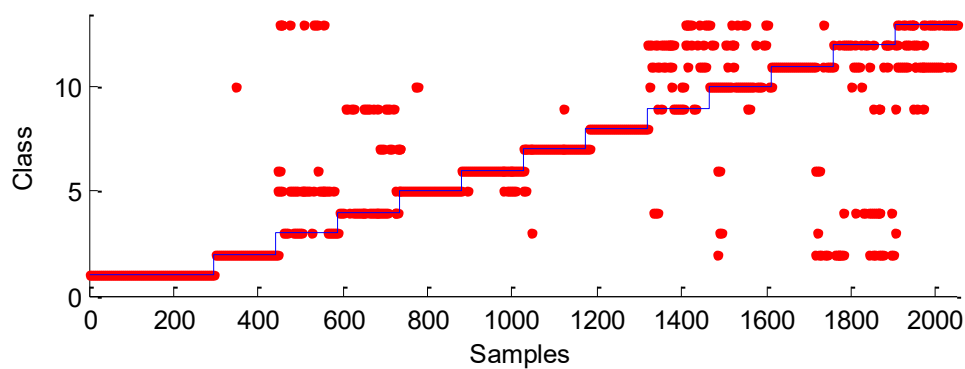


Figure 31. Output stream of predictions for the amputee A7, in validation online for all adopted movements



4.2.1. Post-processing

The results of the classifier were evaluated to reduce the yielding of predictions without an enough reliable. The results of the classifiers generated scores with a probability of association of the current pattern with each one of the classes. The three methods exposed in the methodology were analyzed after the obtainment of the results to identify its suitability in an implementation for real-time applications.

The methods used in the analysis are denoted here as PPI, for the comparison using the agreement through the *Kappa's* coefficient, PP2, for the comparison using a defined threshold; and MV for majority vote. Table II details the results of the methods for all amputees. By inspection, it can be seen that in most of cases PPI produces better results than other methods, followed by MV and PP2, respectively. PPI showed differences up to 5.3% in relation to PP2. A slight difference was found between PP2 and MV (up to 1.9%).

On the overall results, PPI improved the performance up to 10.7%, in relation to the cases when no post-processing techniques were applied. However, it can be also observed that the improvements were accomplished for the same subjects, while other ones did not have difference, over all movement categories. The percentage of trials discarded are also included in Table II, denoted as Disc1 and Disc2, for PPI and PP2 methods, respectively. For MV, it was not calculated this measure, due to at the end, the output is changed and not discarded.

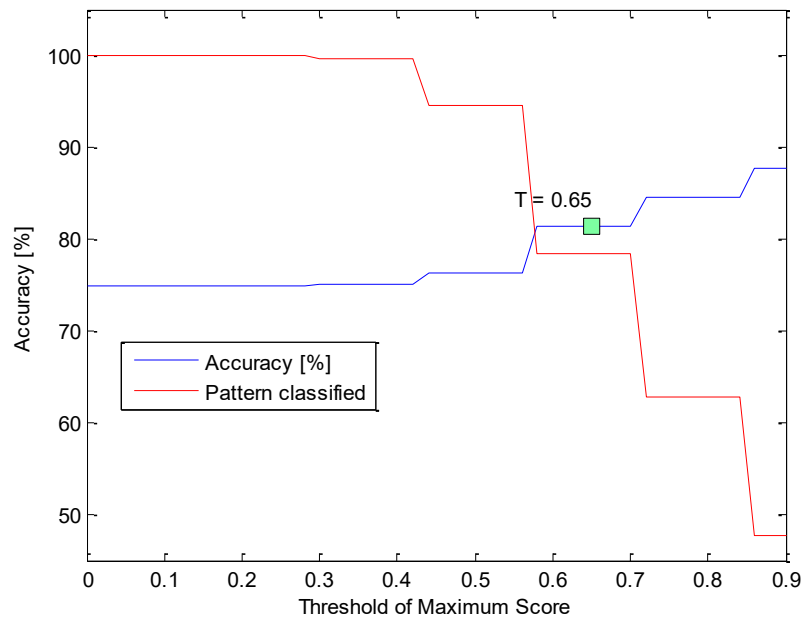
As a specific case, results for amputee A10 in the online experiment, for CA, were considered to analysis. Figure 32 describes the performance using PPI method by iteration of the threshold of maximum score used for comparison. It is shown the accuracy across the iterated threshold, T , from 0 to 0.9 (blue line), and the percentage of the total of trials that were classified (red line). The value $T = 0.65$ was obtained for the eight-class problem according to Equation 2.17.

Table II. Post-processing analysis results.

Subjects	NoPP	PPI	PP2	MV	Disc1	Disc2
Category A (CA)						
1	65.8	76.5	71.7	73.5	0.3	19.8
2	49.3	49.3	49.3	49.3	0.0	0.0
3	51.9	56.2	54.1	55.0	0.2	13.7
4	50.3	50.3	50.3	50.7	0.0	0.0
5	40.3	46.1	43.2	43.2	0.5	28.5
6	43.4	44.7	44.2	46.1	0.1	3.4
7	90.1	90.1	90.1	90.4	0.0	0.0
8	69.7	74.2	72.3	72.8	0.2	12.4
9	58.7	61.2	60.4	60.6	0.2	12.7
10	74.8	81.4	78.4	80.6	0.2	14.8
Category B (CB)						
1	49.7	57.5	54.8	55.0	0.4	22.7
2	47.1	47.1	47.1	48.2	0.0	0.0
3	18.5	20.2	19.1	19.3	0.7	39.3
4	42.5	42.4	42.5	42.7	0.0	0.0
5	39.3	41.1	40.4	40.8	0.5	25.0
6	26.1	26.5	26.3	25.8	0.0	2.2
7	55.1	55.1	55.1	55.8	0.0	0.0
8	39.6	40.0	40.2	40.1	0.3	17.5
9	42.1	40.7	42.5	43.6	0.4	20.9
10	43.9	44.9	44.6	44.4	0.3	17.7
Category C (CC)						
1	55.4	64.9	59.5	61.6	0.4	22.8
2	42.7	42.7	42.7	42.8	0.0	0.0
3	32.0	33.8	32.8	32.7	0.4	21.4
4	43.8	43.8	43.8	44.2	0.0	0.0
5	30.3	32.3	32.2	33.5	0.6	29.9
6	35.2	35.6	35.6	36.5	0.1	2.8
7	65.6	65.6	65.6	66.4	0.0	0.0
8	45.1	49.0	47.0	47.4	0.3	18.8
9	41.3	41.6	41.8	41.3	0.3	18.4
10	50.8	57.0	53.3	54.6	0.4	20.4

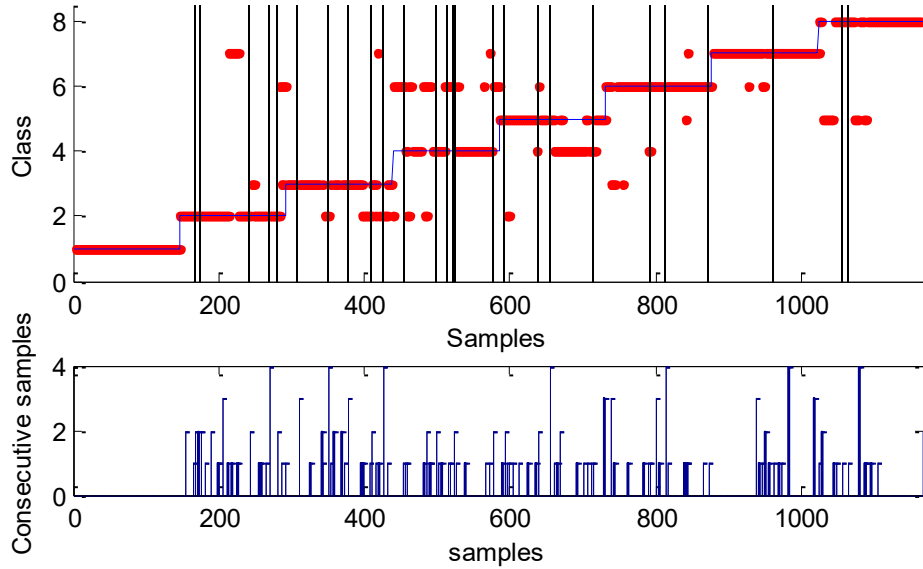
Output without post-processing technique applied (NoPP); method 1 for post-processing (PPI); method 2 for post-processing (PP2); results using majority vote (MV); rate of discarded trials using PPI (Disc1); rate of discarded trials using PPI (Disc2).

Figure 32. Post-processing response by iteration of level of agreement.



The stream of the class decisions from the classifier in the online results were plotted to illustrate the suitability of this scheme. In Figure 33, in the upper diagram, the unclassified trials are represented by vertical black lines. The blue line indicates the target class related to the real movement performed by the user and, the outputs that were classified are represented by red point dot. Such as aforementioned, due to the requirements of the system to be applied in real time, it is necessary to guarantee a response with a delay lower than 300ms. Thus, it is important that consecutive unclassified trials do not yield an extend time without a command to be sent. As the increment window defined in the data extraction was 100 ms, then, it is accepted no more than five consecutive unclassified trials to meet this constraint. The Figure 33, illustrates the occurrence and number of consecutive unclassified trials in the execution of the experiment. Figure 33 also shows the post-processing results using PPI, for A10 in CA, showing the cases with up to 3 consecutive unclassified trials. The performance for this amputee achieved 81.4% of accuracy, in relation to 74.8% when no post-processing technique was applied. Thus is, a correction of 6.6% was accomplished, with 14.8% of trials discarded.

Figure 33. Temporal diagram using post-processing method 1. (Up) predicted decision with discarded patterns; (down) consecutive discarded trials.

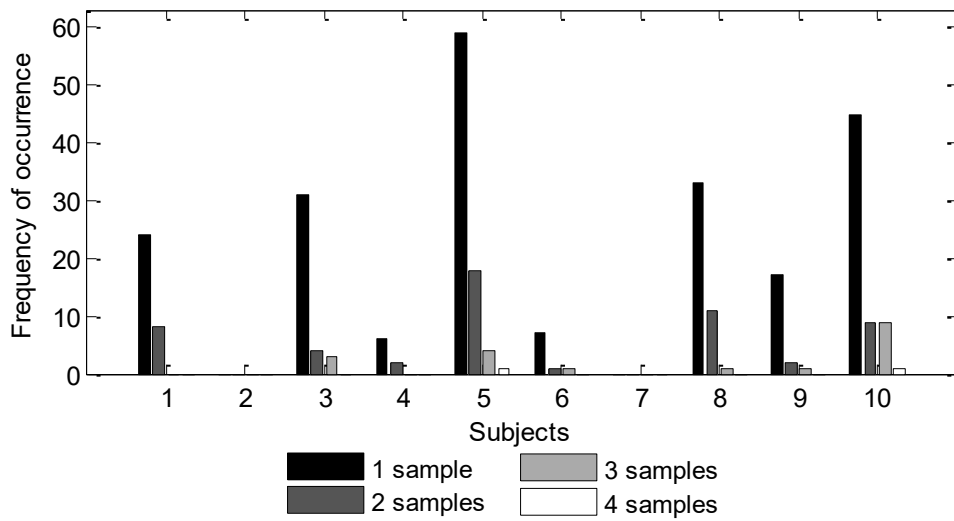


An analysis made from the results of all subjects indicated that some of the unclassified trials were actually true positives, i.e., correctly recognized patterns. Nevertheless, it was noted that the post-processing improved the overall performance. However, the overall results using PPI showed to have no more than four consecutive samples discarded, as shown in Figure 34. It can be noted that subjects A2 and A7 did not present discarded trials, while A3, A5, A8 and A10 had the highest rates of which indicates that recognition had a low rate of discarded trials. It is worth to note that discarding trials is intended to reject likely false positives, according to the scatter distribution of the feature space.

4.3. Online applications

Experiments were conducted using a robotic hand of 5 Degrees of Freedom (DOF), one DOF per finger, shown in Figure 35, including individual articulations for five fingers. Five servomotors were controlled by an Arduino, which receives the control commands via serial port using an UDP protocol.

Figure 34. Histogram of consecutive unclassified samples.



Posterior experiments were conducted with a second prototype of a robotic hand, built with a 3D printing (Figure 36). This prototype has similar configuration to the robotic hand previously described, with five DOF for each one of fingers. Servomotors use the same control developed in Arduino. It is worth to mention that this prototype does not represent a solution to replace an amputee limb because it is not wearable and its physical characteristics are not developed to be used as a prosthetic device. Inside the 3D printed robotic hand, an array of string pulls the artificial fingers through the servomotors controlled by the user interface. Both prototypes described before were adapted to be used in the experiments and to represent a visual response for the MES recognition system proposed in this thesis.

For the experiments using the robotic hand, the system showed a success rate of 96.36% and high concordance ($k = 0.97$). This test in online mode was performed initially without visual feedback, showing 54.3% of accuracy and $K = 0.45$. Finally, visual feedback was provides for the subject with 94.6% of accuracy and a very high concordance ($k = 0.94$). These results means that it is possible to obtain an important improvement in performance when is provide a feedback in the experiments.

Figure 35. Robotic hand used for the experiments.

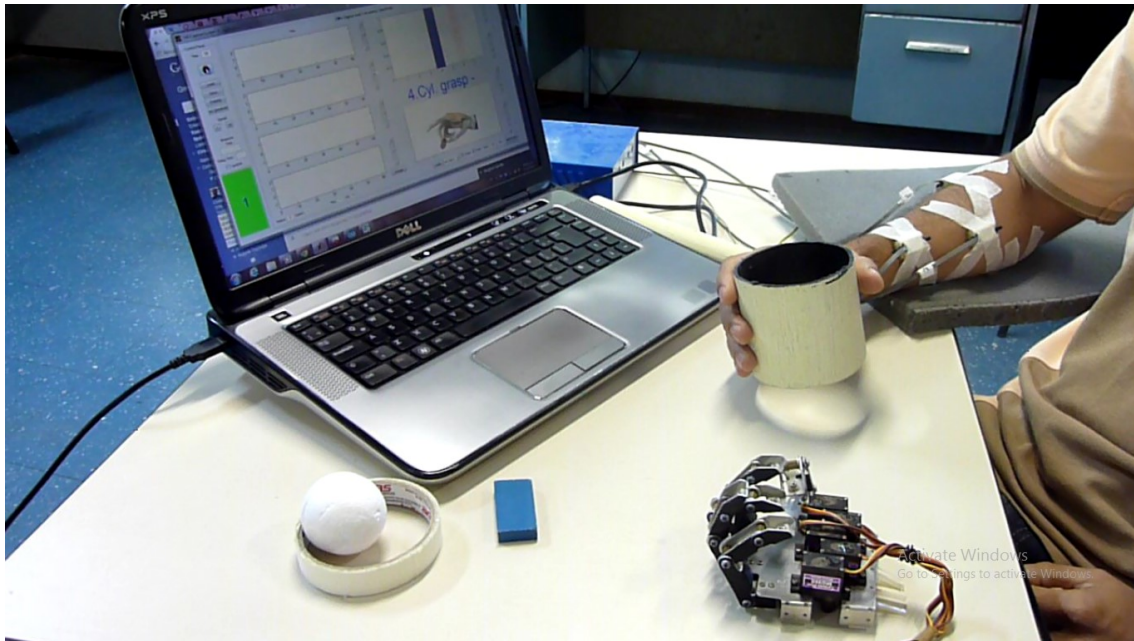
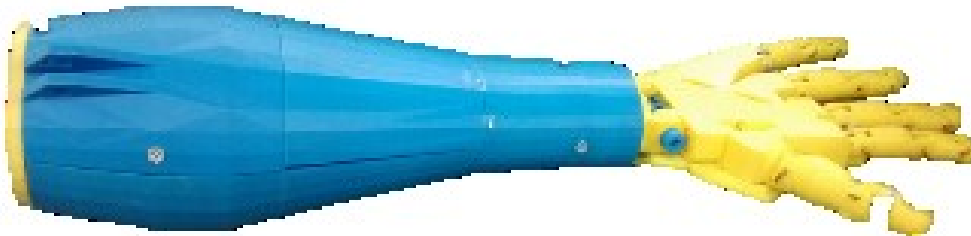
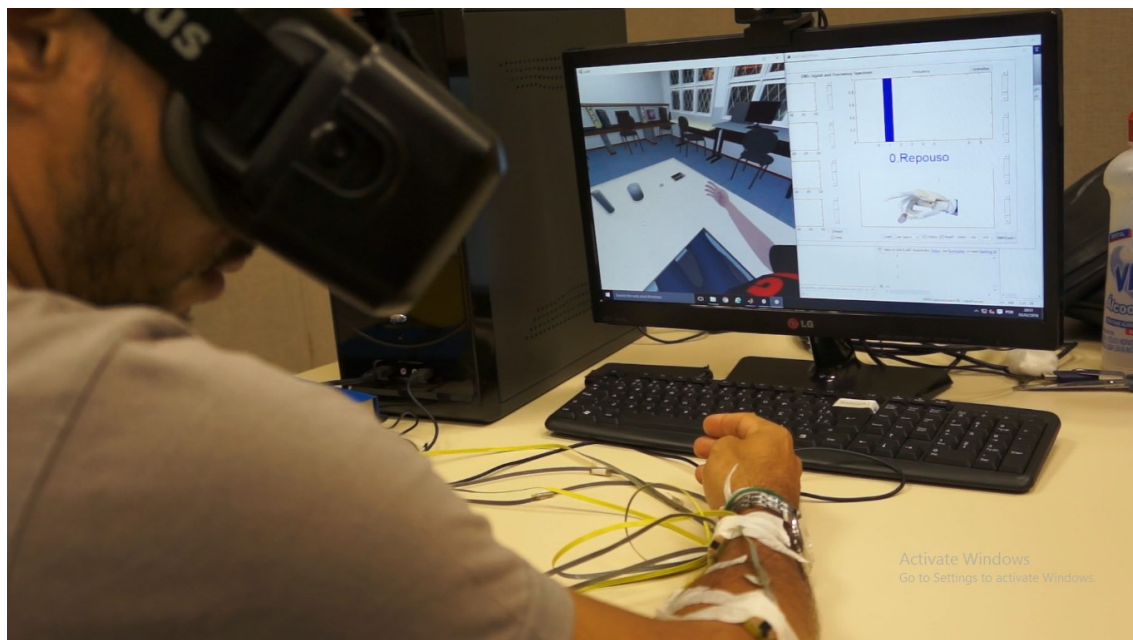


Figure 36. Robotic hand built with a 3D printing.



Additionally, experiments with a virtual reality environment (VRE) were also conducted (Figure 37). The VRE was built to allow a visual biofeedback during the experiments, and can be used as a training system for the use of myoelectric prosthesis. The VRE includes all the movements adopted in this research by controlling the individual articulations resembling human fingers. Only finger flexions were controlled, while the return to the state position is an implicit action when a command control indicates a change at the movement.

Figure 37. Virtual reality environment for training the control of a myoelectric prosthesis.



4.4. Towards a single-channel recognition system

The effect of using a reduced number of electrodes to recognized dexterous hand/finger movements was analyzed, in order to identify the scope of the proposed method focused on low-density MES. All the possible combinations using four electrodes were tested, in order to compare the improvement of the performance when increasing the number of MES channels. Fifteen different MES channel combinations were used to train the MES pattern recognition system, grouped into four sets according to the number of channels, referred as four-channel (4-CH), to a single-channel (1-CH) system. From the results, the best channel combination for these sets were summarized in Table 12. A comparison of performance from each amputee is presented, underlining the best accuracy.

This analysis was performed for each one of the categories of movements proposed in this research.

For GA movements, it was found that 3-CH and 4-CH systems had performances very similar in most of cases, with difference in accuracy between both systems from 0.1% to 3.9%. Four amputees showed having the best performance when 4-CH system was tested (A1, A3, A8 and I0). Moreover, the 3-CH system achieved the best performance for four amputees (A4, A5, A7 and A9). However, there were amputees who achieved the best performance using 3-CH and 2-CH systems, such as A6 and A9, respectively. At overall, it was found that the use of more channels improves the performances for most of amputees, however, these differences are not significant ($p = 0.9397$).

Table 12. Comparison of accuracy for different number of MES channels.

CH	Subjects										Mean	SD
	1	2	3	4	5	6	7	8	9	10		
CA												
1	53.7	54.4	43.5	41.3	39.0	48.2	90.4	48.9	50.6	51.0	52.1	13.7
2	67.3	63.0	43.1	45.2	44.2	44.5	93.8	62.6	63.8	70.3	59.8	15.2
3	71.4	61.9	46.1	52.0	44.9	43.9	96.3	72.8	65.6	77.1	63.2	16.1
4	74.9	57.4	46.6	49.7	44.8	43.3	94.2	76.7	61.3	78.6	62.7	16.6
CB												
1	60.2	56.6	21.6	42.0	49.7	34.2	68.1	45.4	47.5	57.8	48.3	12.9
2	67.2	54.1	15.8	46.0	57.7	36.0	70.4	49.4	51.4	57.3	50.5	14.9
3	77.6	51.7	14.3	46.9	55.3	44.7	67.3	50.9	48.0	60.9	51.8	15.8
4	75.4	44.2	12.7	41.4	50.2	40.4	64.4	47.1	47.7	55.1	47.9	15.6
CC												
1	40.6	36.8	24.5	29.8	25.9	32.3	68.4	33.3	43.1	39.2	37.4	11.9
2	59.6	50.7	27.3	33.1	31.1	34.9	68.4	46.9	55.9	55.6	46.3	13.3
3	69.8	50.7	28.9	37.3	32.9	37.1	71.3	52.1	53.8	62.6	49.6	14.5
4	73.8	49.7	27.6	35.4	33.2	34.6	68.9	58.8	48.4	59.2	49.0	15.2

Number of channels (CH). All values corresponds to accuracy [%].

However, for CB movements, five amputees showed the best performances with the 3-CH system, followed by 2-CH and 1-CH, as shown in Table 12. Although the 4-CH system showed similar performance in comparison to the 3-CH ($p = 0.2899$), it did not improve the results by including more MES channels. Similarly, for CC movements, the 3-CH system showed the best performance for most of amputees, followed by 4-CH and 2-CH, respectively.

Figure 38 shows the error obtained for 4-CH to 1-CH systems, for all amputees and all movements. It can be concluded that the increasing of MES channels does not necessarily improve the ability of discrimination of the pattern recognition system. Possibly, it could be due to the addition of irrelevant information that makes more difficult the separability among classes. In particular, for CB, it was noted that for all cases three channels provides better results.

The relationship between the accuracy and the number of channels is represented in Figure 39. It was obtained that single-channel systems is significant different ($p < 0.0286$) from 3-CH and 4-CH schemes in relation to the accuracy for CA movements; moreover, for CB, it was not found significant difference ($p > 0.2257$); and finally, for CC, the same scheme is significant different ($p < 0.0036$) for 3-CH and 4-CH.

From these results, it can be established that it is possible to obtain a pattern recognition system using a single-channel, with similar results compared with other ones based on low-level MES. However, it is worth to mention that it is expected a decreased performance in the recognition when increasing the number of classes. Thus, it is concluded that an interesting problem in this research area is the identification of a reduced set of movements, suitable for each amputee, according to his/her abilities to obtain a more accurate system.

Figure 38. Comparison among performance for four-channel to single-channel systems, for all categories of movements.

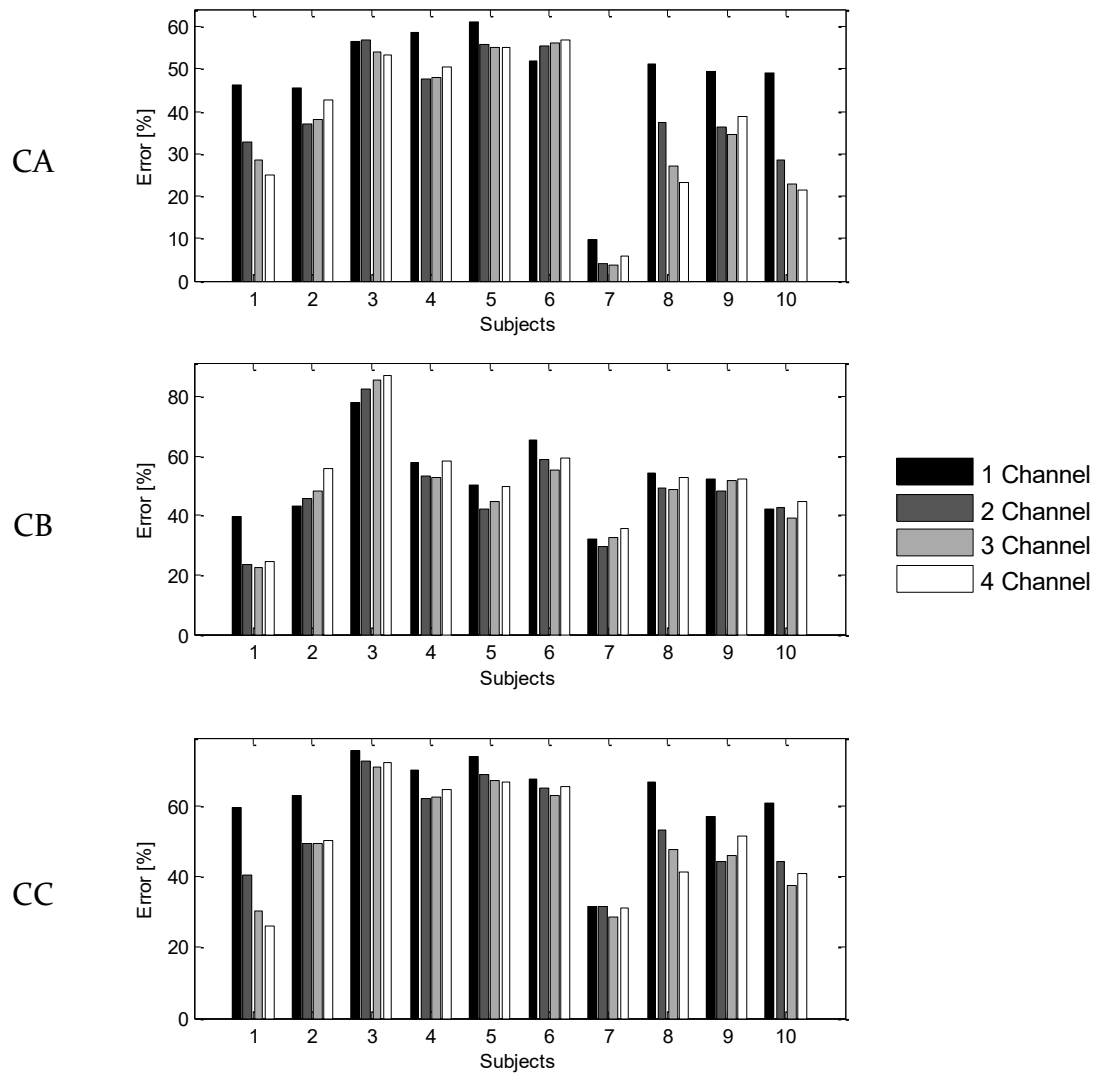
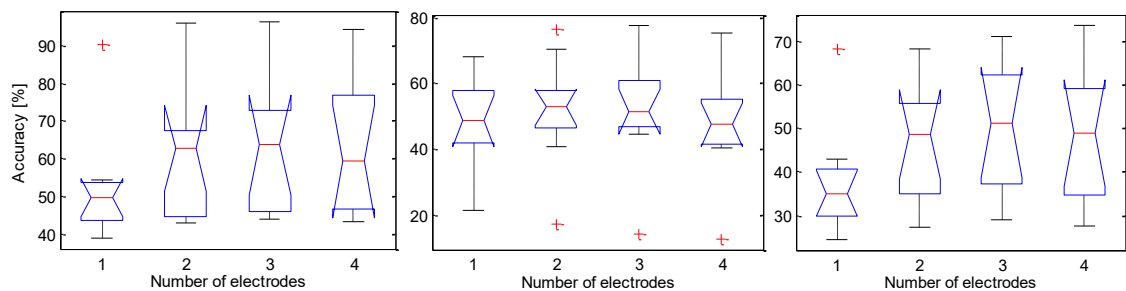


Figure 39. Graphic representation of the relationship between the number of electrodes and the accuracy of the pattern recognition system.



Due to the difference on the accuracy in relation to the number of channels, Table 13 summarizes the main selected muscle groups from previous results, which provide the better performance.

Table 13. Channels selected for the configurations with reduced number of electrodes.

Electrodes (Ch)	CA				CB				CC			
	1	2	3	4	1	2	3	4	1	2	3	4
Number of channels												
1		2				2				2		
2		2	3		1	2				2	3	
3		2	3	4	1	2		4		2	3	4

From this results, it can be found that a second channel provides relevant information to be selected for all channel configurations. This is expected, as this additional channel collects information from the finger flexion muscles, which plays an important role in the execution of all hand/finger movements here proposed. Moreover, a third channel is necessary for system configurations using two channels, when finger movements are involved, as this third channel collects information from the wrist flexion muscles, which are contracted along other muscles in hand movements using fingers. For grasp movements, the first channel has an important contribution, such as expected, due to this channel collecting information from deep muscles of the first chirodactyl, which have an important action for most of movements for grasp purposes. Finally, a fourth channel may be considered on all three-channel configurations, as it provides information about the extensors muscles.

4.5. Assessment of suitable dexterous movements

An assessment of the movements performed by amputees regarding discrimination abilities, taking into account his/her ability to repeat patterns belonging to the same movement and to distinguish patterns from other movements was performed. The analysis was divided into the categories of movements for individual finger movements (CA) and grasp movements (CB). The overall results are shown in Table 14.

Table 14. Results for PNM index for movements of CA and CB.

Mov.	Amputees										PNM
	1	2	3	4	5	6	7	8	9	10	Average
Individual finger movements (CA)											
RT	0.98	1.00	0.39	0.95	0.44	0.48	1.00	0.97	0.89	1.00	0.81 ± 0.25
F1	0.75	0.00	-0.04	-0.85	-0.41	-0.57	0.99	-0.61	-0.96	0.41	-0.13 ± 0.64
F2	0.50	-0.20	-0.59	-0.44	-0.60	-0.57	0.10	0.10	-0.27	0.52	-0.14 ± 0.41
F3	-0.16	-0.29	0.00	0.17	-0.28	-0.66	0.59	0.55	0.74	0.25	0.09 ± 0.43
F4	-0.16	-0.50	-0.25	-0.31	-0.86	-0.19	0.62	0.71	-0.65	-0.09	-0.17 ± 0.47
F5	-0.07	-0.72	-0.85	-0.24	-0.55	-0.10	0.75	0.45	0.10	0.20	-0.11 ± 0.48
HC	-0.42	-0.24	-0.22	-0.29	0.08	-0.55	0.99	-0.05	0.20	0.57	0.01 ± 0.45
HO	0.68	0.41	-0.26	-0.01	-0.04	0.59	0.99	0.65	0.94	0.57	0.45 ± 0.40
Grasp movements (CB)											
RT	0.99	1.00	-0.76	1.00	0.68	0.97	1.00	1.00	1.00	0.99	0.79 ± 0.52
LD	0.90	0.45	-0.91	-0.06	-0.58	-0.51	0.49	-0.47	0.56	0.30	0.02 ± 0.57
LT	0.24	-0.04	-0.66	-0.49	-0.19	-0.59	0.06	-0.52	-0.53	-0.12	-0.28 ± 0.30
T	0.45	-0.24	-0.70	-0.36	0.19	-0.61	0.06	-0.53	-0.32	0.01	-0.21 ± 0.35
TP	-0.07	-0.01	-0.64	-0.37	0.30	0.08	0.05	-0.71	-0.39	-0.02	-0.18 ± 0.31

4.5.1. Individual Finger Movements

A comparison conducted for eight movements using PNM index showed that the rest state is easily differentiated from the others. Opening hand movement was the most distinguished among others (0.45), followed by third

chirodactyl (0.09) and closing hand (0.01). The second and fourth chirodactyls had the greatest difficulty for discrimination, with values below of -0.14, followed closely by first chirodactyl and fifth chirodactyl. However, amputees A1, A7 and A10 showed easiness to recognize correctly the first chirodactyl (from 0.41 to 0.99) and the second chirodactyl (from 0.10 to 0.52). Also, A7, A8, A9 and A10 showed high separability for third and fifth chirodactyls.

An individual assessment of subjects showed that A7, A8 and A10 had indices above 0.4 in at least five movements, while A7 had the second chirodactyl almost 0.6. However, A2, A3, A4, A5 and A6 had indices below -0.2 for second, fourth and fifth chirodactyls. Also, most participants had negatives indices for first chirodactyl and closing hand.

4.5.2. Grasp Movements

In general, full hand wrap grasp (LD) had the second best PNM index (0.02) after rest state (0.79), followed by tip pinch (-0.18). The hardest movement was lateral grasp (LT) with 0.28. For amputees A1, A2, A7, A9 and A10, LD grasp had a very high performance in relation to the other functional movements, with indices from 0.3 up to 0.9, which means a highlighted easiness to accomplish this movement. However, A3 and A5 had the worst performance for this movement among the others, with indices from -0.58 to -0.91. For A5 and A6, the tip pinch showed highest indices (0.3 and 0.08, respectively), while A8 had the worst value among the other movements (-0.71). Amputees A3, A4 and A9 also showed trouble to accomplish this movement. In relation to tripod grasp, A1 showed a high ability to hold similar patterns across repetitions (0.45), while A5, A7 and A10 had a medium performance, with indices from 0.01 up to 0.19. Among all amputees, A3 had a strong difficulty, showing a high confusion of grasp movements with rest state. A8 and A4 also showed good results, distinguishing very well functional movement from rest state (PNM=1). A4 also showed an

easiness to differentiate LD grasp from the other movements. Details of the above results can be found in Table 15.

The amputees showed two different tendencies according to their abilities for movement learning. In the first one, some amputees achieved a high performance with differentiated patterns among the proposed movements. In the second one, some amputees showed difficulties to generate repeatable patterns in some movements, implying that they would require additional sessions using the protocol proposed to accomplish better results. In relation to the amputee's characteristics, low correlations of accuracies with age ($\rho = -0.365$ for GA and $\rho = 0.134$ for GB), and time since amputation ($\rho = -0.290$ for GA and $\rho = -0.068$ for GB) showed a reduced impact on the results

5. Discussion

The objective of this thesis was to propose a method able to recognize patterns from dexterous hand/finger movements from amputees based on low-density MES. A research was conducted with different feature combinations to define an optimal set able to improve the results of classification. The results indicate that a feature selection using SFS-based methods was highly variable between subjects, while GA-based methods provide more homogeneous feature subsets. Moreover, the methods SFS and SFS-CH (SFS applied by channel independently) showed different results according to the algorithm used for classification.

In terms of the nature of the features, GA selected, in most of cases, DFA and HFD features, which means the suitability of these features to characterize the complexity of the MES. However, the feature AR model was also considered with high relevance in the proposed feature set, which is consistent with literature as shown in Several factors are taken into account both in the motor learning and acquisition of abilities during the training with an upper-limb prosthesis, as verbal instructions, characteristics and variability of practice, active participation and motivation of the user, feedback, among others. Some studies have been focused on developing multifunctional upper limb prosthesis combined to training environments to provides biofeedback (CUNHA, 2002). However, a methodology to assess the amputees' abilities to control a prosthesis is a lack in the literature (BOUWSEMA; VAN DER SLUIS; BONGERS, 2014).

Table 1. Other features from the time domain, such as SSC and ZC, were also found to be relevant in solving the problem in this research, which provide information about frequency properties of the signal. Similar results were achieved by the method SFS, which suggests the relevance of these features to be

selected according both SFS and GA methods. However, SFS includes the feature MNF in the frequency domain, which involves a transformation. Moreover, SFS uses the classification accuracy as criteria for selection, which makes it dependent on the selection of the classifier and time consumption for training and validation. Otherwise, GA is based on the entropy of the feature distribution, which provides high-quality results for feature selection and avoids local solutions, as was here reported. In terms of computational cost, GA provides a suitable method for feature selection in comparison with methods SFS. As a result of the factors mentioned above, the selection of the outcome of GA was proposed to provide a better characterization of dexterous patterns from MES. It should also be noted that extraction of same features from all channels is more convenient for simpler implementations. However, this study showed that it is possible to obtain better results with a single-channel approach, but it would require a specific method for each subject. Thus, a suitable scheme to get the best results is based on the best performance achieved with GA + SVM. It is worth to comment that KNN also could be considered as a good classifier, due to present a performance close to SVM and have a lower computational cost.

In relation to the number of classes, CA includes eight, CB includes six and CC has thirteen. Notice that a high number of classes makes the recognition to be more complex. A comparison of the overall results showed that grasp movements had a lower performance, even when the scheme included fewer classes. CB movements had lower accuracy than gestures of CA, for all amputees, except for amputee A5, with difference between categories from 0.21% to 5.66%. Note that the classification accuracy was calculated by post-processing (offline). Although each subject's performance was different (i.e. amputees A7, A10 and A8 achieved generally better performance than the other ones), most of them presented clear abilities for movements recognizing. Specifically, the amputee A3 showed difficulties when performing grasp movements, which reflects in the results.

However, results for recognition of individual finger for this amputee (A3) was similar to other participants ($96.4 \pm 1.3\%$).

In all cases, it was found a lower accuracy for the amputees in comparison with subjects of the control group, which may be due to several reasons, such as disuse of the muscles or damage of the remaining muscles (Kumar et al., 2013). All analyses of the movement categories lead to understand the abilities from amputees to send commands to control a prosthetic hand. This study about dexterous movements also covered the use of individual fingers to understand the abilities of amputees to perform grasps movements. Thus, grasp movements recognition seems to be more difficult than individual finger movement, mainly due to the simultaneous use of more fingers during grasp. The category including all the movements showed the possibility of identifying both individual finger and grasp movements with high accuracy.

In addition, it is known from the literature that the relation between strength of contraction and MES amplitude is non-linear for muscle contractions on dexterous movements, making difficult the differentiation of muscular activities of rest state at these conditions (Arjunan and Kumar, 2010; Arjunan et al., 2014). However, MES from dexterous movements have a poor SNR (Signal to Noise Ratio), while strongest contractions produce a bigger SNR, making the features based on amplitude feasible to obtain better performance. Also, in the experiments with amputees, it was found greater difficulty to accomplish lower contractions during the performance of movements in comparison with able-bodied subjects, mainly because the amputation effect. However, spasms and difficulty for contraction of selective muscles while conducting dexterous movements for a long time were also reported by the amputees, mainly A3 and A5, although we think these issues can be overcome with a more frequent use of the muscles. Also, we think that the level of amputation has influence in the results, specifically for subjects A4, A6 and A9, who also had some changes on the insertion point of the muscles due to the amputation height.

For all experiments, the participants were required to concentrate whilst the movements were carried out. Muscle fatigue was attempted to be avoided leaving enough time between repetitions during the tests, and no more than one hour was considered for tests, in order to avoid mental stress. This is due to the protocol used, in which all the participants held the arms on the table, but a final application would not have this limitation.

Despite the system was validated in offline mode, the time to record and process the raw MES was lower than 300 ms, which agrees with the criteria reported in (Englehart et al., 2001) to be used in real time application. A comparison of our technique with previous works can be unbalanced because of the difference in number of electrodes and muscles selected, number of classes, whether amputees were included in the study and the kind of movements used in relation to the level of dexterity. However, it is possible to obtain a ratio (R) shown in Equation 5.1, which is proposed in this thesis, to get the relation between the number of classes and the number of electrodes, meaning that the higher is value of R , the better is the method. Table 15 shows a summary of previous works which we calculate the value of R for comparison with our work. The overall accuracy and details about the system used were also included, such as number of channels, number of classes, and number and kind of participants, whether able-bodied or amputee. Moreover, the kind of movements recognized is also evaluated, as if movements related to finger, hand, wrists, forearm and grasps were specified. Finally, the ratio R here proposed was calculated, which is defined by the relation shown in Equation 5.1.

$$R = \frac{N.Cl}{N.Ch} \quad 5.1$$

where $N.Cl$ is the number of classes to be recognized and $N.Ch$ is the number of channels used to collect the information from the system. In this sense, our work presents value of R equal 2 (for CA), 1.5 (for CB) and 3.25 (for CC), which means the highest value in comparison with the other researches.

Table 15. Comparison of previous research with this current work.

Authors	N. Ch	N. Cl	Kind movements	of Subjects	Acc [%]	Ratio R
2002, Peleg et al.	2	5	Fingers	4 C	93	2.50
2006, Tsenov et al.	2	4	Finger hand	and 1 C	98	2.00
	4	4				1.00
2008, Oskoei and Hu	4	5	Wrist	11 C	97	1.25
2009, Tenore et al.	19	12	Finger	5 C and 1 A	88	0.63
	32	12	Finger	5 C and 1 A	94	0.38
2009, Chu and Lee	4	10	Wrist	and 11 C	97	2.50
			grasp			
2011, Cipriani et al.	8	7	Finger	5 C and 5 A	48 to 98	0.88
2011, Li et al.	12	11	Wrist	and 5 C	71.3	0.92
			grasp	8 A		
2012, Phinyomark et al.	1	2	Forearm, wrist and hand	20 C	78 to 91	2.00
2013, Al-Timemy et al.	6	15	Finger	10 C	89	2.50
	6	12	Finger	6 A	79	2.00
2013, Wang et al.	2	8	Grasp	6 C	98	4.00
2015, Castro et al.	5	6	Finger	4 C	97	1.20
	5	10	Finger	and 4 C	80	2.00
			grasp			
This study	4	8	Finger	and 10 C and 10 A	99	2.00
			hand			
	4	6	Grasp	10 C and 10 A	97	1.50
	4	13	Finger	and 10 C and 10 A	97	3.25
			grasp			

Number of channels (N.Ch); Number of classes (N.Cl); Control group (C); Amputees (A); Accuracy (Acc).

Thus, our research represents a contribution in the study of non-linear techniques to characterize MES for accurately recognized dexterous hand/finger movements. The validation of the proposed method to recognize all thirteen movements considered in this research, with high accurate results, represents also a contribution for the literature. Additionally, the use of low-density MES represents an important advantage for the acceptance of prostheses by amputees, according to (KHUSHABA et al., 2012), who state that the reduction in the

number of electrodes, without compromising the classification accuracy, would significantly simplify the requirements to control myoelectric prostheses.

Analyzing Table 15, from the studies considering dexterous movements, (CHU; LEE, 2009) included only two grasp movements (cylindrical and lateral grasps). It is worth mentioning the study of LI et al. (2011), which recognizes four different grasps among eleven movements, with 71.3% of accuracy, validated on amputees. However, their work included high-density MES (twelve channels). Moreover, AL-TIMEMY et al. (2013) included twelve different based-finger movements with six amputees and six MES channels, with 89% of accuracy. However, their study did not include grasp movements, a drawback that our research has overcome. However, CASTRO; ARJUNAN; KUMAR (2015) included finger and grasp movements, but using five channels, with 80% of accuracy and only was validated offline on able-bodied subjects.

Additionally, our study included the most important movements from a user-centered perspective according to PEERDEMAN et al. (2011), which improve significantly the functionality of the prostheses for activities of daily living. Moreover, results presented in this research can be considered quite relevant, due to the validation of signal processing techniques with ten amputees, even in both offline and online modes. For our knowledge, no studies for recognition of dexterous hand/finger movements in more than eight amputees were found in literature.

The analysis performed for the selection of the suitable dexterous hand/finger movements sought identifying the abilities from an amputee to use a reliable myoelectric control. This lead the assessment of the movement-learning abilities of upper-limb amputees using a myoelectric prosthesis and performing distinguishable muscle patterns associated with hand, individual finger and grasp movements. The method developed in this thesis can be used in clinical

environments for cross-sectional studies to assess both amputees' abilities and training in prosthesis control.

One approach is to develop technologies and training methods that take advantage of the innate control and learning strategies used by the brain to control a biological limb. In fact, the central nervous system (CNS) uses strategies to efficiently perform the task of grasping and manipulating objects. Thus, the control system would modify ongoing motor commands based on sensory input, producing predictive motor commands used to accomplish the task, such as found for different authors (DOSEN et al., 2015; LEVIN; WEISS; KESHNER, 2015). The improvements throughout new experiments can be associated with a familiarization with the movements themselves. In addition, due to a series of repetition movements, the brain inputs associated with motor learning are training, and therefore, could be affected, improving the abilities for prosthesis control purposes.

In relation to the discrimination abilities, variations in the performances among amputees suggest differences in their learning abilities, which could determine the duration of the training process. For example, amputees A7 and A1 showed the highest performance, for hand/finger movements and for grasp movements, respectively. However, A3 showed the lowest performance with grasp movements. Thus, the response variability among subjects reported in this thesis may be influenced by factors like level of education, number of sessions, fatigue and postural control, such as also detected by CANO-DE-LA-CUERDA et al. (2015) and ENGDAHL et al. (2015). Likewise, clinical and physiological parameters might affect in the discrimination and learning abilities for a natural prosthesis control (ATZORI et al., 2016).

6. Conclusion

The method proposed in this thesis lead to identify a more skilled group of movements considering individual finger flexion, opening/closing hand and grasps movements, for a prosthetic hand, using weak signals and low-density MES. The system is divided into three categories for the study: individual finger movements, opening/closing hand and grasps movements. A set of feature combining non-linear techniques and statistical parameters of the MES amplitude were also proposed to be used as input to the classifiers. In terms of classification, LDA had poor results, with the best results obtained by SVM, followed closely by KNN. However, KNN is faster than SVM, which implies an advantage over SVM for real time applications, taking into account the not significant difference on statistic tests. These results are encouraging for the development of real-time control strategies based on the use of small number of MES channels to accurately control dexterous prosthetic hands. In comparison with others works in the literature, the method proposed in this thesis reached the highest average accuracy (98.9%) and the highest value of R (3.25) in works including amputees, which means that this method is reliable and efficient. The validation of the method here proposed was performed in offline mode. Future works include tests about the validity of the proposed method in real-time applications using embedded hardware, towards a single-channel system for the recognition of dexterous hand/finger gestures of amputees.

The design and control of versatile upper limb prostheses is a very challenging task. While many breakthroughs have been made over the last several decades, the difference in performance and quality between human hands and artificial hands is quite substantial. Robotic hands have many degrees of freedom distributed among several kinematic chains, the fingers. The complexity of the mechanical design is needed to adapt hands to the many kinds of movements

required in unstructured environments. Although it has been acknowledged that a prosthetic limb does not provide all of the amputation functionality of a human limb, there have been many recent advances to improve the upper limb prosthetic restoration.

A limitation of this research is the fact that we did not divide the participants into different learning capacities for the analysis. We do not know if all subjects could be treated as a homogeneous experimental group, due to the low number of participants, and we did not expect to find differences in learning beforehand, related to the characteristics of the subjects. However, this interesting finding was worth mentioning. In future experiments, it is recommended to define possible differences in learning ability in advance. Moreover, we had some limitations for this research. First, we had a limited number of tests to capture data from amputees. Second, we did not include the use of visual feedback of classification response to amputees while validation was carried out. We could identify that is need to perform an enough number of previous experiments for a better understanding of the abilities of the amputee, before presenting biofeedback, to avoid frustration and dejection to the volunteer.

Future research and development of upper limb prostheses continue to be held to mimic the human hand in terms of dexterity and adaptive capacity. The literature shows that movement intention should be recognized and selected by the user, while the control of the actuators for setting the joint angles, trajectories, level of pressures should be performed automatically in a low level control system (ANTFOLK et al., 2010), making sure to hold objects and avoid slippage. Recent works show an increasingly interest to provide more functionality to the current prostheses for better acceptance on amputees, which are addressed to be able to identify dexterous hand/finger movements and different precision grasps to increase the skills on tasks of daily living. Further, different works use weak MES instead of high muscle forces to obtain a better muscle-computer interaction. Non-linear techniques like fractal analysis (used in this thesis) are being used also

in other works of the literature to model these weak MES, in order to develop high level control systems. However, also low density is desirable to improve the accuracy of these systems, avoiding interferences, training and decreasing computational cost for real time implementations. However, implementation of these techniques could require embedded systems with mid-range microcontrollers or digital signal processors (DSP). Future studies should investigate changes of results including simultaneous knowledge of performance during validation. Simulators with virtual prosthesis could motivate the amputees by providing this feedback. Nevertheless, this study did not included able-bodied participants according to the precept that learning skills of the amputees are similar to the unimpaired participants.

6.1. Acknowledgements

This work has been supported by CAPES and FAPES/Brazil (Project Number 007/2014: Use of Robotics and Assistive Technology for Children and Adults with Disabilities).

6.2. Publications

During the development of this research, the following publications were realized:

Journals:

Accepted:

- **Villarejo Mayor, J.J.**; Mamede Costa, R.; Frizera Neto, A.; Freire Bastos, T.F. Decodificación de Movimientos Individuales de los Dedos y Agarre

a Partir de Sinales Mioelétricas de Baja Densidad. Revista Iberoamericana de Automática e Informática Industrial, ISSN 1697-7912. Accepted 21-November-2016.

- **Villarejo Mayor, J.J.**; Mamede Costa, R.; Frizera Neto, A.; Freire Bastos, T.F. Dexterous Hand Gestures Recognition Based on Low-Density sEMG Signals for Upper-Limb Forearm Amputees. Research on Biomedical Engineering, ISSN 2446-4740 / 2446-4732. Submitted 28-Janeiro-2016.

Submitted:

- Mamede Costa, R.; **Villarejo Mayor, J.J.**; Freire Bastos, T.F. User adaptation to myoelectric prostheses: implications in learning hand movements. Disability and Rehabilitation. Submitted 14-February-2017.
- Mamede Costa, R.; **Villarejo Mayor, J.J.**; Freire Bastos, T.F. Assessment of Dexterous Hand Movements of Amputees Based on Myoelectric Patterns for Prosthesis Control. Archives of Physical Medicine and Rehabilitation. Submitted 11-September-2016.

Conferences:

- **Villarejo Mayor, J.J.**; Frizera Neto, A.; Freire Bastos, T.F. Towards an Online Upper-Limb Myoelectric Control for Transradial Amputees. XII Brazilian Symposium of Intelligent Automation (SBAI), 2015, Natal, Brasil.
- **Villarejo Mayor, J.J.**; Giracca, C.N.; Frizera Neto, A.; Freire Bastos, T.F. Real Time Control of an Artificial Hand Prosthesis Using Low Density sEMG Signals. 1st International Workshop on Assistive Technology, 2015, Vitória, Brasil. p.336 – 338

- **Villarejo Mayor, J.J.**; Giracca, C.N.; Frizera Neto, A.; Freire Bastos, T.F. Myoelectric Control for an Individual Finger Artificial Robotic Hand. XVI Brazilian Congress of Biomechanics, 2015, Florianópolis, Brasil.
- **Villarejo Mayor, J.J.**; Mamede Costa, R.; Freire Bastos, T.F.; Frizera Neto, A. Identification of low level sEMG signals for individual finger prosthesis. 5th IEEE Biosignals and Biorobotics conference (BRC 2014), Salvador, Brasil. p.1 – 6
- **Villarejo Mayor, J.J.**; Frizera Neto, A.; Freire Bastos, T.F. Detección de la flexión de los dedos y tareas de agarre para una prótesis de mano usando sEMG. VI Day AITADIS of Rehabilitation and Technologies for Disability Support, 2014, Asunción, Paraguay.
- **Villarejo Mayor, J.J.**; Frizera Neto, A.; Freire Bastos, T.F. Towards a Hand Gestures Recognition Using Weak and a Single-Channel Surface EMG Signals. XXIV Brazilian Congress on Biomedical Engineering (XXIV CBEB), 2014, Uberlandia, Brasil.
- **Villarejo Mayor, J.J.**; Frizera Neto, A.; Freire Bastos, T.F.; Sarmiento Vela, J.F. Pattern recognition of hand movements with low density sEMG for prosthesis control purposes. 2013 IEEE 13th International Conference on Rehabilitation Robotics (ICORR 2013), Seattle, USA.
- **Villarejo Mayor, J.J.**; Mamede Costa, R.; Sarmiento Vela, J.F.; Frizera Neto, A.; Freire Bastos, T.F.; Kant Kumar, D. Sistema de Control Individual de Dedos de una Prótesis Utilizando Señales Electromiográficas de Superficie. VII Iberoamerican Congress of Technologies for Disability Support (VII IBERDISCAP), 2013, Santo Domingo, Dominican Republic.
- Sarmiento Vela, J.F.; **Villarejo Mayor, J.J.**; Frizera Neto, A.; Freire Bastos, T.F. Protocolo de Captura de Señales sEMG para el Reconocimiento de Gestos de la Mano. VII Iberoamerican Congress of Technologies for Disability Support (VII IBERDISCAP), 2013, Santo

Domingo, Dominican Republic.

- López Delis, A.; **Villarejo Mayor, J.J.**; Mamede Costa, R.; Freire Bastos, T.F. Proposal of a Characterization Method for Movement Dysfunction Detection. ISSNIP- Biosignals and Robotics for Better and Safer Living, 2013, Rio de Janeiro, Brasil.
- Mamede Costa, R.; **Villarejo Mayor, J.J.**; Tello, R.G.; Freire Bastos, T.F. Survey on sEMG Signal Analysis and Changes in the Somatosensory and Motor Cortices in Amputees. ISSNIP- Biosignals and Robotics for Better and Safer Living, 2013, Rio de Janeiro, Brasil.
- **Villarejo Mayor, J.J.**; Tello, R.G.; Mamede Costa, R.; Frizera Neto, A.; Freire Bastos, T.F. Reconocimiento de Tareas para una Prótesis Mioeléctrica Basado en Wavelet Packet. V Day AITADIS of Technologies for Disability Support, 2012, Vitória, Brasil.

Chapters of books:

- **Villarejo Mayor, J.J.**; Mamede Costa, R.; Frizera Neto, A.; Freire Bastos, T.F. Movement Identification Using Weak sEMG Signals of Low Density for Upper Limb Control. Tecnologias, Técnicas e Tendências em Engenharia Biomédica.1 ed.: Canal6 Editora, 2014, v.1, p. 280-300.
- Poosapadi Arjunan, S.; Kant Kumar, D.; Bueno, L.; **Villarejo Mayor, J.J.**; Freire Bastos, T.F. Upper Limb Prosthesis Devices. Devices for Mobility and Manipulation for People with Reduced Abilities (Rehabilitation Science in Practice Series).1 ed.: CRC Press, 2014, v.1, p. 179-196.

7. References

AL-TIMEMY, A. H. et al. Classification of finger movements for the dexterous hand prosthesis control with surface electromyography. **IEEE Journal of Biomedical and Health Informatics**, v. 17, n. 3, p. 608–618, 2013.

Anatomy of the hand. Disponível em: <<http://www.eatonhand.com/hom/hom033.htm>>. Acesso em: 10 oct. 2016.

ANTFOLK, C. et al. Using EMG for real-time prediction of joint angles to control a prosthetic hand equipped with a sensory feedback system. **Journal of Medical and Biological Engineering**, v. 30, n. 6, p. 399–406, 2010.

ARJUNAN, S. P. et al. Upper Limb Prosthesis Devices. In: **Devices for Mobility and Manipulation for People with Reduced Abilities**. [s.l: s.n.]. p. 121–127.

ARJUNAN, S. P.; KUMAR, D. K. Fractal theory based Non-linear analysis of sEMG. **2007 3rd International Conference on Intelligent Sensors, Sensor Networks and Information**, p. 545–548, 2007.

ARJUNAN, S. P.; KUMAR, D. K. Decoding subtle forearm flexions using fractal features of surface electromyogram from single and multiple sensors. **Journal of neuroengineering and rehabilitation**, v. 7, n. 1, p. 53, 2010a.

ARJUNAN, S. P.; KUMAR, D. K. Decoding subtle forearm flexions using fractal features of surface electromyogram from single and multiple sensors. **Journal of neuroengineering and rehabilitation**, v. 7, n. 1, p. 53, 2010b.

ATZORI, M. et al. Electromyography data for non-invasive naturally-controlled robotic hand prostheses. **Scientific data**, v. 1, p. 140053, 2014.

ATZORI, M. et al. Effect of clinical parameters on the control of myoelectric robotic prosthetic hands. **Journal of rehabilitation research and development**, v. 53, n. 3, p. 345–58, 2016.

BASMAJIAN, J. V. **Muscles Alive—their functions revealed by**

electromyography. 4th Ed. ed. Baltimore: Williams & Wilkins, 1978.

BOUWSEMA, H.; VAN DER SLUIS, C. K.; BONGERS, R. M. The Role of Order of Practice in Learning to Handle an Upper-Limb Prosthesis. **Archives of Physical Medicine and Rehabilitation**, v. 89, n. 9, p. 1759–1764, 2008.

BOUWSEMA, H.; VAN DER SLUIS, C. K.; BONGERS, R. M. Changes in performance over time while learning to use a myoelectric prosthesis. **Journal of neuroengineering and rehabilitation**, v. 11, n. 1, p. 16, 2014.

BUENO, L. et al. Human–robot cognitive interaction. In: PONS, J. L. (Ed.). **. Wearable Robots: Biomechatronic Exoskeletons**. Chichester, England: John Wiley & Sons, Ltd, 2008. p. 87–125.

CANO-DE-LA-CUERDA, R. et al. Teorías y modelos de control y aprendizaje motor. Aplicaciones clínicas en neurorrehabilitación. **Neurología**, v. 30, n. 1, p. 32–41, 2015.

CARLSEN, B. T.; PRIGGE, P.; PETERSON, J. Upper extremity limb loss: Functional restoration from prosthesis and targeted reinnervation to transplantation. **Journal of Hand Therapy**, v. 27, n. 2, p. 106–114, 2014.

CARROZZA, M. C. et al. The development of a novel prosthetic hand - Ongoing research and preliminary results. **IEEE/ASME Transactions on Mechatronics**, v. 7, n. 2, p. 108–114, 2002.

CARVALHO, J. A. **Amputações de membros inferiores**. 2. ed. São Paulo: Manole, 2003.

CASTILLO GARCIA, J. F. **Interfaz cerebro computador adaptativa, basada en agentes software para la discriminación de cuatro tareas mentales**. [s.l.] Universidad del Valle, 2015.

CASTRO, M. C. F.; ARJUNAN, S. P.; KUMAR, D. K. Selection of suitable hand gestures for reliable myoelectric human computer interface. **BioMedical Engineering OnLine**, v. 14, n. 1, p. 1–11, 2015.

CHEN, Y. et al. Upper Limb Motion Recognition Based on Two-Step SVM Classification Method of Surface EMG. v. 6, n. 3, p. 249–266, 2013.

CHOWDHURY, R. H. et al. Surface electromyography signal processing and

classification techniques. **Sensors (Basel, Switzerland)**, v. 13, n. 9, p. 12431–12466, 2013a.

CHOWDHURY, R. H. et al. Surface electromyography signal processing and classification techniques. **Sensors**, v. 13, n. 9, p. 12431–66, 17 Jan. 2013b.

CHU, J. U.; LEE, Y. J. Conjugate-prior-penalized learning of gaussian mixture models for multifunction myoelectric hand control. **IEEE Transactions on Neural Systems and Rehabilitation Engineering**, v. 17, n. 3, p. 287–297, 2009.

CIPRIANI, C. et al. Online myoelectric control of a dexterous hand prosthesis by transradial amputees. **IEEE Transactions on Neural Systems and Rehabilitation Engineering**, v. 19, n. 3, p. 260–270, 2011.

CUNHA, F. L. DA. **São Carlos hand, a multifunction upper limb prosthesis: a study of the mechanism, actuators and sensors**. [s.l.] University of Sao Paulo, 2002.

DOSEN, S. et al. Building an internal model of a myoelectric prosthesis via closed-loop control for consistent and routine grasping. **Experimental Brain Research**, v. 233, n. 6, p. 1855–1865, 2015.

DUDA, R. O.; HART, P. E.; STORK, D. G. **Pattern Classification**. 2nd. ed. New York, NY: Wiley, 2001.

ENGDAHL, S. M. et al. Surveying the interest of individuals with upper limb loss in novel prosthetic control techniques. **Journal of neuroengineering and rehabilitation**, v. 12, n. 1, p. 53, 2015.

ENGLEHART, K.; HUDGINS, B. A robust, real-time control scheme for multifunction myoelectric control. **IEEE transactions on bio-medical engineering**, v. 50, n. 7, p. 848–854, 2003.

ENGLEHART, K.; HUDGINS, B.; PARKER, P. A. A wavelet-based continuous classification scheme for multifunction myoelectric control. **IEEE Transactions on Biomedical Engineering**, v. 48, n. 3, p. 302–311, 2001.

ESTELLER, R. et al. A Comparison of waveform fractal dimension algorithms. **IEEE Transactions on Circuits and Systems I: Fundamental**

Theory and Applications, v. 48, n. 2, p. 177–183, 2001.

FARINA, D.; NEGRO, F. Accessing the neural drive to muscle and translation to neurorehabilitation Technologies. **IEEE Reviews in biomedical engineering**, n. 5, p. 3–14, 2012.

FEIX, T. et al. The GRASP Taxonomy of Human Grasp Types. **IEEE Transactions on human-machine systems**, p. 1–12, 2015.

GERDLE, B. et al. Acquisition, Processing and Analysis of the Surface Electromyogram. In: WINDHORST, U.; JOHANSSON, H. (Eds.). . **Modern Techniques in Neuroscience Research**. [s.l.] Springer Berlin Heidelberg, 1999. p. 705–755.

GOFFI, F. S. **Técnica Cirúrgica: Bases Anatômicas, Fisiopatológicas e Técnicas da Cirurgia**. Rio de Janeiro: Editora Atheneu, 2004.

GUO, S. et al. Comparison of sEMG-Based Feature Extraction and Motion Classification Methods for Upper-Limb Movement. **Sensors (Basel, Switzerland)**, v. 15, n. 4, p. 9022–38, 16 Jan. 2015.

HARGROVE, L. J. et al. Principal components analysis preprocessing for improved classification accuracies in pattern-recognition-based myoelectric control. **IEEE Transactions on Biomedical Engineering**, v. 56, n. 5, p. 1407–1414, 2009.

HSU, C.-W.; CHANG, C.-C.; LIN, C.-J. **A Practical Guide to Support Vector Classification** *BJU international*. [s.l.: s.n.].

HUANG, C.; WANG, C. A GA-based feature selection and parameters optimization for support vector machines. **Expert Systems with Applications**, v. 31, p. 231–240, 2006.

IBGE. **Census 2010**. Disponível em: <<http://www.ibge.gov.br/home/estatistica/populacao/censo2010/default.shtm>>. Acesso em: 2 feb. 2015.

JAPKOWICZ, N.; SHAH, M. **Evaluation Learning Algorithms a Classification Perspective**. [s.l.] Cambridge University Press, [s.d.].

KHUSHABA, R. N. et al. Toward improved control of prosthetic fingers

using surface electromyogram (EMG) signals. **Expert Systems with Applications**, v. 39, n. 12, p. 10731–10738, 2012.

KONRAD, P. **The ABC of EMG. A Practical Introduction to Kinesiological Electromyography**. Scottsdale, Arizona: Noraxon U.S.A, Inc., 2006.

KUMAR, D. K.; POOSAPADI ARJUNAN, S.; SINGH, V. P. Towards identification of finger flexions using single channel surface electromyography - able bodied and amputee subjects. **Journal of neuroengineering and rehabilitation**, v. 10, n. 1, p. 50, 2013a.

KUMAR, D. K.; POOSAPADI ARJUNAN, S.; SINGH, V. P. Towards identification of finger flexions using single channel surface electromyography-- able bodied and amputee subjects. **Journal of neuroengineering and rehabilitation**, v. 10, n. 1, p. 50, 2013b.

LEVIN, M. F.; WEISS, P. L.; KESHNER, E. A. Emergence of virtual reality as a tool for upper limb rehabilitation: incorporation of motor control and motor learning principles. **Physical Therapy**, v. 95, n. 3, p. 415–425, 2015.

LI, G. et al. Conditioning and sampling issues of EMG signals in motion recognition of multifunctional myoelectric prostheses. **Annals of Biomedical Engineering**, v. 39, n. 6, p. 1779–1787, 2011.

LIU, J. Adaptive myoelectric pattern recognition toward improved multifunctional prosthesis control. **Medical Engineering and Physics**, v. 37, n. 4, p. 424–430, 2015.

MERLETTI, R.; PARKER, P. J. **Electromyography. Physiology, Engineering and Non-Invasive Applications**. New York, NY: J. Wiley - IEEE Press, 2004.

NAIK, G. R.; KUMAR, D. K. Identification of hand and finger movements using multi run ICA of surface electromyogram. **Journal of Medical Systems**, v. 36, n. 2, p. 841–851, 2012.

NAIK, G. R.; KUMAR, D. K.; ARJUNAN, S. Use of sEMG in identification of low level muscle activities: Features based on ICA and Fractal dimension.

Proceedings of the 31st Annual International Conference of the IEEE Engineering in Medicine and Biology Society: Engineering the Future of Biomedicine, EMBC 2009, p. 364–367, 2009.

NAIK, G. R.; KUMAR, D. K.; ARJUNAN, S. P. Pattern classification of Myo-Electrical signal during different Maximum Voluntary Contractions: A study using BSS techniques. **Measurement Science Review**, v. 10, n. 1, p. 1–6, 2010.

OSKOEI, M. A. Evaluation of Support Vector Machines in Upper Limb Motion Classification Using Myoelectric Signal. p. 3–8, 2008.

OSKOEI, M. A.; HU, H. Myoelectric control systems-A survey. **Biomedical Signal Processing and Control**, v. 2, n. 4, p. 275–294, 2007.

OSKOEI, M. A.; HU, H. Support Vector Machine-Based Classification Scheme for Myoelectric Control Applied to Upper Limb. **IEEE Transactions on Biomedical Engineering**, v. 55, n. 8, p. 1956–1965, 2008.

PEERDEMAN, B. et al. Myoelectric forearm prostheses: State of the art from a user-centered perspective. **The Journal of Rehabilitation Research and Development**, v. 48, n. 6, p. 719, 2011.

PELEG, D. et al. Classification of finger activation for use in a robotic prosthesis arm. **IEEE Transactions on Neural Systems and Rehabilitation Engineering**, v. 10, n. 4, p. 290–293, 2002.

PHINYOMARK, A.; LIMSAKUL, C.; PHUKPATTARANONT, P. A Novel Feature Extraction for Robust EMG Pattern Recognition. **Journal of Computing**, v. 1, n. 1, p. 71–80, 2009.

PHINYOMARK, A.; PHUKPATTARANONT, P.; LIMSAKUL, C. Feature reduction and selection for EMG signal classification. **Expert Systems with Applications**, v. 39, n. 8, p. 7420–7431, 2012a.

PHINYOMARK, A.; PHUKPATTARANONT, P.; LIMSAKUL, C. Fractal analysis features for weak and single-channel upper-limb EMG signals. **Expert Systems with Applications**, v. 39, n. 12, p. 11156–11163, 2012b.

PHINYOMARK, A. et al. Feature extraction and reduction of wavelet transform coefficients for EMG pattern classification. **Elektronika ir**

Elektrotechnika, v. 122, n. 6, p. 27–32, 2012.

PONS, J. L. et al. Objectives and technological approach to the development of the multifunctional MANUS upper limb prosthesis. **Robotica**, v. 23, n. 3, p. 301–310, 2005.

SCHULZ, S. et al. A hydraulically driven multifunctional prosthetic hand. **Robotica**, v. 23, n. 3, p. 293–299, 2005.

SENIAM. **Seniam recommendations**. Disponível em: <<http://seniam.org>>. Acesso em: 2 feb. 2015.

SENSINGER, J. W.; LOCK, B. A.; KUIKEN, T. A. Adaptive pattern recognition of myoelectric signals: Exploration of conceptual framework and practical algorithms. **IEEE Transactions on Neural Systems and Rehabilitation Engineering**, v. 17, n. 3, p. 270–278, 2009.

SHENOY, P. et al. Online electromyographic control of a robotic prosthesis. **IEEE Transactions on Biomedical Engineering**, v. 55, n. 3, p. 1128–1135, 2008.

TENORE, F. V. G. et al. Decoding of individuated finger movements using surface electromyography. **IEEE Transactions on Biomedical Engineering**, v. 56, n. 5, p. 1427–1434, 2009.

THEODORIDIS, S.; KOUTROUMBAS, K. **Pattern Recognition**. 4th. ed. [s.l.] Academic press, 2008.

TOMMASI, T. et al. Improving control of dexterous hand prostheses using adaptive learning. **IEEE Transactions on Robotics**, v. 29, n. 1, p. 207–219, 2013.

TSENOV, G. et al. Neural Networks for Online Classification of Hand and Finger Movements Using Surface EMG signals. **8th Seminar on Neural Network Applications in Electrical Engineering (NEUREL)**, p. 167–171, 2006.

WANG, N.; CHEN, Y.; ZHANG, X. The recognition of multi-finger prehensile postures using LDA. **Biomedical Signal Processing and Control**, v. 8, n. 6, p. 706–712, 2013.

ZECCA, M. et al. Control of multifunctional prosthetic hands by processing the electromyographic signal. **Critical reviews in biomedical engineering**, v. 30, n. 4–6, p. 459–485, 2002.

ZHANG, H. et al. An adaptation strategy of using LDA classifier for EMG pattern recognition. **Proceedings of the Annual International Conference of the IEEE Engineering in Medicine and Biology Society, EMBS**, p. 4267–4270, 2013.

Appendices

Appendix A – Human Ethics Committee



UNIVERSIDADE FEDERAL DO ESPÍRITO SANTO
COMITÊ DE ÉTICA EM PESQUISA DO
CENTRO DE CIÊNCIAS DA SAÚDE

Vitória-ES, 15 de dezembro de 2011.

De: Prof. Dr. Adauto Emmerich Oliveira
Coordenador do Comitê de Ética em Pesquisa do Centro de Ciências da Saúde

Para: Prof. (a) Teodiano Freire Bastos Filho
Pesquisador (a) Responsável pelo Projeto de Pesquisa intitulado **“Mão artificial inteligente. Controle de mão e dedos de uma prótese artificial.”**

Senhor (a) Pesquisador (a),

Informamos a Vossa Senhoria, que o Comitê de Ética em Pesquisa do Centro de Ciências da Saúde da Universidade Federal do Espírito Santo, após analisar o Projeto de Pesquisa nº. 302/11 intitulado **“Mão artificial inteligente. Controle de mão e dedos de uma prótese artificial.”** e o **Termo de Consentimento Livre e Esclarecido**, cumprindo os procedimentos internos desta Instituição, bem como as exigências das Resoluções 196 de 10.10.96, 251 de 07.08.97 e 292 de 08.07.99, **APROVOU** o referido projeto, em Reunião Ordinária realizada em 14 de dezembro de 2011.

Lembramos que, cabe ao pesquisador responsável elaborar e apresentar os relatórios parciais e finais de acordo com a resolução do Conselho Nacional de Saúde nº 196 de 10/10/96, inciso IX.2. letra “c”.

Atenciosamente,

Coordenador do
Comitê de Ética em Pesquisa
CEP/UFES

Appendix B - Assessment sheet for amputees

1- Identificação																					
Nome: _____																					
Data de Nascimento: ____/____/____ Idade: ____anos Sexo: () M () F																					
Escolaridade: _____																					
2- Anamnese																					
Mão dominante: () direita () esquerda																					
Etiologia da amputação: () vascular () neoplásica () infecciosa () congênita () traumática () outros																					
Tempo de amputação: ____ anos																					
<table border="1"> <thead> <tr> <th colspan="2">Nível da Amputação</th> <th>Direito</th> <th>Esquerdo</th> </tr> </thead> <tbody> <tr> <td rowspan="3">Amputação de Antebraço</td> <td>Terço proximal</td> <td></td> <td></td> </tr> <tr> <td>Terço médio</td> <td></td> <td></td> </tr> <tr> <td>Terço distal</td> <td></td> <td></td> </tr> <tr> <td colspan="2">Desarticulação de Punho</td> <td></td> <td></td> </tr> </tbody> </table>		Nível da Amputação		Direito	Esquerdo	Amputação de Antebraço	Terço proximal			Terço médio			Terço distal			Desarticulação de Punho					
Nível da Amputação		Direito	Esquerdo																		
Amputação de Antebraço	Terço proximal																				
	Terço médio																				
	Terço distal																				
Desarticulação de Punho																					
3- Exame Físico (geral e do coto)																					
Exame físico geral																					
Já fez uso de prótese? () Sim () Não																					
Tipo: _____ Há quanto tempo? ____ anos																					
AVDs: Dependente (D) Parcialmente Independente (PI) Independente (I) () alimentação () higiene oral () higiene genital () banho () vestuário																					
Exame físico do coto																					
Cicatrização																					
Localização da cicatriz _____																					
Cicatriz:																					
() Regular () Normotrófica () Hipotrófica () Aderida a planos profundos																					

Coxim terminal				
Características do Coxim Adiposo:				
() Firme () Flácido () Escasso () Ideal () Volumoso				
Perimetria				
Comprimento do coto: ____ cm Referência óssea: _____				
Circunferência do coto: ____ cm Referência óssea: _____				
Membro Fantasma				
Paciente apresenta sensação de membro fantasma?	() Sim () Pressão () Dormência () Coceira	() Formigamento () Temperatura () Posição do membro	() Não	
Dor Fantasma				
Paciente apresenta dor fantasma?	() Sim () Disparo doloroso () Queimação	() Aperto () Câimbra	() Não	
Avaliação Articular				
Goniometria: Ativa (A) Passiva (P)				
	Direito		Esquerdo	
	A	P	A	P
Ombro				
Flexão (0 - 180°)				
Abdução (0 - 180°)				
Extensão (180° - 0)				
Rotação Interna (0 - 65°)				
Rotação Externa (0 - 90°)				
Cotovelo				
Flexão (0 - 145°)				
Extensão (145° - 0)				
Pronação (0 - 90°)				
Supinação (90° - 0)				

Data: ____/____/____

Assinatura do Avaliador